Schweizerische Eidgenossenschaft
Confédération suisse
Confederazione Svizzera
Confederaziun svizra

Eidgenössisches Departement für Umwelt, Verkehr, Energie und Kommunikation UVEK
Département fédéral de l'environnement, des transports, de l'énergie et de la communication DETEC
Dipartimento federale dell'ambiente, dei trasporti, dell'energia e delle comunicazioni DATEC

Bundesamt für Strassen
Office fédéral des routes
Ufficio federale delle Strade

Thermophysical and Thermomechanical Behavior of Cold-Curing Structural Adhesives in Bridge Construction

Thermophysikalisches und thermomechanisches Verhalten von kalthärtenden strukturellen Klebstoffen im Brückenbau

Comportement thermophysique et thermomécanique des adhésifs structuraux à basse température dans la construction des ponts

ÉCOLE POLYTECHNIQUE FÉDÉRALE DE LAUSANNE EPFL
Composite Construction Laboratory CCLab
O. Moussa, MSc, dipl.-Ing. EPF
T. Keller, Prof. Dr. sc. techn., dipl. Bau-Ing. ETH

Research Project AGB 2005-008 commissioned by the Bridge Research Working Group

Juni 2013 **654**

Schweizerische Eidgenossenschaft
Confédération suisse
Confederazione Svizzera
Confederaziun svizra

Eidgenössisches Departement für Umwelt, Verkehr, Energie und Kommunikation UVEK
Département fédéral de l'environnement, des transports, de l'énergie et de la communication DETEC
Dipartimento federale dell'ambiente, dei trasporti, dell'energia e delle comunicazioni DATEC

Bundesamt für Strassen
Office fédéral des routes
Ufficio federale delle Strade

Thermophysical and Thermomechanical Behavior of Cold-Curing Structural Adhesives in Bridge Construction

Thermophysikalisches und thermomechanisches Verhalten von kalthärtenden strukturellen Klebstoffen im Brückenbau

Comportement thermophysique et thermomécanique des adhésifs structuraux à basse température dans la construction des ponts

ÉCOLE POLYTECHNIQUE FÉDÉRALE DE LAUSANNE EPFL
Composite Construction Laboratory CCLab
O. Moussa, MSc, dipl.-Ing. EPF
T. Keller, Prof. Dr. sc. techn., dipl. Bau-Ing. ETH

Research Project AGB 2005-008 commissioned by the Bridge Research Working Group

June 2013 **654**

Imprint

Research centre and project team

Project leader
Prof. Dr. Thomas Keller EPFL-CCLab

Members

Omar Moussa EPFL-CCLab
Dr. Anastasios P. Vassilopoulos EPFL-CCLab
Dr. Julia de Castro EPFL-CCLab

Review board

President
Dr. Armand Fürst

Members

Dr. Manuel Alvarez
Heinrich Figi
Dr. Hans Rudolf Ganz
Prof. Dr. Aurelio Muttoni
Dr. Dario Somaini

Applicant

Federal Road Office (FEDRO)

Source of supply

This document can be downloaded at http://www.mobilityplatform.ch

Table of contents

Summary

The use of the structural adhesive bonding technique is well established in the aircraft and automotive industries where, in most cases, joints can be fabricated indoors under controlled conditions. In the civil engineering domain, however, load-bearing structures are normally erected on-site in outdoor conditions, i.e. joint fabrication is exposed to varying outdoor temperature and humidity profiles and particularly in winter, when long periods of very low temperatures are frequent, the on-site joining of structural components must remain possible. Consequently, and due to the generally large scale of the structural components, cold-curing adhesives are used, unlike in other fields where hot-curing adhesives are applied.

Although it offers many potential advantages in bridge construction, structural adhesive bonding is not yet widely used in civil engineering structures. This can be attributed, amongst other things, to the lack of knowledge regarding adhesive behavior during exposure to varying environmental conditions. Despite significant research efforts concerning the characterization of structural adhesives, the question of the changes that occur in the thermophysical and thermomechanical properties of cold-curing structural adhesives during their service life, and particularly at early age and low temperatures, is yet to be addressed. The objective of this work was therefore, based on experimental and analytical investigations, to understand the thermophysical and thermomechanical behavior of cold-curing structural adhesives from the time of the mixing of the different components and throughout the long-term service life.

Investigations of curing at early age and low temperatures (during winter) showed that curing already takes place at temperatures slightly above 0°C. The process is very slow however and several days of curing are required to attain significant curing degrees. The glass transition temperature, T_g, develops even more slowly due to early initiation of vitrification. A new and practical experimental method was developed to establish the relationship between glass transition temperature and curing degree for different types of cold-curing adhesives. Furthermore, cure kinetics (developed for hot-curing adhesives) proved its applicability for cold-curing adhesives at low temperatures.

In contrast to thermophysical properties, mechanical properties start developing significantly only after the onset of material vitrification. Lower curing temperatures also significantly decelerate the development process. An empirical model to predict strength and stiffness as a function of simple or complex curing temperature profiles particularly for curing at low temperatures was developed, taking the temperature-dependent vitrification into account.

During summer, the temperature at specific locations of certain joints (e.g. joints below the asphalt) may exceed T_g, which may lead to a significant drop in mechanical properties. The investigations showed that when cooled to temperatures below T_g, the mechanical properties fully recovered and even a significant increase in properties is achieved due to post-curing. An existing model to predict temperature-dependent mechanical properties was extended to predict the change in stiffness and strength due to exceeding of T_g and subsequently after recovery.

Over the long term and during ambient curing, a significant increase in mechanical and thermophysical properties occurs over the years and decades due to the completion of curing. A model based on the similar long-term increase of concrete properties was revised to also predict the long-term strength and stiffness of cold-curing structural adhesives.

Finally several case studies demonstrate how the results of this research can be applied, particularly to predict mechanical properties at early age and low temperatures. Such results can be used to plan construction stages or estimate the required waiting periods prior to a bridge being brought into service.

Zusammenfassung

Tragende Klebeverbindungen sind mittlerweile etablierte Verbindungstechniken in der Automobil- und Flugzeugindustrie, wo sie meistens im Werk und unter kontrollierten Bedingungen eingesetzt werden. Im Bereich des Bauwesens, wo Bauwerke in der Regel im Freien errichtet werden, unterliegen Klebeverbindungen den klimatischen Bedingungen vor Ort, Temperaturen und Feuchtigkeitsgrade variieren. Insbesondere im Winter während langen Perioden niedriger Temperaturen muss es dabei möglich bleiben, geklebte Verbindungen komplexer Bauteile herzustellen. Deshalb, aber auch wegen der Größe der zu verbinden Bauteile, kommen meist kalthärtende Klebstoffe zum Einsatz – im Gegensatz zu in den andern Industriezweigen verwendeten warmaushärtenden Klebstoffen.

Obwohl tragende Klebeverbindungen im Brückenbau sehr viele Vorteile aufweisen können, werden diese bisher nur selten verwendet. Dies ist unter anderem auf fehlende Kenntnisse über das Langzeitverhalten unter den variierenden klimatischen Bedingungen zurückzuführen. Trotz vieler Erkenntnisse auf dem Gebiet der Charakterisierung von strukturellen Klebstoffen besteht weiterhin Forschungsbedarf hinsichtlich der thermo-physikalischen und thermomechanischen Eigenschaften, insbesondere in der frühen Härtungsphase sowie unter tiefen Temperaturen. Das Ziel der vorliegenden Arbeit ist es deshalb, basierend auf experimentellen und analytischen Untersuchungen, das thermophysikalische und thermomechanische Verhalten kalthärtender Klebstoffe, von der Mischung der verschiedenen Komponenten bis hin zum Langzeitverhalten, zu verstehen und zu beschreiben.

Die Untersuchungen der Anfangsphase des Härtungsverhaltens unter tiefen Temperaturen (im Winter) haben gezeigt, dass der Härtungsprozess bereits bei Temperaturen geringfügig über 0°C einsetzt. Allerdings verläuft der Prozess sehr langsam, sodass mehrere Tage nötig sind um signifikante Härtungsgrade zu erzielen. Die Glasübergangstemperatur, T_g, entwickelt sich infolge des frühen Einsetzens der Vitrifikation noch langsamer. Eine neue und praxisorientierte Methode wurde entwickelt um den Zusammenhang zwischen Glas-übergangstemperatur und Härtungsgrad für verschiedene Klebstoffe zu beschreiben. Des Weiteren konnte gezeigt werden, dass die für warmhärtende Klebstoffe entwickelten Härtungsmodelle auch für kalthärtende Klebstoffe unter tiefen Temperaturen anwendbar sind.

Im Gegensatz zu den thermophysikalischen Eigenschaften entwickeln sich die thermomechanischen Eigenschaften erst nach dem Einsetzen der Vitrifikation. Geringere Härtungstemperaturen führen auch zu einer signifikanten Verlangsamung der Entwicklung. Ein empirisches Modell zur Vorhersage von Festigkeit und Steifigkeit wurde entwickelt - dies in Abhängigkeit von einfachen oder komplexen Temperaturprofilen, insbesondere von tiefen Temperaturen und unter Einbezug der temperaturabhängigen Vitrifikation.

Im Sommer kann die Temperatur an exponierten Stellen, z.B. unter dem Asphalt, T_g übersteigen, was zu einer signifikanten Reduktion der mechanischen Eigenschaften führen kann. Die Untersuchungen haben gezeigt, dass wenn die Klebeverbindung sich wieder abgekühlt (unterhalb T_g), die mechanischen Eigenschaften sich wieder vollständig erholen. Dank einer erfolgten Nachhärtung werden diese sogar leicht erhöht..

Die Untersuchungen haben weiter gezeigt, dass die mechanischen Eigenschaften langfristig, über Jahre und Jahrzehnte, infolge Nachaushärtung signifikant zunehmen. Ein Modell zur langzeitigen Entwicklung von Festigkeit und Steifigkeit von kalthärtenden strukturellen Klebstoffen wurde entwickelt. Das Modell basiert auf einem bestehenden Modell zur entsprechenden Vorhersage für Beton.

Abschließend zeigen verschiedene Fallbeispiele wie die Ergebnisse dieser Arbeit praktisch angewendet werden können, insbesondere zur Vorhersage der mechanischen Eigenschaften in der Anfangsphase der Aushärtung unter tiefen Temperaturen. Diese Ergebnisse können beispielsweise zur Planung von Bauphasen oder Wartezeiten bis zur Inbetriebnahme von Brücken verwendet werden.

Résumé

Le collage structurel est bien établi dans les industries aéronautique et automobile, où, dans la plupart des cas, les joints sont fabriqués à l'intérieur dans des conditions de température et d'humidité contrôlées. Dans le domaine du génie civil, cependant, les éléments porteurs sont généralement assemblés sur site dans les conditions environnementales. Ainsi, la réalisation des joints est exposée à différents profils de température et d'humidité extérieures. En hiver particulièrement, de longues périodes de très basses températures sont fréquentes, au cours desquelles le collage des éléments structurels sur site doit toutefois rester possible. Par conséquent, et en raison de la grande taille des éléments structuraux, les adhésifs à basse température sont utilisés, contrairement à d'autres domaines où adhésifs à haute température sont appliqués.

Bien que le collage structural offre de nombreux avantages dans le domaine de la construction de ponts, il n'est actuellement que faiblement utilisé dans les structures de génie civil. Cela peut être partiellement attribué, au manque de connaissances concernant le comportement des adhésifs pendant leur durée de vie lorsqu'ils sont exposés aux conditions environnementales. Malgré les importants efforts entrepris dans la caractérisation des adhésifs structuraux, les changements des propriétés thermo-physiques et thermomécaniques des adhésifs structuraux à basse température pendant leur durée de vie, et plus particulièrement ceux exposés à basse température à un âge précoce, doivent encore être abordés. L'objectif de ce travail était donc de comprendre le comportement thermomécanique et thermophysiques des adhésifs structuraux à basse température dès l'instant du mélange des différents composants jusqu'au comportement à long terme en se basant sur des études expérimentales et analytiques.

Les études effectuées sur le durcissement des adhésifs exposés à de basses températures (en hiver) à un age précoce ont montré que le durcissement se déroule à des températures légèrement au-dessus de 0°C. Le processus de durcissement est cependant très lent et plusieurs jours sont nécessaires pour atteindre des degrés de polymérisation significatifs. La température de transition vitreuse, T_g, se développe encore plus lentement en raison de l'initiation précoce de la vitrification. Une nouvelle méthode expérimentale et pratique a été développée permettant d'établir la relation entre la température de transition vitreuse et le degré de polymérisation de différents types d'adhésifs à basse température. Par ailleurs, il est démontré que la cinétique de réticulation, développée pour des adhésifs à haute température, peut aussi être appliquée aux adhésifs à basse température.

Contrairement aux propriétés thermophysiques, les propriétés mécaniques commencent à se développer de façon significative après le début de la vitrification. L'exposition aux basses températures ralenti aussi de manière significative le processus. Un modèle empirique permettant de prédire la résistance et la rigidité de l'adhésif en fonction de l'historique simple ou complexe des températures, en particulier pour le durcissement à basse température, a été développé en prenant en considération la dépendance de la vitrification.

Pendant l'été, la température à des endroits particuliers de certains joints (par exemple sous l'asphalte) peut dépasser la température de transition vitreuse T_g et conduire à une baisse significative des propriétés mécaniques. Les études ont montré que lorsque les adhésifs sont refroidis à des températures inférieures à T_g, les propriétés mécaniques sont complètement récupérées et qu'une augmentation importante des propriétés est atteinte en raison de la post-cure. Un modèle existant permettant d'estimer les propriétés mécaniques en fonction de la température a été étendu pour prédire la rigidité et la résistance lors du dépassement de T_g et par la suite après la récupération.

A long terme et au cours du durcissement à une température ambiante, une augmentation significative des propriétés mécaniques et thermophysiques survient au cours des années et des décennies en raison de l'achèvement de durcissement. Un modèle basé sur le comportement à long terme de béton, qui est similaire à celui de l'adhésif, a été développé pour estimer la résistance et la rigidité des adhésifs structuraux à basse température à long terme.

Enfin, plusieurs études de cas montrent l'application des résultats de cette recherche, en particulier la prédiction des propriétés mécaniques à l'âge précoce sous basses températures. Ces résultats permettent de planifier les étapes de construction ou d'estimer les délais d'attente nécessaire à la mise en service d'un pont.

1 Introduction

1.1 Motivation and context

The use of adhesives in the construction industry has been established for many decades. Cold-curing resin systems have been extensively used in repair and refurbishment applications to enhance the service life of existing structures [1-2]. In bridge engineering too, structural adhesives have already been used for more than 50 years, although only in specific applications. Advances have been made in the bonding of structural and semi-structural elements of bridges, such as bearings, expansion joints, concrete deck slabs to steel girders in composite bridges and joining of precast concrete segments, as a substitute for or in combination with conventional joining methods [1-2].

Adhesive bonding is being introduced for different engineering applications due to the opportunities offered for increased design flexibility and innovation in design concepts. In bridge construction specifically, recourse to structural adhesives can be primarily attributed to the following advantages [2-5]:

- Structural adhesives are characterized as high-strength materials that are designed to support loads. The mechanical strength of commercial adhesives is usually higher than that of concrete, although they are less stiff. Adhesives are also adequately resistant to high/low temperature cycles and aggressive environments. They are often used for bonding rigid structural elements, providing uniform stress distribution through continuous bonding and at the same time sufficient flexibility to counter the effects of movement, impact or vibration.
- Adhesives can be easily applied to the surfaces of structural elements thanks to their good wetting properties. They are simply applied to one of the surfaces to be bonded, thus keeping the bonded element intact, unlike mechanical connections where drilled holes are usually required.
- In addition to having a reasonable service lifetime, adhesives offer the advantage of easy and rapid maintenance. Degraded adhesive can be easily removed and replaced by a new material after treating the bonded surface.
- Adhesives possess low density and usually only a thin layer is applied, thus avoiding a weight penalty compared to mechanical connections.
- The fatigue performance is improved through adhesive bonding in comparison to conventional joining methods such as bolted and welded joints that usually have limited fatigue resistance.

The use of structural adhesives for primary load-bearing joints in bridge construction started in the late sixties. In eastern Germany from 1968 to 1992, seven bridges in which concrete slabs were bonded to steel girders and with spans of 15-32 m were built. The deck was bonded to the steel girders' upper flanges using a 5-15 mm-thick epoxy adhesive, as shown in *Figure 1.1*. The main reasons for such bonding were the fast erection and optimal stress transfer between the deck and steel girders [6-8].

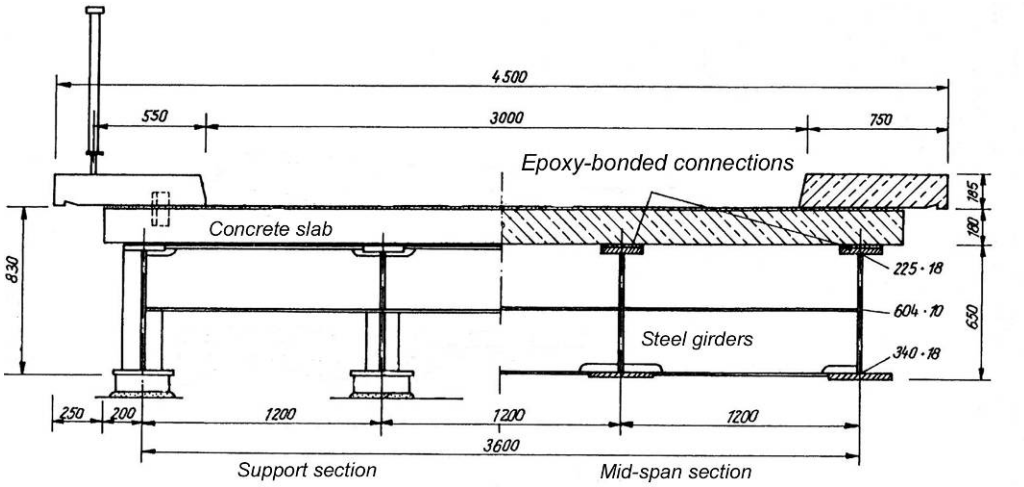

Figure 1.1 Görlitz bridge with bonded slab, Germany, 1973 [8]

Also in Germany in the sixties, adhesively-bonded joints were developed for steel bridges [9]. Compared to prestressed-only connections, bonded-prestressed connections showed a load resistance up to 60% higher than traditional connections as well as good fatigue behavior. The bonded connections are considered as being an economical solution, and also appropriate for corrosion protection. A total of 15 pipeline-bridges with a 20-m span were built. The nodes of the truss structures were formed using bonded connections, as shown in *Figure 1.2*. In addition, a composite bridge in which a deck and steel girders were bonded using prestressed-bonded connections was erected [10].

Recent applications include structural strengthening using bonded steel plates or CFRP strips. *Figure 1.3* shows bonded CFRP strips used for the shear and flexural strengthening of a bridge beam [2, 11].

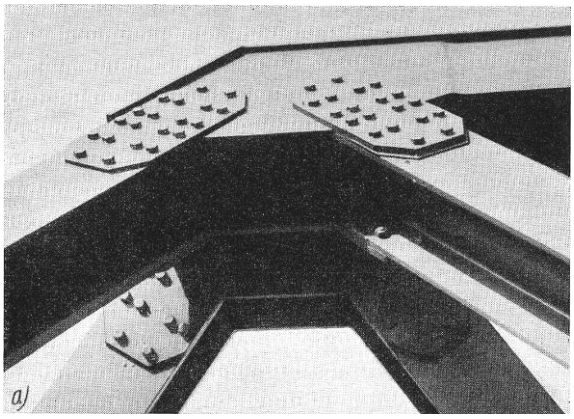

Figure 1.2 Prestressed-bonded steel-truss nodes [9]

Figure 1.3 Beams reinforced with bonded CFRP strips (CCLab) [11]

In all the previously described applications, a two-component epoxy adhesive was used. Epoxy adhesives are characterized by high strength and stiffness, but also exhibit a brittle behavior. Efforts are therefore being made to use flexible and/or ductile polyurethane or acrylic adhesives to provide more robust adhesive bonds [12-13]. *Figure 1.4* shows the variation in lap shear strength and stiffness of a variety of structural adhesives.

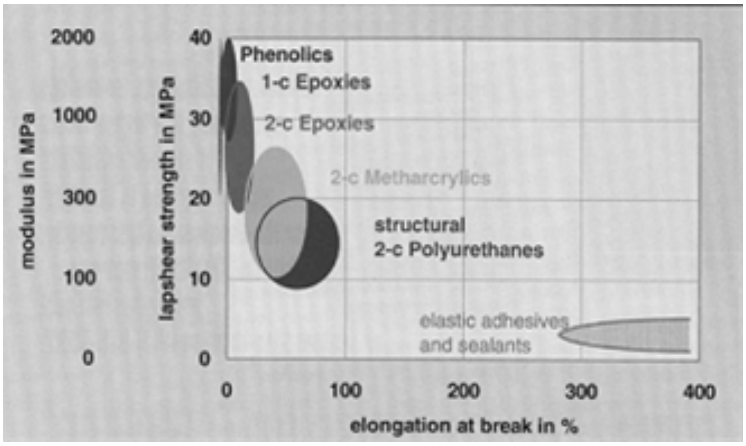

Figure 1.4 Shear strength and stiffness of brittle and flexible/ductile adhesives

Due to the enormous variety of adhesives available in industry, the selection of the tailored adhesive is of prime importance. Besides the adhesive's cohesive properties, the selection is dependent on different parameters such as the adhesion to the adherend, the type of applied load and environmental conditions.

The successful performance of a bonded joint depends on adequate adhesion between the adhesive and the substrate [2, 14-16]. The strength of the bonded joints depends not only on the cohesive strength of the adhesive, but also on the degree of adhesion to the bonding surface. Adhesive bonding requires clean surfaces in order to obtain a satisfactory degree of contact (adhesion) and therefore surface pre-treatment is required. Optimization of surface pre-treatment is the key to maximizing joint performance and durability. The purpose of surface preparation is to remove contamination and weak surface layers, and to change the substrate surface geometry. Various surface pre-treatment methods, according to the type of adherend, are proposed in literature (e.g. [17-18] for steel and [19-21] for concrete).

The design of bonded joints dictates the required properties of the adhesive used as it should transfer stresses between the adherends. Therefore, the level and type of applied load (i.e. peel, shear, cleavage or compression) should be analyzed in order to select a suitable adhesive. Also bond thickness and bond area have an effect on load transfer and consequently joint performance [22].

It is essential during the selection phase to investigate the environmental conditions on the construction site in which the adhesive is used. Humidity may damage the adhesive through cracking due to swelling during moisture inclusion, whereas its stiffness may be reduced by plasticization. The subsequent scission of the polymer chains provoked by hydrolysis and the leaching out of low molecular weight material from the bulk resin further damages the polymer. Since the ability of an adhesive to maintain adhesion while exposed to harsh environments varies [14-15, 23], it is important to investigate the behavior of structural adhesives under extreme conditions. These conditions involve low-temperature curing at early age and elevated temperature exposure (exceeding the adhesive's glass transition temperature, T_g) during serviceability. At early age, the curing of structural adhesives used in outdoor applications might take place at low temperatures (particularly during winter), but low-temperature curing is not desirable and could alter the performance of the adhesive. Moreover, during service the adhesive might be subjected to temperatures exceeding its T_g due to variable environmental temperatures or temperature increases at certain joint locations. Despite the existence of knowledge of

the adhesive's response to high temperatures, the recovery behavior (when cooled from temperatures above T_g) is yet to be investigated.

However, and in order that adhesive bonding can be widely accepted in bridge engineering, in particular for new constructions, an understanding of the basic adhesive behavior (in terms of themophysical and thermomechanical performance) from the initiation of curing to the long-term performance is required in a first step. Once this objective is achieved, other critical aspects such as the complex stress states in joints, various failure modes and long-term durability need to be addressed. Finally, a design standard for adhesive bonding in construction needs to be formulated.

The purpose of this research is to fill the first of these gaps and provide engineers with theoretical and practical knowledge concerning adhesive behavior starting with the mixing of the components up to long-term performance where changes in thermophysical and thermomechanical properties take place. The research focuses on cold-curing adhesives which are widely used in civil engineering applications.

1.2 Objectives

This research concentrates on studying the curing behavior of structural adhesives during their service life in bridge applications (from fabrication up to long-term performance). Extensive experimental and analytical investigations of the thermophysical and mechanical properties of a cold-curing structural epoxy adhesive were carried out. Finally recommendations for the use of structural adhesives in bridge construction are presented. Based on the above, the objectives of this research can be summarized as follows:

1. Understand and investigate the effect of low-temperature curing on the physical state of commercial cold-curing adhesives.
2. Study the effects of low-temperature curing on the early-age development of the mechanical properties of commercial cold-curing adhesives. Furthermore, investigate the relationship between thermophysical and mechanical properties.
3. Understand and investigate the effect of the physical changes on the mechanical properties during the thermomechanical recovery of cold-curing adhesives after their glass transition temperature has been temporarily exceeded.
4. Investigate the long-term curing behavior of cold-curing structural adhesives, thus observing the changes in mechanical properties and physical characteristics that occur during the achieving of a fully cured system.
5. Implement the outcome of this research in practical design problems through studying different bridge applications.

1.3 Methodology

In order to achieve the objectives mentioned above, extensive experimental investigations were carried out and theoretical methods originating not only from civil engineering but also from other fields were either applied or modified or new ones were developed, as shown in *Figure 1.5*, as follows:.

1. Investigating the change in the physical state of the adhesive was achieved by experimentally monitoring the change in physical material properties (curing degree and glass transition temperature) with temperature and time (objective 1). Special attention was paid to low-temperature curing. Cure kinetics was applied to model the observed behavior.
2. Investigating the change in mechanical behavior at early-age was achieved by carrying out mechanical experiments under different curing profiles. Corresponding thermophysical experiments were conducted in order to study the relationship between mechanical property development and the related changes in the physical state of the material (objective 2). A new model is proposed for the prediction of property development at early age.
3. Following the results obtained after addressing objectives 1 and 2, the sensitivity of the adhesive to elevated temperatures and the recovery behavior of the mechanical

properties when the adhesive was cooled from temperatures above the glass transition temperature were experimentally investigated. An existing model was extended for the prediction of the thermomechanical recovery response of adhesives.

4. As the results obtained after addressing objective 2 showed the need to investigate the long-term curing performance of cold-curing adhesives, an experimental method was used to predict long-term properties and a model is also proposed.
5. Numerical examples are presented to demonstrate the use of the results obtained during the investigation of objective 2. A discussion based on the results of objective 3 is also included.

1.4 Report Organization

This report comprises eight chapters. Following the introduction (Chapter 1), the adhesives used during this research are presented in Chapter 2. Chapters 3 to 7 correspond to objectives 1 to 5 listed above. Finally, the conclusions and the discussion regarding future work are presented in Chapter 8. The general organization of the report based on each chapter content is shown in *Figure 1.5* and can be described as follows:

Chapter 1: An introduction explaining the use of structural adhesives in bridge construction and their advantages and drawbacks is given. The objectives of the project are derived and the methodology followed by the research is presented.

Chapter 2: The adhesives used in this research are introduced. Available information and material properties, either derived from experiments or obtained from manufacturers' datasheets, are presented for each adhesive.

Chapter 3: An extensive experimental investigation is presented, using the dynamic scanning calorimetry technique (DSC), to monitor changes in the curing degree, α, and glass transition temperature, T_g, of a cold-curing adhesive, particularly at low curing temperatures (between 0 and 10°C). Cure kinetics is applied for modeling the curing behavior of the adhesive at early age and predicting the development of T_g involving physical changes in the material (e.g. vitrification). Finally and due to its observed importance, a new experimental method is presented for establishing the T_g - α relationship.

Chapter 4: An extensive experimental investigation of mechanical properties is presented, carried out on specimens cured at different isothermal and cyclic temperatures (with special attention to low-temperature curing) during different periods. Corresponding thermo-physical characteristics (T_g and α) are also experimentally investigated using DSC. A new empirical method, based on the autocatalytic curing behavior of the adhesive, is proposed to predict the mechanical properties as a function of the curing procedure.

Chapter 5: An extensive experimental investigation shows the response of adhesives to a wide range of temperatures and also the thermomechanical behavior after cooling from exposure temperatures above T_g to recovery temperatures below T_g. The time effect is also investigated by extending time at exposure temperatures and recovery temperatures. An existing model to predict temperature-dependent mechanical properties is extended to also predict the thermomechanical recovery behavior of structural adhesives.

Chapter 6: An experimental study is described to evaluate the long-term curing performance. A method involving accelerated curing based on the results of the previous study (Chapter 5) is presented. An existing model, previously established for concrete, is adapted in order to predict the long-term properties of structural adhesives.

Chapter 7: Numerical examples concerning three different bridge applications are presented to demonstrate the use of the research results. The different parameters affecting the thermophysical and mechanical performance of the adhesive bond layer are taken into account.

Chapter 8: General conclusions concerning this research are presented in addition to highlighting its contributions to both the scientific community and industry. Furthermore, suggestions regarding future works that compliment this field of research are given

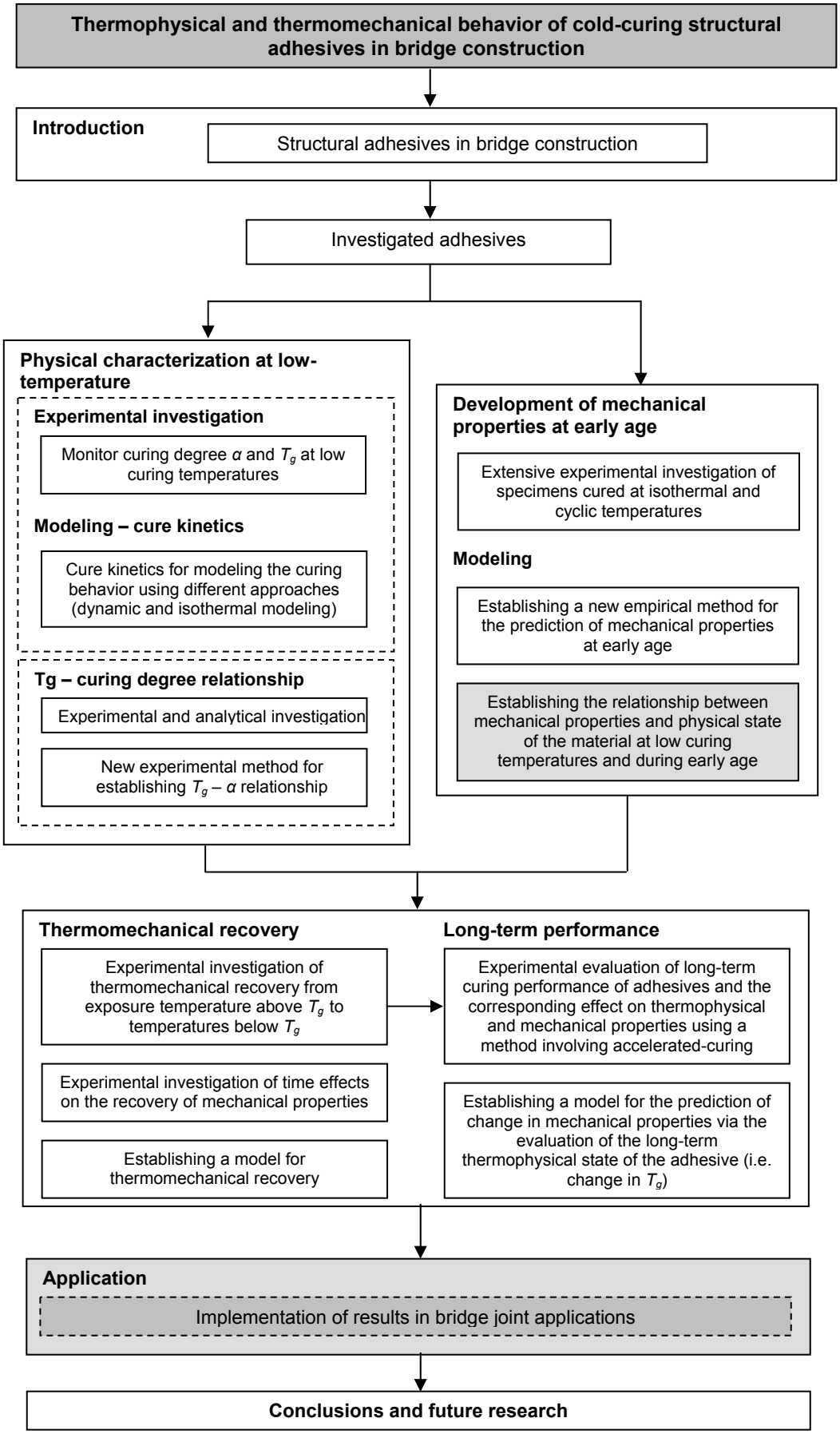

Figure 1.5 Methodology and report organization

1.5 References

D.J. Dunn, "*Engineering and structural adhesives*", Rapra review report, 15 (1), 2004, 1-28. [1]

G.C. Mays and A.R. Hutchinson, "*Adhesives in civil engineering*", Cambridge university press, 1992. [2]

R.W. Messler Jr*., "Joining of Materials and structures", Elsevier*, 2004, 177-226. [3]

R.F. Mander*, "Use of resins in road and bridge construction and repair",* Int. J. Cem. Comp. LW. Conc. Vol3, N1. [4]

M.R. Bowditch, "*The durability of adhesive joints in the presence of wate*r", Int. J. Adhes. Adhes. 16, 1996, 73-79. [5]

H. Hänsch and W. Krämer, "*experiments with bonded composite structures"*. The road in 1968; 3: 137-141. [6]

E. Fiedler, "*The development of the steel bridge in the GDR until the turn of a retrospective*", Stahlbau 2001; 70(5): 317-328. [7]

H. G. Dauner, "*Neue Verbindungstechnik im Verbundbrückenbau"*, ASTRA Report No. 583. Bern: Swiss Federal Roads Authority. [8]

G. Trittler and K. Körnen, "*Die vorgespannte Klebeverbindung (VK-Verbindung eine Weiterentwicklung der Verbindungstechnik im Stahlbau"*, Stahlbau, 1964; 33(9): 257–269 [9]

R.D. Adams, J. Comyn and W.C. Wake, "*Structural adhesive joints in engineering"*. Chapman & Hall, London, 1997. [10]

T. Keller, "*Strengthening of concrete bridges with carbon cables and strips"*. Proceedings of the Sixth International Symposium on FRP Reinforcement for Concrete Structures (FRPRCS-6). [11]

M. Schmid and R. Kieselbach, New Leimen, EMPA Report No. 200'171 scientific e02 / 2, 2002. [12]

J. de Castro, *"System ductility and redundancy of FRP structures with ductile adhesively-bonded joints"* PhD thesis No 3214, Ecole Polytechnique Fédérale de Lausanne (EPFL), 2005. [13]

J. Comyn, "*Developments in adhesives - 2*", (Ed. Kinloch, A.J.), Applied science publishers, London, 1981, chapter 8. [14]

A.J. Kinloch, "*Durability of structural adhesives*", Applied science publishers, London, 1983. [15]

W.A. Zisman, "*Handbook of adhesives, 2nd edn.*", Van Nostrand Rheinhold company, New York, 1977, Chapter 3. [16]

J.M. Sykes, "*Surface analysis and pretreatment of plastics and metals*", (Ed. Brewis, D.M.), Applied science publishers, London, 1982, Chapter 7. [17]

W. Brockmann, "*Durability of structural adhesives*", (Ed. Kinloch, A.J.), Applied science publishers, London, 1983, P. 281. [18]

P.C. Hewlett and J.D.N. Shaw, "*Developments in adhesives - 1*", (Ed. Wake, W.C.), Applied science publishers, London, 1977, Chapter 2. [19]

J.D.N. Shaw, *"A review of resins used in construction. Types of resin - applications - case histories"*, Int. J. Adhes. Adhes., 1982; 2(2): 77–83. [20]

H.R. Sasse and M. Fiebrich, *"Bonding of polymer materials to concrete"*, Mater. Struct., 1983; 16(4): 293–301. [21]

M. Petronio, "*Handbook of adhesives, 2nd edn.*", (Ed. Skeist. I.), Van Nostrand Rheinhold company, New York, 1977, Chapter 6. [22]

A.J. Kinloch, *"Interfacial fracture mechanical aspects of adhesive bonded joints – a review"*, J. Adhes., 1979; 10(3): 193–219. [23]

2 Investigated Adhesives

2.1 Overview

Six structural cold-curing adhesives from three manufacturers were considered during this research, see *Table 2.1*. The Sikadur-30 adhesive was used to develop the work presented in Chapters 3, 4 and 5, while Sikadur-330 was used in the investigation presented in Chapter 6. In addition, four other adhesive systems were used to validate the results, whereby different resin systems (epoxy, polyurethane and polyester) and filler contents were taken into account. One of the adhesives (Sikadur-30 unfilled) is a non-commercial adhesive, specially prepared by the manufacturer for this study. The characteristics of each adhesive are given below.

Table 2.1 Adhesives used in this research

Adhesive	Manufacturer	Type	Fillers		Density (Kg/m^3)	Mixing ratio	T_g[1] (°C)
			Type	*Content (%)*			
Sikadur-30	Sika	Epoxy	Silica quartz	55	1650	3:1	62
Sikadur-30 (unfilled)[2]	Sika	Epoxy	None	0	-	4:1	-
Sikadur-330	Sika	Epoxy	Silica-based	< 20	1310	4:1	> 40
Sikaforce-7851	Sika	Polyurethane	None	0	1130	2:1	45
Adesilex PG1	Mapei	Epoxy	Sand grains	20-25	1580	3:1	> 40
VM-K 300	MKT	Polyester	None	0	1570	10:1	-

[1] According to manufacturer
[2] Non-commercial adhesive

2.1.1 Sikadur-30

Sikadur-30 is a filled bi-component thixotropic adhesive mortar from Sika Schweiz AG, the base resin being a solvent-free bisphenol-A-based epoxy. The hardener consists of aliphatic amines. The base resin contains silica quartz fillers. To determine filler size and quantity, the surfaces of three adhesive samples were investigated using optical microscopy, as shown in *Figure 2.1*, and burn-off tests were performed respectively. The resulting filler sizes are between 0.2 and 0.5 mm and the content is approximately 55% by weight fraction. The epoxy system is mixed at room temperature at a ratio of 3:1 by weight of the respective constituents (resin and hardener). According to the manufacturer's data sheets, the tensile strength and modulus of elasticity for fully cured materials are 31 MPa and 11.2 GPa respectively (according to DIN 53 455 and ISO 527 respectively). The glass transition temperature is 62°C resulting from a torsion pendulum test after curing at 45°C during one week.

Figure 2.1 Bi-component epoxy Sikadur-30

This adhesive is characterized by good workability, waterproofness and good adherence to concrete, masonry, steel and aluminum. The curing of this adhesive is not affected by humidity and no shrinkage is observed during cure. Besides high strength properties, this

adhesive presents high resistance to creep during permanent loading and to abrasion and impact loading. Applications include structural bonding between steel or FRP plates and concrete, different concrete elements and bridge segments.

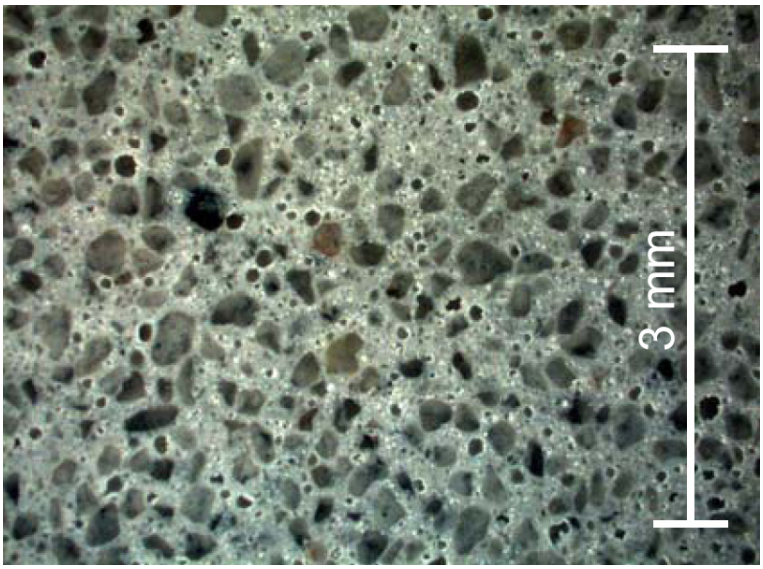

Figure 2.2 Optical microscopy photo showing adhesive filler size for epoxy Sikadur-30

As mentioned above, a non-commercial version of this adhesive with a mixing ratio of 4:1 and containing no fillers was prepared to demonstrate the effect of filler content.

2.1.2 Sikadur-330

Sikadur-330 is another thixotropic bi-component adhesive from Sika Schweiz AG. The base resin is a bisphenol-A-based epoxy. The hardener consists of aliphatic amines but in a higher concentration than that of Sikadur-30. This adhesive contains a small quantity of silica-based fillers (<20% by weight, based on burn off tests, see also optical microscopy photo in *Figure 2.2*). The mixing ratio is 4:1 resin to hardener. In order to confirm the material properties of this adhesive, quasistatic tension experiments and dynamic mechanical analysis (DMA) were performed on specimens cured under laboratory conditions (T=23±5°C and RH=50±10%). The tensile strength and modulus of elasticity are 38.1 MPa and 4.6 GPa respectively (according to EN ISO 527-1) as reported in [1]. The glass transition temperature is around 44°C determined by the drop in storage modulus, as shown in *Figure 2.5*. This adhesive is fabricated for manual application to surfaces and is used to impregnate FRP fabrics employed to strengthen existing concrete or steel structures.

Figure 2.3 Bi-component epoxy Sikadur-330

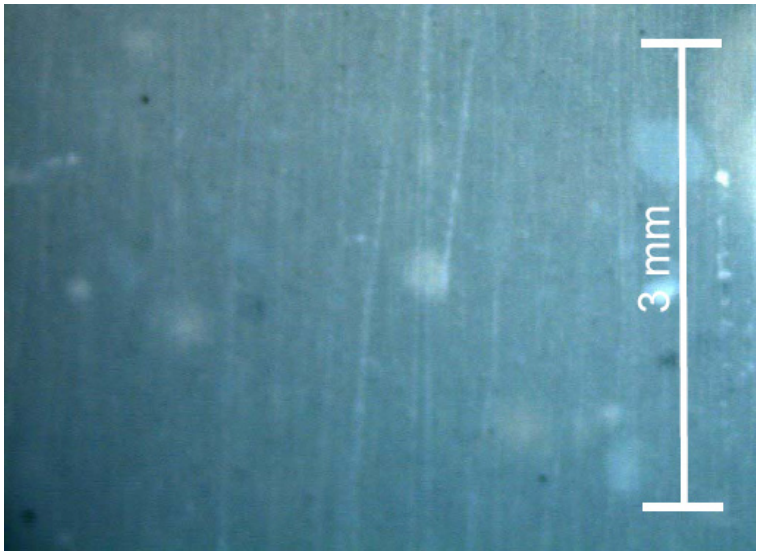

Figure 2.4 Optical microscopy photo of epoxy Sikadur-330 showing silica-based fillers (white spots)

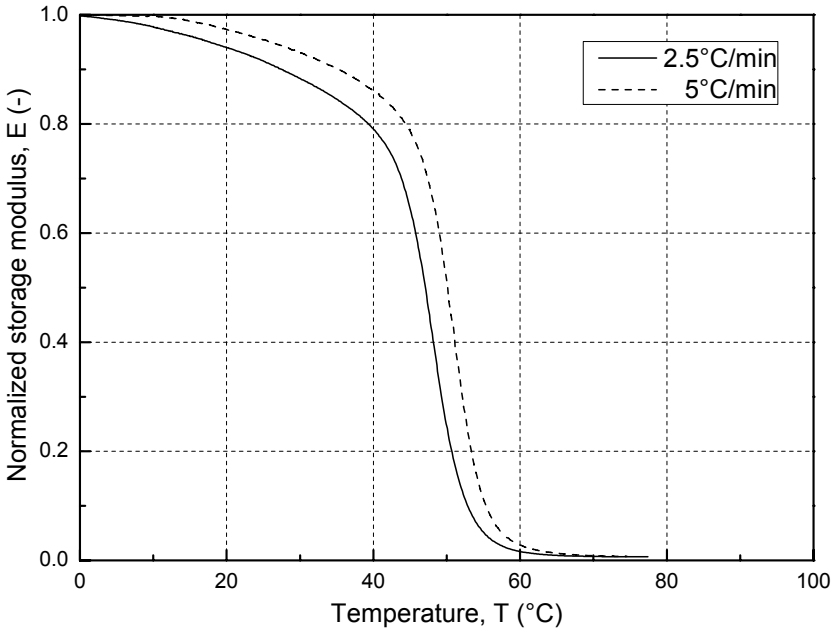

Figure 2.5 DMA results at different heating rates for epoxy Sikadur-330

2.1.3 Sikaforce-7851

Sikaforce-7851 is a thixotropic, bi-component, solvent-free polyurethane adhesive from Sika Schweiz AG. The components are mixed mechanically using a dispenser with a ratio of 2:1. The glass transition temperature is approximately 45°C according to the manufacturer. This adhesive is used for joining prefabricated structural elements and also provides a certain joint ductility which favors for stress redistribution [2].

Figure 2.6 Bi-component polyurethane Sikaforce-7851

2.1.4 Adesilex PG1

Adesilex PG1 is a thixotropic bi-component epoxy adhesive from Mapei, Italy. The base resin is a bisphenol-A-based epoxy with a different hardener type than that used in Sikadur-30 and Sikadur-330. The mixing ratio is 3:1 resin to hardener. Selected fine grains of free crystalline silica of a diameter >0.01 mm are added (20-25% by weight) according to the manufacturer. Modulus of elasticity and bond strength are 6 GPa and >18 MPa according to EN 13412 and EN 12188 respectively. The glass transition temperature is > 40°C according to EN 12614. Main applications are strengthening of concrete by bonded steel or FRP plates and structural bonding of precast concrete elements.

Figure 2.7 Bi-component epoxy Adesilex PG1

2.1.5 VM-K 300

VM-K 300 is a fast-curing bi-component polyester adhesive from MKT Deubel, Germany. A manual dispenser is used to mix the two components with a ratio of 10:1. The adhesive is mainly used for fastening of anchors into concrete and masonry.

Figure 2.8 Bi-component polyester VM-K 300

2.2 References

J. de Castro and T. Keller, "*Ductile double-lap joints from brittle GFRP laminates and ductile adhesives. Part I: Experimental investigation*", Compos Part B-Eng, 2008; 39(2): 271-281. [1]

J. de Castro and T. Keller, "*System ductility and redundancy of FRP beam structures with ductile adhesive joints*", Compos Part B-Eng, 2005; 36 (8): 586-596. [2]

3 Physical characterization at low temperatures

3.1 Overview

3.1.1 Curing mechanism

Thermosetting resins (such as the adhesives used in this study) undergo cross-linking after the base components are mixed either at ambient temperature (cold-curing adhesives) or during heating to the required elevated temperatures. This process is known as the curing of the resin or conversion as shown in *Figure 3.1*. The properties of thermosetting materials depend greatly on their chemical formulation or composition as well as the curing conditions, such as temperature and time, to which the resin is exposed during processing. Small changes in the formulation or processing conditions can affect the curing of the resins, and can thus have a significant influence on the properties of the end product [1-2].

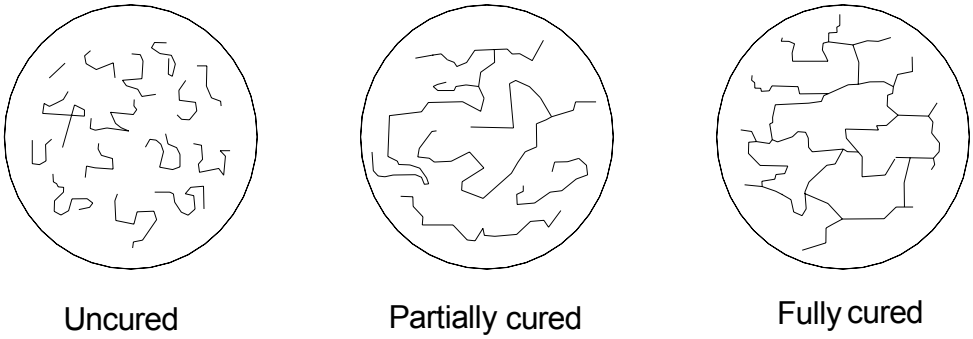

Figure 3.1 Representation of increase in cross-link density of a thermosetting material

Thermosetting resins undergo an irreversible chemical reaction during cure. As the components in the resin system cure, heat is evolved by the resin. The curing degree (degree of cross-linking) differs from one system to another according to the chemical constituents of the material as well as the curing conditions (in terms of temperature and time).

For the wider application of adhesive joints in bridges, an understanding of the curing behavior and associated development of the mechanical properties of cold-curing adhesives, particularly when exposed to low temperatures, must be acquired. The curing rate produced at low-curing temperatures must be predicted in order to decide when a bridge can be opened for traffic for example. Although adhesive curing theories do exist, they were developed for hot-curing adhesives only and the proof of their applicability to describe the physical behavior of cold-curing adhesives, especially at low temperatures, is still lacking.

The main material characteristics involved and of interest are the curing degree, α, and the glass transition temperature, T_g, beyond which mechanical properties decrease. The relationship between the curing temperature, T_{cure}, and T_g (which increases during curing) not only defines the physical state of the material (liquid, rubbery or glassy) but also the reaction rate during the curing process [2-3]:

$T_{cure} > T_g$: the reaction proceeds rapidly at a rate driven by chemical kinetics

$T_{cure} \approx T_g$: vitrification takes place, i.e. the material solidifies

$T_{cure} < T_g$: the reaction rate decelerates and becomes diffusion-controlled

Based on the above analysis, the effect of low-temperature curing on the physical states of a commercial cold-curing epoxy adhesive (Sikadur-30) was experimentally investigated. Temperatures down to 5°C were taken into account. The applicability of existing curing models - previously developed for hot-curing adhesives - to the present

cold-curing adhesive was examined. The results of this work and their impact on the design and fabrication of bridge joints are discussed in this chapter.

3.1.2 Differential scanning calorimetry (DSC)

One important aspect of thermosetting resins is the cure kinetics associated with the material. Kinetics refers to the modeling of the effect of temperature and time on the degree of cure. One of the easiest ways of determining the cure kinetics of a resin is Differential Scanning Calorimetry (DSC).

DSC is a well-established thermoanalytical technique in which the difference in the amount of heat required to increase the temperature of a sample and an empty reference is measured as a function of temperature. Both the sample and the reference sample are maintained at the same temperature throughout the experiment [1]. When the sample undergoes a physical transformation, more or less heat flows to it than to the reference sample to maintain both at the same temperature. This heat flow during the curing of adhesives is monitored by the DSC machine. *Figure 3.2* represents the change in heat flow taking place by scanning an uncured or partially cured epoxy resin undergoing a constant increase in temperature. The resin eventually undergoes curing and this is observed as the large exothermic peak at which the heat flow deviates from a linear response (horizontal line) at the onset temperature of cure and a maximum rate of curing is reached at the peak temperature, T_p. Upon the completion of curing or cross-linking, the DSC heat flow returns to a quasi-linear response. The curing degree is obtained by the integration of the area under the exothermic peak. The corresponding glass transition temperature of the adhesive, T_g, is obtained from the step preceding the exothermic peak. Moreover, by increasing the temperature beyond the curing exotherm, another peak appears at higher temperatures describing the decomposition of the adhesive (usually endothermic). The maximum decomposition rate is characterized by the temperature T_d.

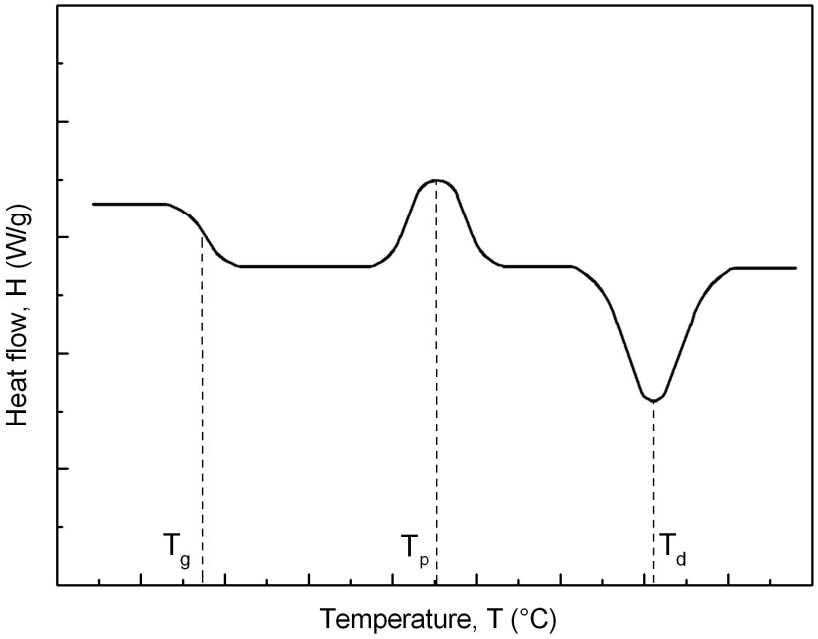

Figure 3.2 Typical DSC curve of an uncured or partially cured adhesive

The curing of thermosetting resins can also be monitored by another technique, which involves running an isothermal test (heating at constant temperature) where the cumulative heat can be calculated i.e. recording the maximum attainable heat flow at a certain isothermal temperature.

3.2 Experimental investigation

3.2.1 Experimental set-up

A heat-flux differential scanning calorimeter (DSC-TA Q100) connected to a thermal analyzer was used to detect the heat released during the cure reaction. The equipment is supplied by a liquid nitrogen cooling system providing an inert atmosphere, thus allowing the DSC cell to reach very low temperature ranges as shown in *Figures 3.3a* and *b*.

The weight of each sample was measured prior to scanning by a microbalance. Sample weight ranged between 5 and 10 mg according to preliminary tests carried out to specify the heating rate, curing temperature and suitable sample weight ranges. The samples were placed in a steel pan covered with a lid and sealed with a manual press, as shown in *Figure 3.3c*. An empty steel pan of the same type and size was used as a reference during every scan. Data acquisition was performed using the accompanying software (TA Analysis).

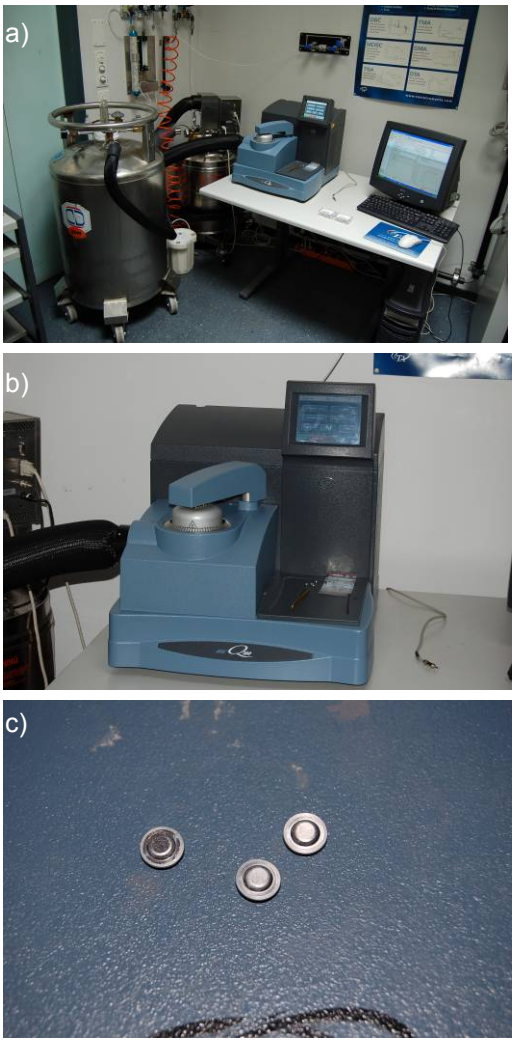

Figure 3.3 DSC experiments, a) Full set-up, b) DSC machine, c) DSC samples (scale in cm)

3.2.2 Experimental Program

Uncured samples were used to determine a) the total heat of reaction released during a complete curing process of a dynamic scan and b) the maximum heat of reaction reached at different isothermal temperatures.

Dynamic scans were conducted in the temperature range of -50°C to 250°C at constant heating rates of 2.5, 5, 10, 15 and 20°C/min. By extending the scanning temperature

range, the decomposition reaction of the material was found to initiate at a temperature of 297±2°C (result from 3 scans at 15°C/min).

Isothermal scans were conducted at temperatures ranging between 5 and 80°C. This range was chosen in accordance with the planned bridge application. Samples were placed in the DSC cell and then scanned at a rate of 20°C/min when the temperature equilibrium was reached in the sample holder. The samples were scanned until the heat flow curve approached a plateau.

When samples were scanned at high temperatures above T_g, part of the initial data was not recorded. The curing process was too rapid and part of the reaction heat was released before detection by the calorimeter. Furthermore, at low curing temperatures of 5, 10 and 25°C, a large scatter in the results was obtained. Therefore, an alternative method, which proved to be efficient in [4], was used to determine the development of the curing degree at low (5, 10 and 25°C) and high (70°C) curing temperatures. The samples were pre-conditioned in a climate chamber (according to ASTM D618-05) at the different curing temperatures (5, 10, 25, and 70°C) during different time periods, t_{cure}, (ranging from several minutes at the highest temperature to 10 days at the lowest temperature). Constant humidity (50±2%) was maintained in order to eliminate any possible effect on the curing process. After removal from the chamber, the samples were rapidly quenched in liquid nitrogen to stop the reaction. The residual cure and the corresponding glass transition temperature of the partially cured samples were then obtained by running a dynamic scan. Three samples were investigated for each combination (T_{cure} and t_{cure}).

This procedure was also used to investigate the development of the glass transition temperature as a function of time as well as the relationship between the glass transition temperature and the curing degree. In some cases, at a low curing degree and low T_g (at short t_{cure}), difficulty in detecting the corresponding T_g was encountered. Modulated DSC was then used to separate reversible and non-reversible reactions, which enabled the T_g to be detected from the reversible heat capacity (midpoint of the step in the curve preceding the curing exotherm).

A half-life validation (according to ASTM E-698) was performed to assess the results. A sample was preconditioned at the determined half-life temperature, $T_{h\text{-}l}$, for 60 minutes in the DSC chamber and then rapidly quenched in liquid nitrogen to stop the reaction. The sample was subsequently scanned at 10°C/min (an intermediate heating rate) between -50 and 250°C.

3.3 Cure kinetics

3.3.1 Kinetic analysis

The change in heat flow vs. temperature and time during dynamic scans at different heating rates is shown in *Figure 3.4a* and *b*. The peak temperature, T_p, the onset of cure temperature, T_{onset} (defined according to ASTM E2041), and the shape of the exotherm were heating rate- dependent. The value of the heat released was determined by integrating heat flow vs. time under the exotherm along a straight base line, as shown in *Figure 3.4b*. This heat of reaction, ΔH_T, was independent of the heating rate, see *Table 3.1* (95.1 ± 1.56 J/g). The scatter of samples scanned at the same heating rate was examined by scanning three samples at 15°C/min and was found to be small (95.5 ± 0.5 J/g).

The heat flow vs. time of isothermal scans at temperatures between 35 and 60°C is shown in *Figure 3.5*. Reducing the curing temperature delayed the maximum heat flow due to the deceleration of the reaction and corresponding movement of the particles. The heat released during isothermal scanning, ΔH_{iso}, was calculated as the area under each isothermal curve considering the plateau as a horizontal base line; the results are listed in *Table 3.2*.

Table 3.1 Dynamic scanning results at different heating rates

Parameter	***dT/dt* (°C/min)**				
	2.5	5	10	15	20
ΔH_T (J/g)	92.64	94.50	96.36	95.52	96.36
T_{onset} (°C)	41.4	50.5	58.0	73.6.0	77.0
T_p (°C)	80.8	89.7	107.8	116.8	120.8
α_p (%)	0.49	0.46	0.54	0.54	0.49
$(d\alpha/dt)_p$ (min^{-1})	0.069	0.12	0.22	0.33	0.39
$(d\alpha/dT)_p$ ($°C^{-1}$)	0.0278	0.024	0.022	0.022	0.019

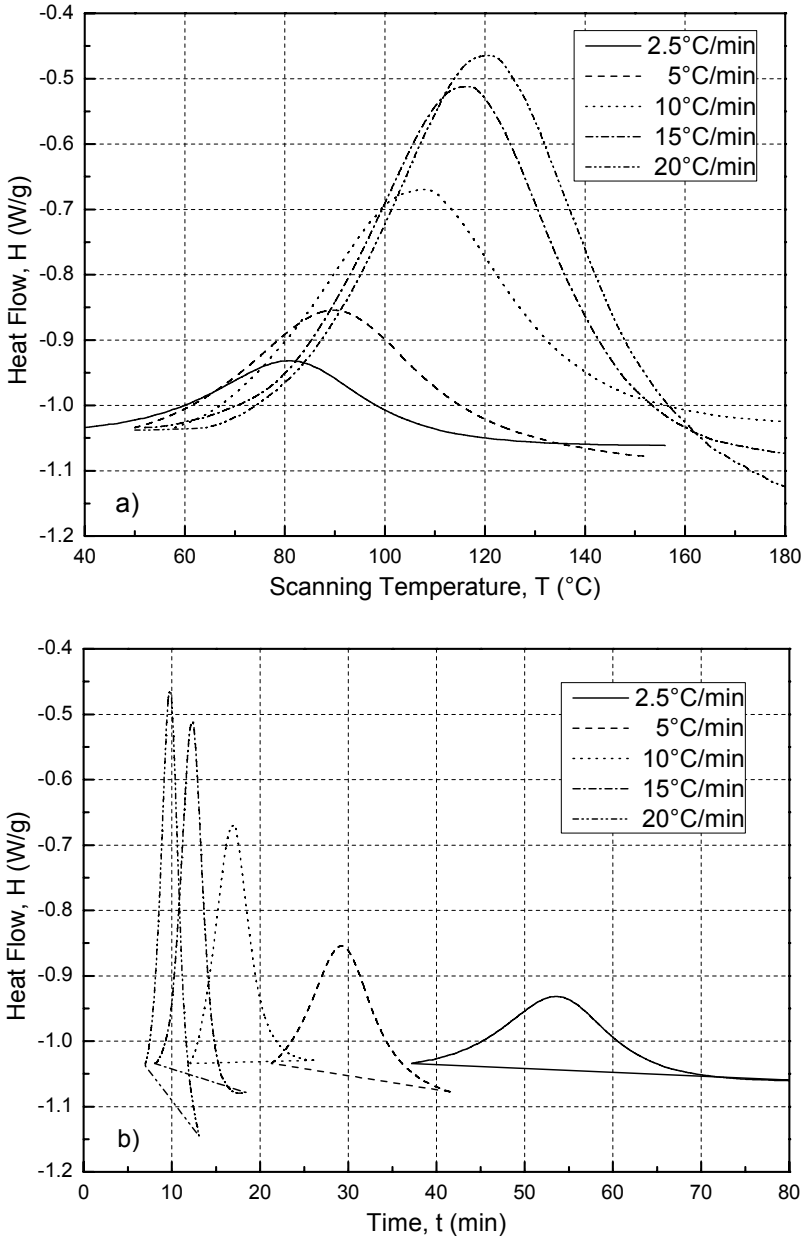

Figure 3.4 Heat flow at different heating rates during dynamic scanning as function of, a) temperature, b) time (between onset and end of cure) (Sikadur-30)

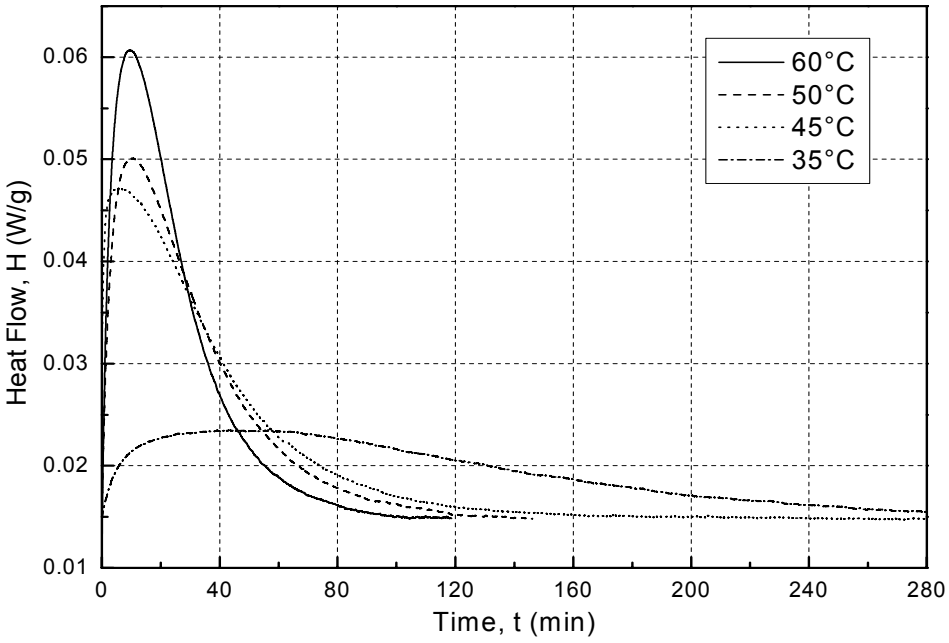

Figure 3.5 Heat flow at different isothermal curing temperature s(Sikadur-30)

Table 3.2 Isothermal scanning results at different temperatures until onset of diffusion control

Parameter	T_{cure} (°C)							
	5[a]	10[a]	25[a]	35	45	50	60	70[a]
ΔH_{iso} (J/g)	-------	-------	-------	91.54	94.44	96.36	96.36	-------
α (%)	-------	-------	-------	0.95	0.98	1	1	-------
t (hrs)	-------	-------	-------	3.73	2.42	2.05	1.58	-------
t_{50} (hrs)	11.85	6.67	1.54	0.97	0.45	0.4	0.38	0.15

[a] Results from alternative pre-conditioning method

Based on dynamic and isothermal results, the curing degree, α, was calculated as $\Delta H_{iso}/\Delta H_T$. The resulting values vs. time are shown in *Figure 3.6* for the two experimental methods (pre-conditioning and subsequent dynamic scans vs. isothermal scans, see Section 3.2.1). At high temperatures, full curing was attained after a few hours. At lower temperatures curing was delayed: at 5°C for example, 70% of curing required almost one day and 90% was attained after 3 days at 10°C. *Figure 3.6a* also shows the onset of diffusion control (for derivation see below) after which curing was further delayed.

According to the time required to attain 50% curing, t_{50} (see *Table 3.2*), the 60-min half-life temperature was found to be 34°C. The integrated peak area of the partially cured sample represented 49.7% of the peak area of the uncured sample and was thus within the standard range (50 ± 0.5%). The validity of the DSC results was therefore confirmed.

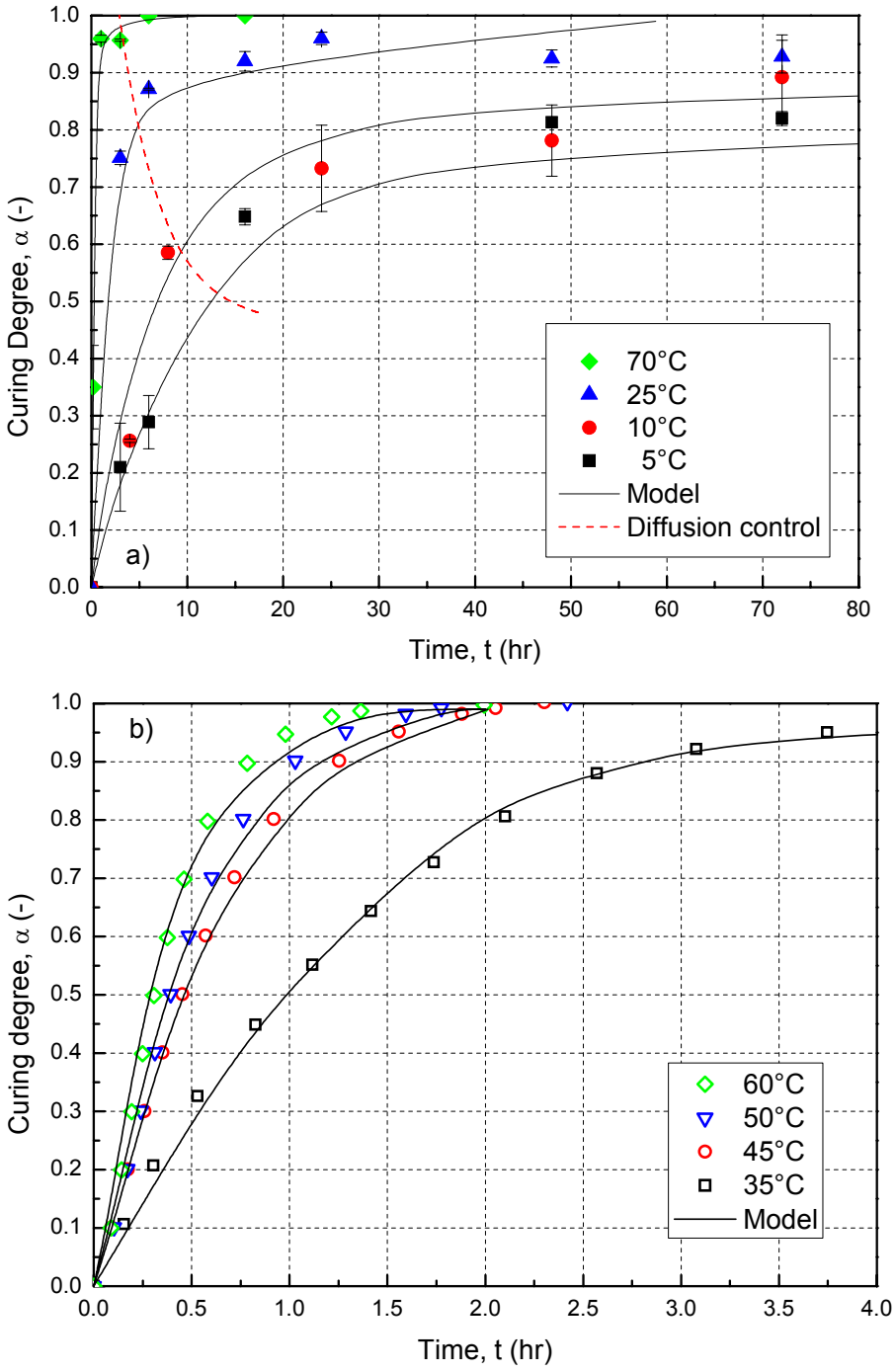

Figure 3.6 Curing degree vs. time a) using pre-conditioning method, b) from DSC isothermal scans (Sikadur-30)

3.3.2 Kinetic modeling

Overview

Up until now, research has been focused on the cure kinetics of hot-curing epoxies [5-11]. Determination of the kinetic parameters has been conducted either by means of a series of isothermal experiments [5-9] or dynamic scans [9-11]. These works focused on temperature ranges above 50°C [6-7, 9]. Dynamic and isothermal modeling developed for hot-curing adhesives are applied in the following to describe the experimental responses of the cold-curing adhesive.

Dynamic modeling

The basic modeling equation relates the curing rate, $d\alpha / dt$, at a specific temperature, to a function of the curing (or chemical conversion) degree, *α,* which depends on the concentration of the reactants, $f(\alpha)$:

$$\frac{d\alpha}{dt} = k\, f(\alpha) \tag{3.1}$$

where *k* is the rate constant. Basically, resins may exhibit two different behaviors, nth order or autocatalytic [8]. The main difference is that nth order resins exhibit a cure rate peak at the beginning of the reaction, while autocatalytic resins show a delayed peak, which occurs during the curing process.

Based on the responses shown in *Figure 3.5*, which exhibited a delayed peak at 20-30% of the total reaction time, an autocatalytic behavior was assumed, as follows:

$$f(\alpha) = \alpha^m (1-\alpha)^n \tag{3.2}$$

where n and *m* are the reaction orders (with $m+n$ being the overall reaction order). Furthermore, the rate constant is temperature-dependant, following the Arrhenius law:

$$k = A\, e^{-E_a / RT} \tag{3.3}$$

where A is the pre-exponential factor, E_a is the activation energy (J/mol), *R*=8.314 J/mol·K is the universal gas constant, and T is the temperature (K). Integrating Eq. (3.3) into Eq. (3.1) results in the rate equation:

$$\frac{d\alpha}{dt} = A\, e^{-E_a / RT}\, f(\alpha) \tag{3.4}$$

The kinetic parameters *n, m, A* and E_a were determined by fitting the experimental results to the autocatalytic model, as demonstrated in [10] for commercial epoxy prepregs. A method based on the Kissinger and Ozawa methods [12-13] was used. Eq. (3.4) was rearranged by multiplying the left hand side by *dT/dt* and taking the natural logarithm of both sides as follows:

$$\ln\left(\frac{dT}{dt}\right) = \ln(A) - \ln\left(\frac{d\alpha}{dT}\right) + \ln(f(\alpha)) - \frac{E_a}{RT} \tag{3.5}$$

where dT / dt is the heating rate. At peak temperature, T_p, the derivative of the curing rate with respect to temperature equals zero, which means that the derivative of the curing degree with respect to temperature is a constant value regardless of the heating rate. Furthermore, since at peak temperature the change in *ln f(α)* with respect to the heating rate is negligible compared to that in *ln A* [10], the general linear form of the previous equation can be written as:

$$\ln\left(\frac{dT}{dt}\right) = K + \left(\frac{-E_a}{R}\right)\frac{1}{T_p} \tag{3.6}$$

where *K* is the intercept of Eq. (3.6). An average activation energy of E_a = 56.3 kJ/mol was calculated from the slope of the plot *ln(dT/dt)* vs. *1000/T_p*, see *Table 3.3*.

Furthermore, the change in activation energy during the whole curing process was obtained from iso-conversional plots *ln(dT/dt)* vs. *1000/T* at different curing degrees, as shown in *Figure 3.7*. It decreased from 65 kJ/mol at the beginning of the curing process to 57 kJ/mol and then slightly increased due to the energy required to increase the mobility of both the reactants and products during the late stages of the curing process. Similar behavior was found for other materials [10-11], particularly in the late stages of curing.

Table 3.3 Kinetic parameters obtained from autocatalytic dynamic model

Model	Parameter	*dT/dt* (°C/min)					
		2.5	5	10	15	20	R^2
Kissinger and Ozawa	E_a (kJ/mol)	←		56.3		→	0.99
	A (min^{-1})	←		44431700		→	
	m	0.52	0.28	0.04	0.27	0.12	0.97
	n	1.99	1.81	1.16	1.47	1.49	
Modified Kissinger and Ozawa	C_f	0.899	1.124	0.897	0.909	0.982	0.97
	A_f (min^{-1})	77732893	58040782	27754751	40959771	31786834	

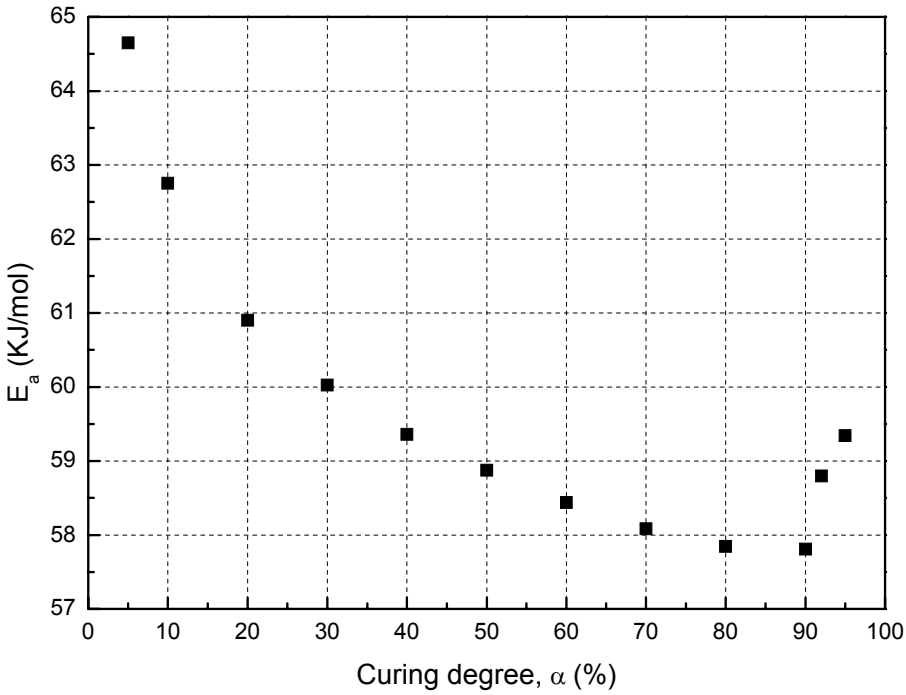

Figure 3.7 Activation energy from isoconversional plots vs. curing degree (Sikadur-30)

An average pre-exponential factor *A* was obtained from the intercept of Eq. (3.6), see *Table 3.3*. Based on this value and Sun et al. [10], heating rate-specific values, A_f, were obtained as follows:

$$A_f = C_f \cdot A_{av} = C_f \frac{e^K \left(da/dt\right)_p}{\alpha_p^m (1-\alpha_p)^n} \tag{3.7}$$

where C_f is the heating rate-dependent correction factor of A_{av}, and $(d\alpha/dt)_p$ and α_p are the curing rate and curing degree at peak respectively, as given in *Table 3.1*. Integerating Eqs. (3.7) and (3.2) in the basic curing rate Eq. (3.4), the curing rate for an autocatalytic model yields to:

$$\frac{d\alpha}{dt} = C_f \cdot e^K \left(\frac{d\alpha}{dT}\right)_p e^{-(E_a/RT)} \frac{\alpha^m (1-\alpha)^n}{\alpha_p^m (1-\alpha_p)^n} \tag{3.8}$$

The correction factors C_f as well as the reaction orders, *m* and *n*, were determined from Eq. (3.8) using the multiple non-linear least square regression method based on the Levenberg-Marquardt algorithm; the results are shown in *Table 3.3*.

Once the kinetic parameters *A*, E_a, *m* and *n* had been estimated, the curing degree was calculated as a function of the temperature by solving Eq. (3.9) numerically using the fourth-order Runge-Kutta method.

$$\frac{d\alpha}{dT} = \frac{A_f}{dT/dt} e^{-(E_a/RT)} \alpha^m (1-\alpha)^n \tag{3.9}$$

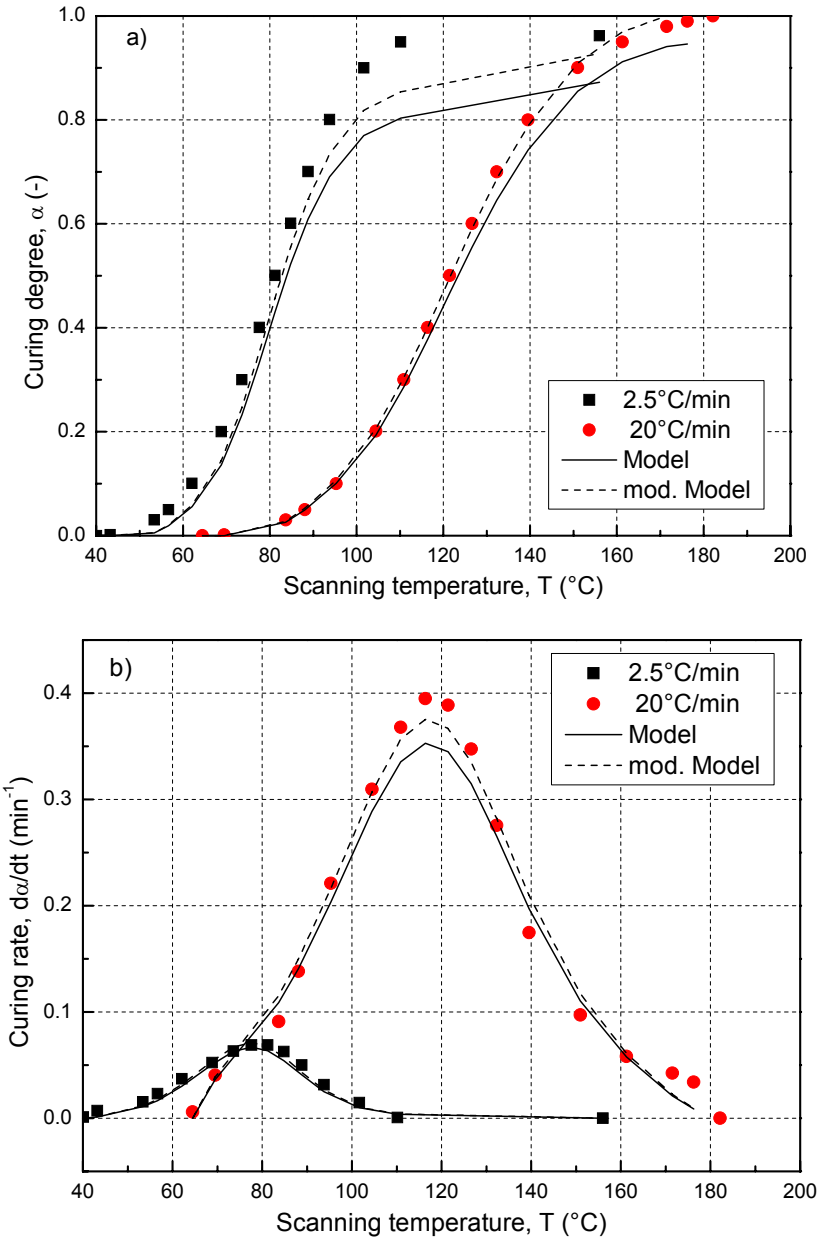

Figure 3.8 a) Curing degree and b) curing rate vs. temperature: comparison of experimental and autocatalytic model results (with and without modified pre-exponential factor) (Sikadur-30)

The results for the heating rates of 2.5 and 20°C/min with and without modification of the pre-exponential factor are shown in *Figure 3.8a*. The modeling curves compare well to the experimental results, particularly with modification of the pre-exponential factor. The late stages of curing at 2.5°C/min were only slightly underestimated, most probably due to disregarding the term *ln f(α)* in Eq. (3.5). At 2.5°C/min, the term *ln (f(α))* was found to be approximately 26% of the term *ln A* at 90% of cure, which is not really negligible. Similarly, *Figure 3.8b* shows the curing rate vs. temperature for the same heating rates. Again, the autocatalytic model with modification of the pre-exponential factor provides good and more accurate results than the model without modification.

Isothermal modeling

A more general model than Eq. (3.1) was used for the isothermal modeling, which takes non-zero values of the initial curing rate into account:

$$\frac{d\alpha}{dt} = (k_1 + k_2\alpha^m)(1-\alpha)^n \tag{3.10}$$

where k_1 and k_2 are curing rate constants with k_1 being the value at the beginning of the reaction at t = 0.

In a first step, Eq. (3.10) was fitted to the experimental data of curing rate vs. curing degree at each of the isothermal temperatures to obtain the rate constants and reaction orders (k_1, k_2, n and m). Results at 70° (clearly above T_g), were not taken into account. A non-linear least-square regression analysis was used as proposed in [6]. The value of the overall reaction order ($m+n$) decreased with increasing temperature, see Table 4, which is in contrast to works which assume this value as being constant ($m+n$ = 2 in [14]). Subsequently, by plotting the logarithms of the rate constants, *ln* k_1 and *ln* k_2, versus *1000/T*, the activation energies, E_{a1}, E_{a2}, and logarithms of the pre-exponential factors, *ln* A_1 and *ln* A_2, were obtained from the slopes and the intercepts respectively, see *Table 3.4*.

Table 3.4 Kinetic parameters obtained from autocatalytic isothermal model

T (°C)	k_1 (min^{-1})	k_2 (min^{-1})	n	m	m+n	R^2	E_{a1} (kJ/mol)	A_1 (min^{-1})	R^2	E_{a2} (kJ/mol)	A_2 (min^{-1})	R^2
60	0.0192	0.0578	1.291	0.553	1.843	0.97						
50	0.0160	0.0435	1.348	0.595	1.943	0.99						
45	0.0143	0.0378	1.408	0.650	2.058	0.99						
35	0.00948	0.0278	1.758	1.168	2.926	0.98	36.6	13226.8	0.97	19.2	54.6	0.97
25	0.0065	0.0251	2.010	1.738	3.748	0.99						
10	0.0025	0.0186	2.950	2.610	5.560	0.98						
5	0.00137	0.0124	3.130	2.720	5.850	0.97						

Approaching the glassy state, the cure reaction became diffusion-controlled, i.e. the movement of the reactants was slowed down and also hindered by the already formed chains. To take this effect into account, an extension of Eq. (3.10) by a diffusion control factor was proposed by Chern et al. [7] and applied as follows:

$$\frac{d\alpha}{dt} = (k_1 + k_2\alpha^m)(1-\alpha)^n \frac{1}{1+e^{C(\alpha-\alpha_c)}} \tag{3.11}$$

where C is an empirical constant and α_c is the critical curing degree at which diffusion control initiates. To obtain these two parameters (which are curing temperature-dependent), the experimental results were non-linearly re-fitted with the already known kinetic parameters (from fitting according to Eq. (3.10)). The resulting values, presented in *Table 3.5*, show that the critical curing degree decreases when the curing temperature

is decreased. At high temperatures (> 50°C), diffusion control is no longer relevant ($\alpha_c \rightarrow$ 1.0).

Table 3.5 Diffusion control parameters obtained from autocatalytic isothermal model

T (°C)	α_c	C	R^2
45	0.98	191.78	0.98
35	0.91	137.91	0.93
25	0.84	72.30	0.95
10	0.58	25.25	0.94
5	0.52	11.93	0.95

A comparison between the experimental and the predicted curing degree according to Eq. (3.11) vs. time shows good agreement, as demonstrated in *Figures 3.6a* and *b*. The values at 5°C curing temperature are only slightly underestimated. The onsets of diffusion control (the critical curing degrees according to *Table 3.5*) are also shown.

The maximum curing rate occurred at a curing degree of approximately 20%, as shown in *Figure 3.9*, in accordance with the DSC results shown in *Figure 3.5* and therefore confirming the assumption of autocatalytic behavior. At lower curing temperatures (<35°C) the curves exhibited a negative (decreasing) slope in the early curing stages when m became >1 (see *Table 3.4* and [13]).

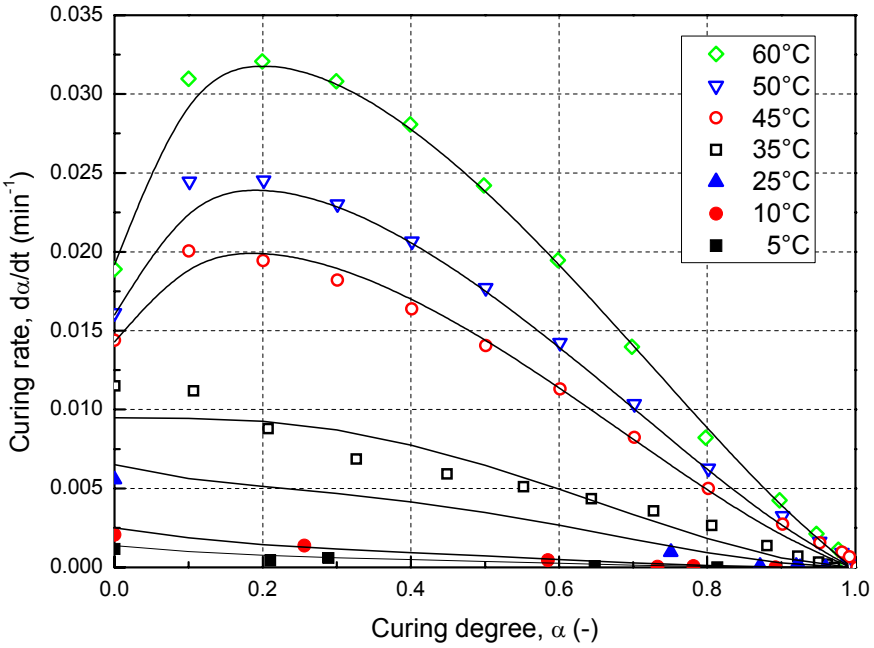

Figure 3.9 Curing rate vs. curing degree: comparison of experimental and autocatalytic model results for different isothermal temperatures (Sikadur-30)

3.4 Glass transition temperature

3.4.1 Effect of low-temperature curing

The development of the glass transition temperature, T_g, during curing and the relationship to the curing degree was extensively investigated for hot-curing adhesives [3, 15-18] and corresponding models were developed [3] whose applicability for cold-curing adhesives will be examined in the following.

The observed development of T_g vs. time, up to around 3 days, is shown in *Figure 3.10*. At 70°C curing temperature, a plateau was reached (at approx. 56°C) after a few hours, which was however clearly below the 62°C value given in the manufacturer's datasheet.

T_g development at lower temperatures was much slower: at 5°C, for example, around 50% of the maximum value was reached after only 3 days. The development decelerated when diffusion control and corresponding vitrification started, i.e. when T_g equaled T_{cure}. Similarly to *Figure 3.6a*, the corresponding onset of diffusion control (or vitrification) is shown in *Figure 3.10* (expressed as $T_g = T_{cure}$ in this case).

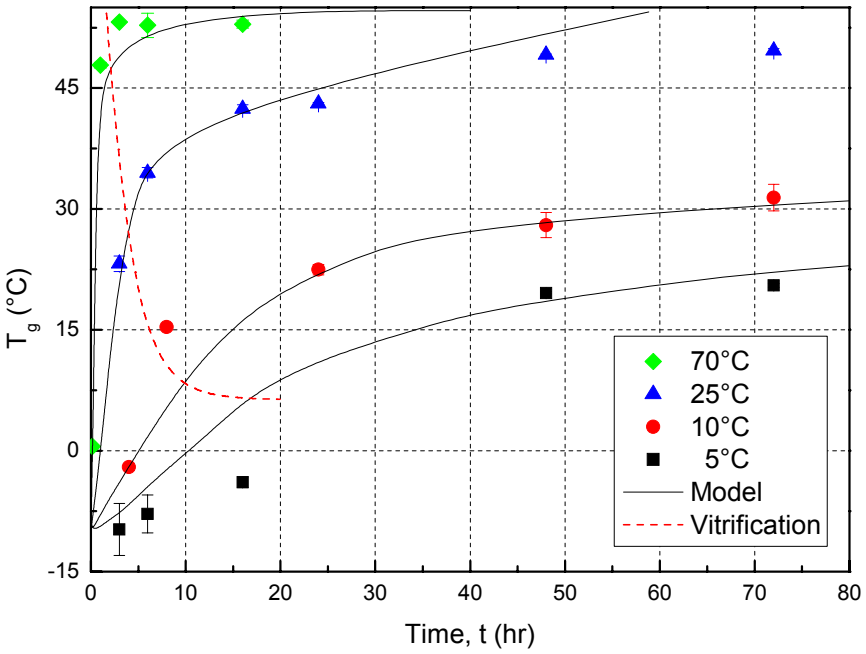

Figure 3.10 Glass transition temperature vs. time for samples partially cured at different temperatures (Sikadur-30)

3.4.2 T_g – α relationship

A model to describe the T_g vs. α relationship (independent of the curing temperature in this case) was proposed by DiBenedetto [19] as follows:

$$\frac{T_g - T_{go}}{T_{go}} = \frac{(\varepsilon_\infty / \varepsilon_o - c_\infty / c_o)x}{1-(1-c_\infty / c_o)x} \tag{3.12}$$

where x being the crosslink density (defined as the fraction of all segments that are crosslinked), ε the lattice energy, *c* the segmental mobility, and subscripts $"0"$ and $"\infty"$ refer to the uncured and fully cured resin, respectively. A modified version of the DiBenedetto equation by Pascault and Williams, replaces x by the curing degree, α, as follows [15]:

$$\frac{T_g - T_{go}}{T_{g\infty} - T_{go}} = \frac{\lambda\alpha}{1-(1-\lambda)\alpha} \tag{3.13}$$

with λ is an adjustable structure-dependent parameter, equal to $\Delta C_{p\infty} / \Delta C_{po}$, where $\Delta C_{p\infty}$ and ΔC_{po} are the differences in heat capacity between the glassy and rubbery/liquid states at full conversion and zero conversion respectively [17].

A further model, based on thermodynamics and proposed by Couchman [20], was adopted by Venditti and Gillham [17] and assumes that the system, at a curing degree α, is a mixture of unreacted end segments with concentration $(1-\alpha)$ and $T_g = T_{go}$, and reacted end segments with concentration α and $T_g = T_{g\infty}$:

$$\ln(T_g) = \frac{(1-\alpha)\ln(T_{go}) + \lambda\alpha\ln(T_{g\infty})}{(1-\alpha)+\lambda\alpha} \tag{3.14}$$

Fitting Eqs. (3.13) and (3.14) to the experimental data resulted in the λ-values listed in *Table 3.6*, which also shows the experimental value calculated as defined previously. There is good agreement between the three values, which also lie within the range obtained for hot-curing epoxy systems (0.16 – 0.69) [17]. The corresponding curves are shown in *Figure 3.11* and show good agreement with the experimental results. However, the experimental data exhibited a significant dependency on the curing temperature (lowest T_g values at 5°C), which could not be captured by the models. This is due to the early vitrification of the material followed by deceleration of the reaction, which becomes controlled by diffusion. In addition, the activation energy is not sufficient to cause secondary amines and sterical hindered amines to react.

Table 3.6 Fitted and experimental λ values

Method	**λ**	**R^2**
Pascault and Williams	0.32	0.96
Venditti Gillham	0.36	0.95
DSC	0.33 ± 0.15	-------

To take the curing time dependency into account, Eq. (3.13) was fitted to the results of each curing temperature separately. The resulting changes in λ with curing temperature are shown in *Figure 3.12*. Taking this result into consideration, the development of T_g over time, shown in *Figure 3.10*, was modeled and good agreement to the experimental results was obtained. Since the isothermal scan and the alternative method are very time-consuming and in view of the importance of the T_g – α relationship, a faster and more easily practicable experimental method was developed, which is presented in the next section.

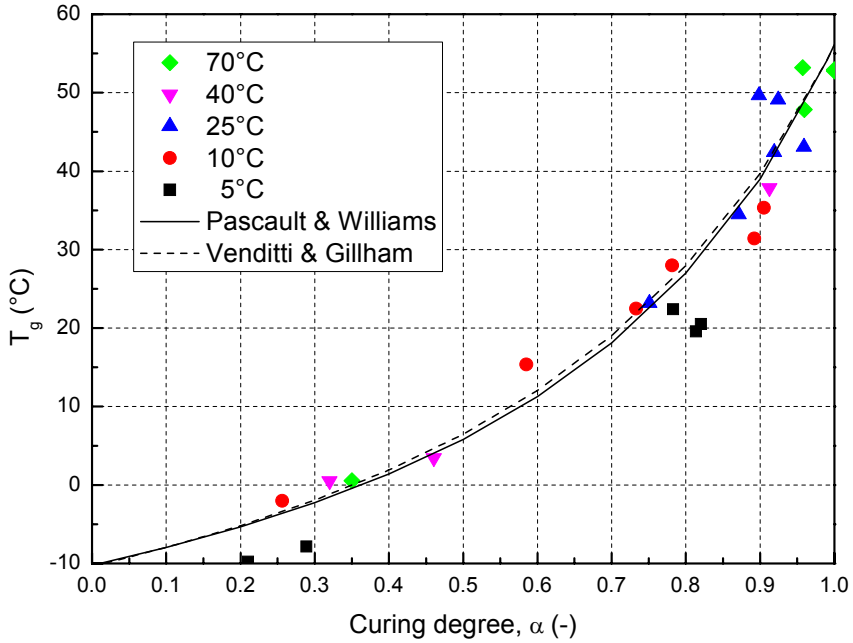

Figure 3.11 Glass transition temperature vs. curing degree for partially cured specimens at different temperatures (Sikadur-30)

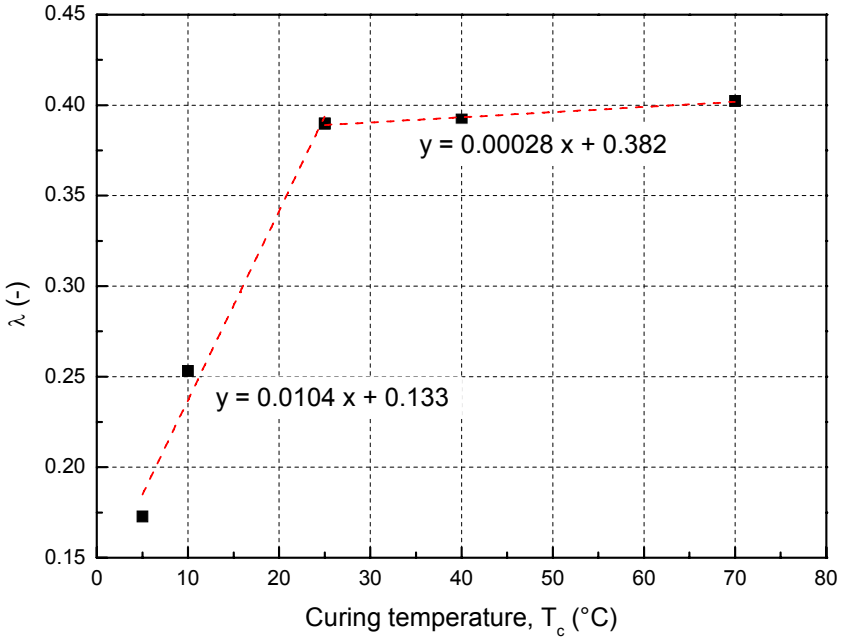

Figure 3.12 Modeling parameter λ vs. curing temperature (Sikadur-30)

3.5 New DSC-based method for establishing $T_g - \alpha$ relationship

3.5.1 Motivation

A basic parameter used to describe curing propagation and link it to mechanical properties is the glass transition temperature, T_g [2]. As curing advances, the molecular network mobility decreases and the T_g increases. This process is dependent on curing temperature and curing time, as previously explained. The corresponding relationship between the T_g and curing degree, α, can be described by the isothermal time-temperature transformation (TTT) [21-22]. The relationship is normally independent of curing temperature, unless the latter is very low - between 0°C and 10°C, where early vitrification of the material takes place as discussed in Section 3.4.2 and [23].

Despite the existence of different experimental techniques that can be used to measure the T_g of polymers [24], only a few – e.g. differential scanning calorimetry (DSC) and infrared spectroscopy – can be used to investigate the $T_g - \alpha$ relationship at early stages of cure where the material is still in the liquid/rubbery state, i.e. freshly mixed and partially cured material. When the DSC technique is applied, the isothermal curing (reaction) is interrupted at different times, usually by quenching the samples in liquid nitrogen, and then applying a dynamic scan to obtain the T_g and residual cure. Isothermal curing, however, is time-consuming, particularly at low temperatures. In the latter case, the accuracy of the method also decreases when the reaction becomes diffusion-controlled and therefore limits its applicability [23]. Analytically, the $T_g - \alpha$ relationship can also be determined using different models based either on fitting an equation to experimental results, e.g. in [22, 25], or on physical assumptions and thermodynamic considerations, e.g. in [15, 17]. Despite the good predictions obtained by these models for some resin systems, their applicability, particularly for highly cross-linked systems, is limited. Therefore, these models cannot be generalized for use with all types of thermosetting resins [16].

In view of the fact that joints must be fabricated during the construction process, a measuring method is required that is able to efficiently and accurately establish the $T_g - \alpha$ relationship. In this section, a new experimental method is presented that is based on DSC but establishes the $T_g - \alpha$ relationship more efficiently than the existing isothermal method described above. Although the method was developed based on a cold-curing

epoxy adhesive, its applicability to other cold-curing epoxy, polyurethane and polyester adhesives is also demonstrated.

3.5.2 New experimental method

The new method is based on dynamic DSC scans and on the fact that the T_g development is slow at early stages of cure and accelerated at later stages, particularly for highly cross-linked systems [18]. A six-step procedure is applied as follows:

- Step 1: A first uncured sample is scanned dynamically at a constant heating rate of 5 °C/min within a temperature range of -50 to 250°C. This range was found to be sufficient to obtain a full exotherm for cold-curing adhesives. The total heat released during the scan is determined by integrating the area under the exotherm, as shown in *Figure 3.13*, according to the ASTM E2041 standard.

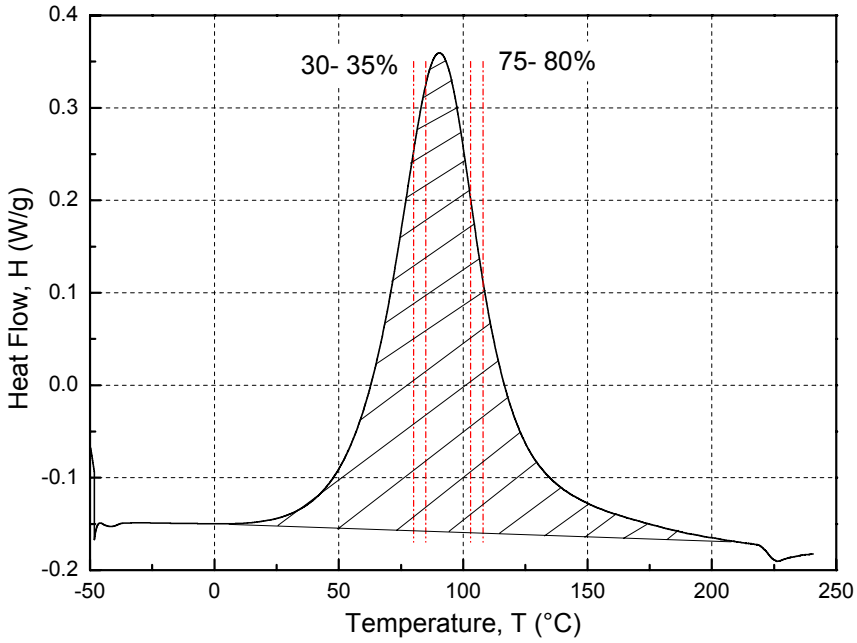

Figure 3.13 Exotherm from dynamic scan of uncured sample and ranges for selection of two-step temperatures (Sikadur-330)

- Step 2: Based on the shape of the exothermic peak, two so-called step temperatures are selected, at which the $T_g - \alpha$ relationship is subsequently established. The recommended ranges for these selections are 30 to 35% and 75 to 80% of cure for the first and second step temperature respectively.
- Step 3: For each of the chosen step temperatures, three successive dynamic scans are carried out on a second and third uncured sample at the same heating rate as that used in Step 1. The first scan is stopped at the step temperature while the second and third scans are stopped at 250°C, as shown in *Figure. 3.14*. After each of the three scans, the sample is quenched in liquid nitrogen to stop the reaction.
- Step 4: From the three consecutive scans, Tg0, Tg, and Tg∞ are determined for each step temperature according to ASTM E 2602, as shown in Figure 3.15. These temperatures correspond to the glass transition temperatures of the uncured, partially cured (at the two step temperatures) and fully cured material.
- Step 5: The curing degree, corresponding to the Tg of the partially cured material, can be calculated for each step temperature by dividing the residual heat of cure, resulting from the 2nd scan (shown in Figure 3.14), by the total heat of cure determined in Step 1 and then subtracting the resulting value from 100%.
- Step 6: Based on the two step temperatures, a trilinear Tg – α relationship is established.

The trilinear curve approaches the continuous curve obtained from the existing isothermal DSC method. The accuracy of the new method is demonstrated and discussed in the

following by comparing the results for various cold-curing adhesives obtained using both methods.

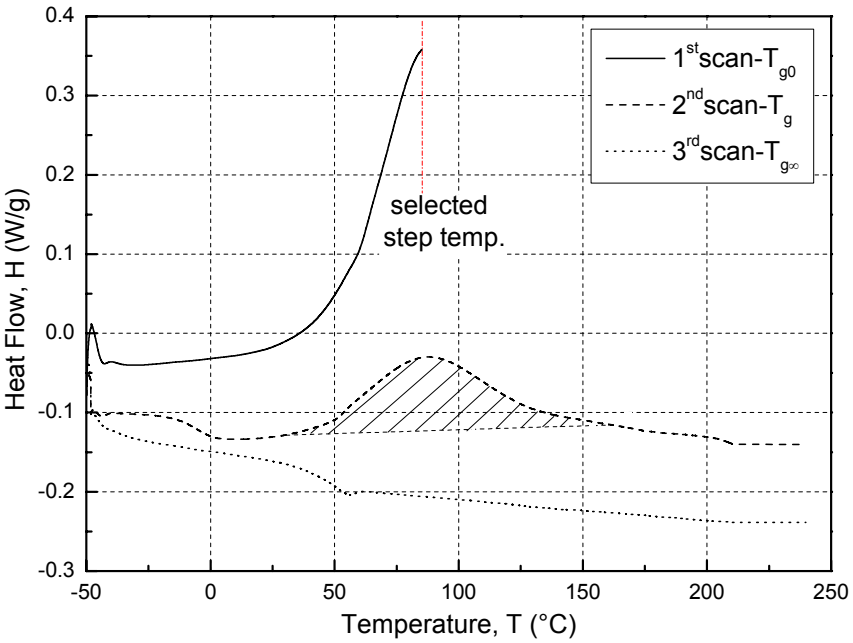

Figure 3.14 Three consecutive dynamic scans for each step temperature to obtain T_{g0}, T_g and $T_{g\infty}$ (Sikadur-330)

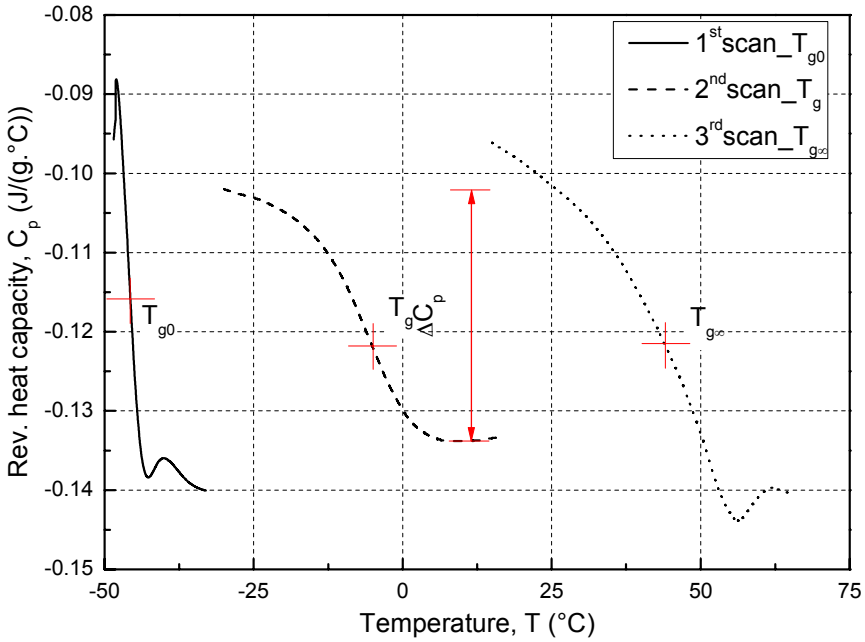

Figure 3.15 Determination of glass transition temperatures T_{g0}, T_g and $T_{g\infty}$ from three successive scans (Sikadur-330)

3.5.3 Experimental set-up

The same DSC machine as that described in Section 3.2 and shown in *Figures 3.3 a* and *b* was used, except that it was calibrated in order to be used for modulated experiments. Modulation was carried out at an amplitude of ±0.5°C every 60 seconds and nitrogen was used as purge gas.

In modulated differential scanning calorimetry, the total heat flow signal is separated into reversing and non-reversing components. The heat capacity change that indicates glass transition can be detected from the reversing heat flow signal, while processes such as curing and enthalpy can be detected from the non-reversing heat flow signal. This allows a reliable detection of T_g, particularly at low curing degrees.

Adhesive samples of between 5 and 10 mg were placed in a steel pan covered with a lid and sealed using a manual press (see *Figure 3.3 c*). An empty steel pan was used as a reference during every scan (as explained in Section 3.2). Data acquisition was performed using the accompanying software (TA Analysis).

3.5.4 Experimental procedure

The $T_g - \alpha$ results obtained using the conventional method (see Section 3.4.2) were used to develop the new experimental method. The new method was then applied as follows: Firstly, the effect of different heating rates was investigated. Uncured samples were scanned between -50 and 250°C at different heating rates (1, 2.5, 5, 10 and 15°C/min), thus providing a complete exotherm for each (Step 1). Two-step temperatures were selected for each heating rate within the previously proposed ranges, which vary according to the heating rate (Step 2). Two uncured samples, one for each selected step temperature, were then scanned (in three successive runs) from -50°C up to the step temperature and then 250°C (Step 3). The trilinear curve $T_g - \alpha$ relationship was then established (Steps 3-6) and compared to the results of the conventional method.

The same procedure was then applied to the other five adhesives, at one single heating rate of 5°C/min only, which was selected based on the above-mentioned study. The trilinear curves were established and compared to corresponding results obtained using the existing isothermal method. For each adhesive, a minimum of three samples were cured isothermally at different temperatures for different time periods.

3.5.5 Experimental results and discussion

The $T_g - \alpha$ relationship of Sikadur-30 at different curing temperatures, resulting from the existing method, is shown in *Figure 3.11*. The T_g development was slow at early stages of cure when the molecular chains formed, with the adhesive developing less than 25% of the T_g up to 50% of cure. At later stages of cure, when chain networks were branched [26], the T_g development accelerated, with 50% taking place between 75 to 100% cure. These ranges may vary for different adhesive systems according to the base resins and reacting groups. However, similar curves were found for hot-curing epoxy adhesives [3, 15, 18 and 26]. The exponential curve also confirms the adequacy of the two ranges of step temperature selection (at 30-35% and 75-80% of cure) to approach the trend by a trilinear curve.

The $T_g - \alpha$ relationship derived for Sikadur-30 using the new method at different heating rates (1, 2.5 and 5°C/min) is shown in *Figure 3.16*. The heating rate did not significantly influence the results up to 5°C/min. At higher rates (10 and 15°C/min), the reaction was fast and difficult to stop within the designated temperature ranges. Furthermore, during opening of the DSC cell and quenching the sample in liquid nitrogen, significant curing continued to take place, which increased the designated curing degree at the two-step temperatures. This difference between designated and effective curing degree was much smaller at lower heating rates, as shown in *Table 3.7*. At very low heating rates, on the other hand, the scan was time-consuming. The time required to scan one sample at 1°C/min was almost 4 times that required for scanning at 5°C/min, see *Table 3.7*. Taking all these results into account, a heating rate of 5°C/min was shown to be the best compromise for the new method. The unintentional increase in curing degree at this rate was approximately 17% (from 30-35% to ~55% and 75-80% to ~90%, see *Figure 3.16*), which however did not affect the accuracy of the trilinear approach of the continuous curve of the existing method. The results obtained using the new and existing isothermal methods agree well, as demonstrated in *Figure 3.16*.

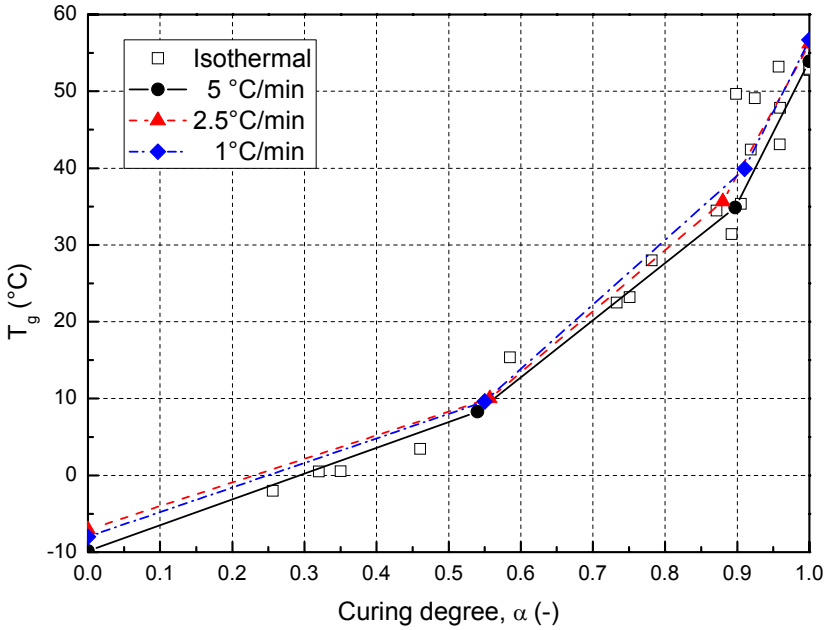

Figure 3.16 Trilinear T_g – α relationship obtained using new method at different heating rates and comparison to results obtained using existing isothermal method for Sikadur-30

The exotherms resulting from an uncured sample of each of the method-validation adhesives are shown in *Figure 3.17*. The values of the heat released during the scan and the exothermic peak temperatures, T_p, are listed in *Table 3.8*. The filler content greatly influenced the amount of heat released, as only 20% of the heat released by the unfilled Sikadur-30 was released by the filled Sikadur-30 (55% fillers by weight). Similarly, Adesilex PG1 (20-25% fillers by weight) released ca. 23% and Sikadur-330 (<20%) released ca. 44% heat compared to the unfilled Sikadur-30. The fillers obviously absorbed parts of the energy depending on the filler quantity in the resin. This is in agreement with the results presented in [27], where it was observed that the total heat of cure was decreased by increasing filler content. The peak temperature was less affected by the filler content, as shown in *Figure 3.17* and *Table 3.8*, which agrees with the results obtained in [28].

Table 3.7 Influence of heating rates on heat losses during one scan and time required for one step temperature

Heating rate (°C/min)	Difference* (%)	Average time per step (hr)
1	5.7	7.5
2.5	16.0	3.9
5	17.7	2.0
10 / 15	> 25	< 2

* *between designated and effective curing degree*

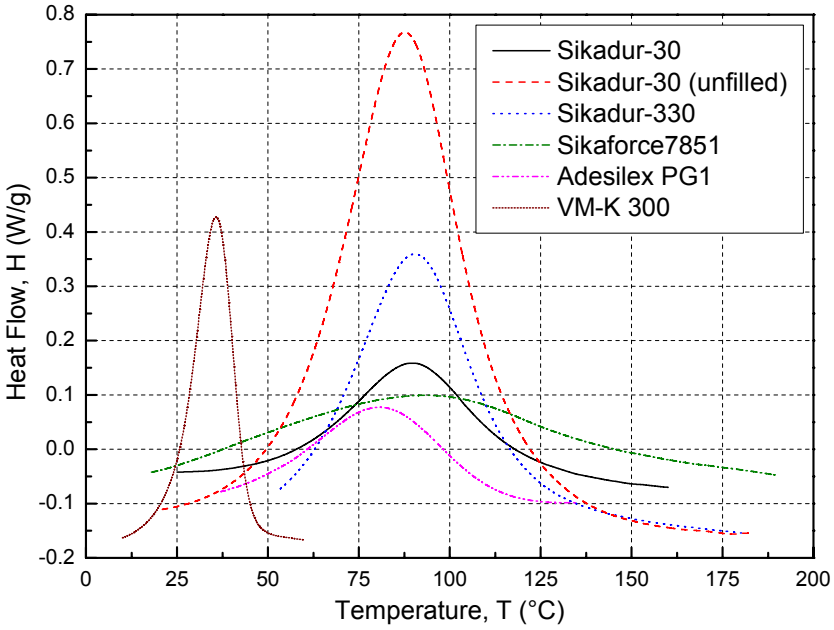

Figure 3.17 Dynamic scan for uncured samples of different adhesives

Table 3.8 Heat released and peak temperatures of exotherms from ynamic scans of uncured samples

Adhesive	Heat (J/g)	T_p (°C)
Sikadur-30	95.1	89.7
Sikadur-30 (unfilled)	471.6	87.7
Sikadur-330	205.8	90.5
Sikaforce-7851	166.8	94.5
Adesilex PG1	110.2	80.7
VM-K 300	97.2	35.7

Figures 3.18 and *3.19* compare the T_g – α relationships for the method-validation adhesives obtained using the new method and the existing isothermal method. A good agreement between the results was found. A further verification of the new method was carried out using the Pascault and Williams model [12]. The λ-factors were calculated by fitting the experimental results for all adhesives, see *Table 3.9* (λ_{mod} values) and directly from the experimental results, from $\lambda = \Delta C_{p\infty}/\Delta C_{p0}$ (see λ_{DSC} values in *Table 3.9*). The results compare well, with the exception of Sikadur-330. This difference may be explained however by the inapplicability of the model to this material. In the case of Sikaforce-7851, λ_{DSC} could not be derived because the T_g-sigmoid of the exotherm was not clearly detectable.

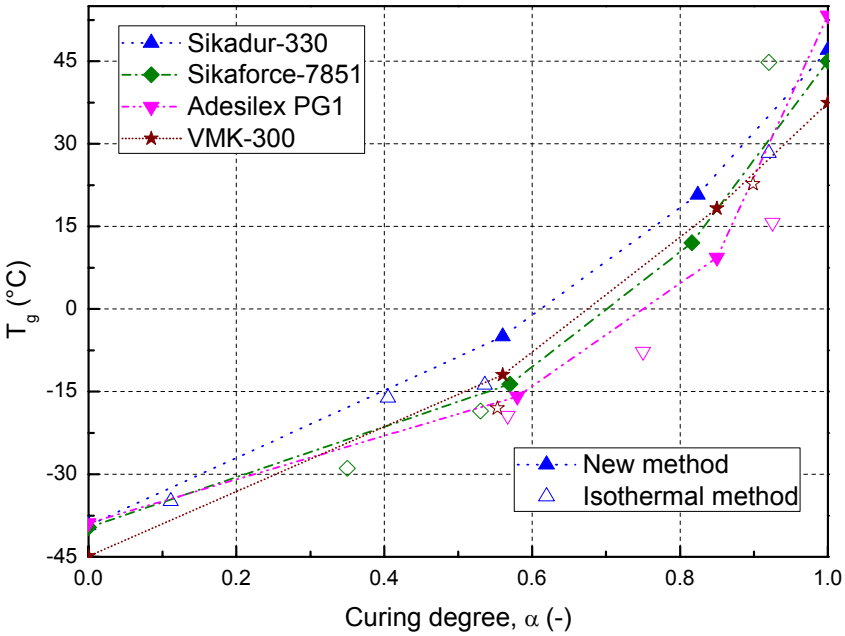

Figure 3.18 Trilinear T_g – α relationship obtained using new method and comparison to results obtained using existing isothermal method for different adhesive

Table 3.9 Predicted and measured λ-values for validation adhesives (new method)

Adhesive	**λ_{DSC}**	**λ_{mod}**	**R^2**
Sikadur-30	0.34	0.32	0.96
Siakdur-30 (unfilled)	0.51	0.45	0.96
Sikadur-330	0.73	0.55	0.96
Sikaforce-7851	-----	0.37	0.95
Adesilex PG1	0.25	0.27	0.97
VM-K 300	0.52	0.58	0.98

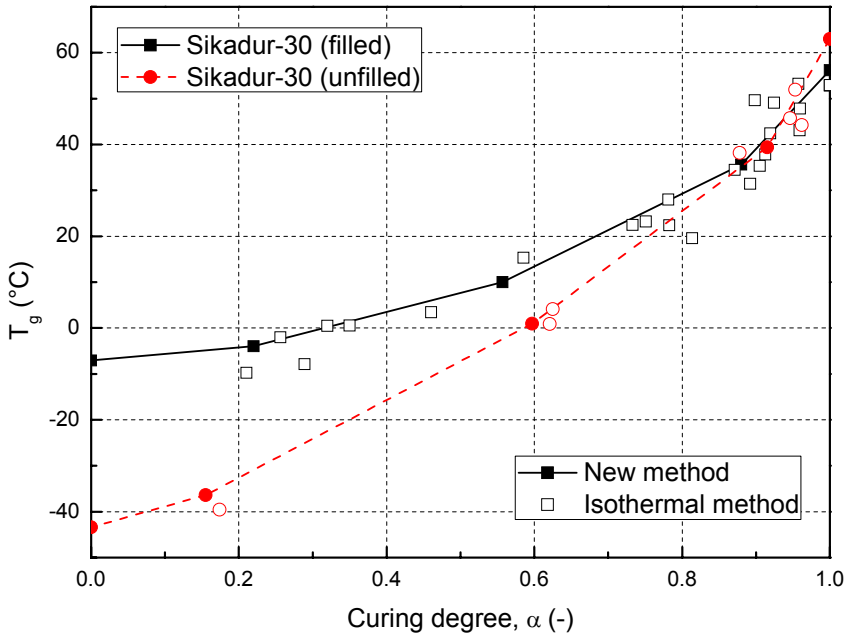

Figure 3.19 Effect of filler content on T_g – α relationship

Similarly to the released heat, high filler content also influenced the $T_g - \alpha$ relationship, as shown in *Figure 3.19*, particularly at lower curing degrees. Much higher values were obtained for the filled Sikadur-30 than for the same unfilled material. This can be explained by the prevention of polymer chain formation and reduction of chain flexibility. The comparatively low filler content of Adeslix-PG1 and Sikadur-330, however, did not influence the $T_g - \alpha$ relationship (see *Figure 3.18*). Also, depending on type and size, fillers with polar groups and fine grains can interact with the polymeric network (Van der Waal interactions, polar or ionic interactions), thus influencing the chain formation and flexibility during cure and, consequently, the T_g.

The results obtained with the new method for all the commercial adhesives used are summarized in *Figure 3.20*. With the exception of Sikadur-30 with high filler content, the curves deviate from each other only marginally, despite the fact that the base resins were very different (epoxy, polyurethane and polyester).

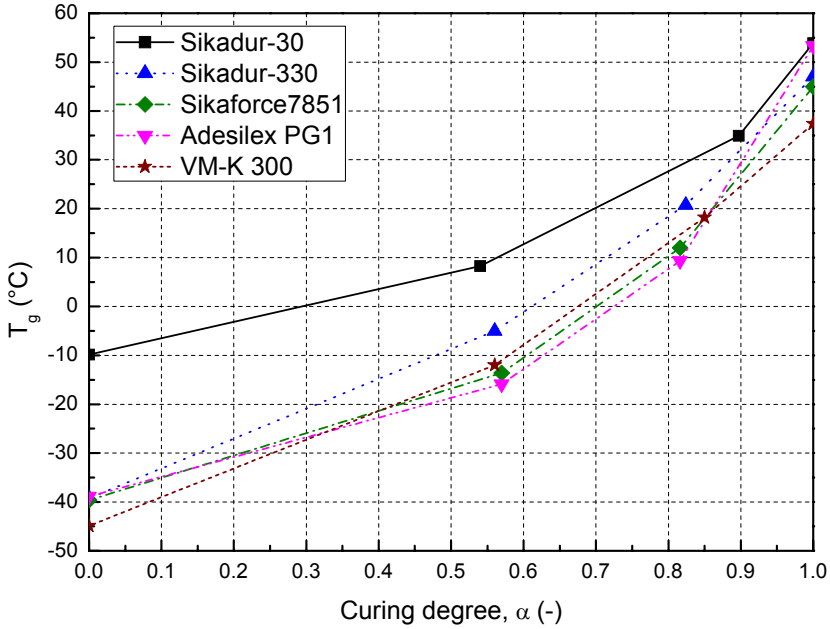

Figure 3.20 Trilinear $T_g - \alpha$ relationship obtained using new method for different adhesives

3.6 Conclusions

The effect of low-temperature curing on the physical characteristics of a commercial cold-curing epoxy adhesive was experimentally and analytically investigated with a view to a potential application in bridge construction during winter. The following conclusions were drawn:

1) Curing did take place at low temperatures of 5-10°C but the curing process significantly decelerated. Several days of curing were required before high curing degrees of >80% were reached. The glass transition temperature developed even more slowly due to initiation of vitrification when the low curing temperature was reached.
2) Existing dynamic and isothermal curing models developed for hot-curing adhesives proved applicable to simulate the curing behavior of the cold-curing adhesive even at low temperatures. However, a heating rate-dependent pre-exponential factor and diffusion control had to be taken into account. The cold-curing adhesive exhibited an autocatalytic behavior.
3) The relationship between the glass transition temperature and the curing degree could also be described by models developed for hot-curing adhesives. However, at low temperatures, the relationship was curing temperature-dependent, something which had to be taken into account in the modeling for accurate simulation.

4) A new DSC-based experimental method to efficiently establish the glass transition temperature vs. curing degree relationship for structural adhesives was developed. The method approaches the continuous $T_g - \alpha$ relationship by a trilinear curve, which is established from several dynamic scans instead of time-consuming isothermal scans. The trilinear curves determined by the new method approached well the $T_g - \alpha$ relationship resulting from the existing isothermal method.

In a next step, the development of the mechanical properties of cold-curing adhesives at low temperatures and their dependence on the physical state will be investigated.

3.7 References

E.A. Turi, "*Thermal characterization of polymeric materials*", 2nd Ed., Vol. 1, Academic press, 1997. [1]

B. Ellis, "*Chemistry and technology of epoxy resins*", Blackie academic professional, an imprint of Chapman & Hall, 1993. [2]

G. Wisanrakkit and J.K. Gillham, "*Glass transition temperature (T_g) as an index of chemical conversion for high-T_g amine/epoxy system: chemical and diffusion-controlled reaction kinetics*", J. Appl. Polym. Sci., 1990; 41(11-12): 2885–2929. [3]

F.Y.C. Boey and W. Qiang, "*Experimental modeling of the cure kinetics of an Epoxy–Hexahydro-4-methylphthalic Anhydride (MHHPA) System*", Polym., 2000; 41(6): 2081-2094. [4]

J.Y. Lee, H.K. Choi, M.J. Shim and S.W. Kim, *"Kinetic studies of an epoxy cure reaction by isothermal DSC analysis"*, Thermochim. Acta, 2000; 343(1-2): 111-117. [5]

L. Sun, S. Pang, A. Sterling. I. Negulescu and M. Stubblefield, *"Thermal analysis of curing process of Epoxy Prepreg"*, J. Appl. Polym. Sci., 2002; 83(5): 1074-1083. [6]

C.S. Chern and G.W. Phoehlein, *"A kinetic model for curing reactions of epoxides with amines"*, Polym. Eng. Sci., 1987; 27(11): 788-795. [7]

A. Yousefi, P.G. Lafleur and R. Gauvin, "*Kinetic studies of thermoset cure reactions: a review*", Polym. Composite., 1997;18(2): 157-168. [8]

A. Atarsia and R. Boukhili, "*Relationship between isothermal and dynamic cure of thermosets via the isoconversion representation*", Polym. Eng. Sci., 2000; 40(3): 607–620. [9]

L. Sun, S. Pang, A. Sterling. I. Negulescu and M. Stubblefield, *"Dynamic analysis of curing process of Epoxy Prepeg"*, J. Appl. Polym. Sci., 2002; 86(8): 1911-1923. [10]

M. R. Kessler and S. R. White, "*Cure kinetics of the ring opening metathesis polymerization of Dicyclopentadiene*", J. Polym. Sci., 2002; 40(14), 2373-2383. [11]

H.E. Kissinger, *"Reaction kinetics in differential thermal analysis"*, Anal. Chem. 1957; 29(11): 1702-1706. [12]

T. Ozawa, *"A new method of analyzing thermogravimetric data",* Bull. Chem. Soc. Jpn. 1965; 38(11): 1881-1886. [13]

M.E. Ryan and A. Dutta, "*Kinetics of epoxy cure: a rapid technique for kinetic parameter estimation*", Polym., 1979; 20(2): 203–206. [14]

J.P. Pascault and R.J.J. Williams, "*Relationships between glass transition temperature and conversion - analyses of limiting cases*", Polym. Bull., 1990; 24(1): 115-121. [15]

A. Hale, C.W. Macosko, and H.E. Bair, "*Glass transition temperatures as a function of conversion in thermosetting polymers*", Macromolecules, 1991; 24(9): 2610-2621. [16]

R.A. Venditti and J.K. Gillham, "*A relationship between the glass transition temperature and fractional conversion in thermosetting system*s", J. Appl. Polym. Sci., 1997; 64(1): 3–14. [17]

F.Y.C. Boey and W. Qiang, "*Glass-transition temperature/Conversion relationship for an Epoxy–Hexahydro-4-methylphthalic Anhydride System*", J. Appl. Polym. Sci., 2000; 78(3): 511–516. [18]

A. T. Dibenedetto, "*Prediction of the glass transition temperature of polymers: Amodel based on the principal of corresponding states*", J. Polym. Sci. Part:B Polym. Phys., 1987; 25(9): 1949–1969. [19]

P.R. Couchman and F.E. Karasz, "*A classical thermodynamic discussion of the effect of composition on glass-transition temperatures*", Macromolecules, 1978; 11(1): 117–119. [20]

J.K. Gillham, "*Formation and properties of thermosetting and high T_g polymeric materials*", Polym. Eng. Sci., 1986; 26(20):1429-1433. [21]

J.B. Enns and J.K. Gillham, "*Time-Temperature-Transformation (TTT) cure diagram: modeling the cure behavior of thermosets*", J. Appl. Polym. Sci., 1983; 28(8): 2567-2591. [22]

O. Moussa, A. Vassilopoulos and T. Keller, "*Effects of low temperature curing on physical properties of structural epoxy adhesive joints in bridge construction"*, Int. J. Adhes. Adhes., 2011; 32(1): 15-22. [23]

J. Rieger, "*The glass transition temperature T_g of polymers- comparison of the values from differential thermal analysis (DTA, DSC) and dynamic mechanical measurements (torsion pendulum)*", Polym. Test., 2001; 20(2): 199-204. [24]

C.C. Riccardi, H.E. Adabbo, and R.J.J. Williams, "*Curing reaction of epoxy resins with diamines*", J. Appl. Polym. Sci., 1984; 29(8): 2481-2492. [25]

G. W. Ehrenstein and S. Pongratz, "*Beständigkeit von Kunststoffen*", Carl Hanser Verlag, München 2007. [26]

H. Kubota, "*Curing of highly reactive polyester resin under pressure: kinetic studies by differential scanning calorimetry"*, J. Appl. Polym. Sci., 1975; 19 (8): 2279-2297. [27]

H. Ng and I. Manas-Zloczower, "*Kinetic studies of a composite thermoset cure reaction - application in pultrusion simulations"*, Polym. Eng. Sci., 1989; 29(16): 302-307. [28]

4 Development of mechanical properties

4.1. Overview

The early-stage mechanical properties strongly depend on the physical state of the adhesive [1]. Curing temperature and curing time govern processes that take place during curing such as gelation and vitrification [2]. As a basis for decisions concerning the duration of construction stages or periods prior to a structure being put into service, there is a need for models allowing prediction of the early-age physical and mechanical properties as a function of (particularly low) curing temperatures and time.

Several studies have been carried out to investigate the effects of curing temperature and curing time on both bulk adhesive materials and adhesively-bonded joints. In [3] the effects of curing time and curing temperature on the tensile strength, yield stress and elastic modulus of two different epoxy-based commercial adhesives were experimentally investigated. Different curing optimization curves were produced for different properties under different curing conditions. It was found that the ultimate strength and stiffness were higher under curing conditions comprising ″lower temperature – long time″ (e.g. 93.3°C/120mins) than ″higher temperature – short time″ (e.g. 143.3°C/20mins). This was attributed to the increase in the randomness of network cross-linking of the adhesive at higher curing temperatures as well as the increase in the magnitudes of the thermal residual stresses during cure. At high temperatures, lower values of tensile properties were obtained, which was attributed to the degradation of the material. The same result was obtained in [1], where mechanical properties were found to be lower at a higher extent of reaction achieved by high temperature-short time curing. In [4], the effect of curing conditions on the mechanical properties of a rubber-modified epoxy adhesive was investigated. The results revealed the pronounced influence of curing time and curing temperature on the mechanical properties of both bulk adhesive and adhesive joints. In [5], an experimental study was carried out to determine the effects of the incomplete curing of resin on the dynamic moduli and tensile strengths of two commercial amine-cured epoxy adhesives. The tensile bond strength for instance was found to be sensitive to the degree of under-cure (incomplete curing), leading to a strength reduction as great as 15 times the results obtained for fully-cured specimens. The degree of under-cure was also investigated in [6], and the change in the mechanical properties of a commercial epoxy adhesive due to incomplete curing was investigated leading to the same conclusion.

Despite the existence of studies that investigate the effects of curing temperature and curing time on the mechanical properties of both bulk adhesive materials and adhesively bonded joints, most of these works focus on hot-curing adhesives and curing temperatures are high compared to those that occur during the winter on a construction site. Furthermore, none of these previous works focused on the relationship between physical properties, such as curing degree or glass transition temperature, and the early-age mechanical properties, particularly under low curing temperatures.

The effects of low temperature curing on the early-age physical properties – curing degree and glass transition temperature – of a commercial structural epoxy adhesive have been presented in Chapter 3 and [7]. This chapter focuses on the early-age development of the mechanical properties – tensile stiffness and strength – of the same adhesive subjected to the same low-temperature curing procedures (isothermal, cyclic and outdoor curing). Additionally, the relationship between physical and mechanical properties is established and an empirical model, based on the autocatalytic curing behavior of the adhesive, is proposed to predict the mechanical properties as a function of the curing procedure.

4.2 Experimental investigation

4.2.1 Curing procedures

Three different curing procedures were applied as follows: A) isothermal curing at five different isothermal temperatures (T_{cure} = 5, 10, 25, 40 and 70°C) during different curing periods, t_{cure}, the latter are summarized in *Table 4.1*. The temperature range covered the minimum curing temperatures according to the adhesive manufacturer and the maximum temperatures that can occur during summer, e.g. below the asphalt layer of a bridge. The maximum curing time was 720 hours (30 days) since only the early age was of interest in this study. B) curing at cyclic temperatures between 5°C and 15°C and between 0°C and 10 °C (once starting at 0°C, and once at 10°C, see *Table 4.2*). The temperatures were kept constant during 12 hours and changes then occurred at a rate of approximately 1°C/min. This curing procedure simulated outdoor situations that can arise during winter time. C) complex outdoor curing in winter at varying temperatures from approximately -6°C to +6°C during 12 days between 27/01/2010 and 09/02/2010, as shown in *Figure 4.1*. The physical experiments and corresponding results of procedure A were presented and discussed in Chapter 3 and will be repeated here for comparison with the results of procedures B and C.

Table 4.1 Overview of isothermal curing procedure and associated physical (p) and mechanical (m) investigations

T_{cure} (°C) / t_{cure} (hr)	5	10	25	40	70
0.17					p
0.33				p	
0.5				p	m
1					p+m
3	p		p		p+m
4		p		p	
6	p		p		p+m
8		p			
16	p		p+m		p+m
24		p+m	p+m		
48	p+m	p+m	p+m		
72	p+m	p+m	p+m		
168	p+m	p+m			
240	p+m	m	m		
720		m			

Table 4.2 Overview of cyclic curing procedure and associated physical (p) and mechanical (m) investigations

T_{cure} (°C) / t_{cure} (hr)	0-10	10-0	5-15
24	p		p+m
48	p+m	m	p+m
72	p+m	m	p+m
96			m
120	m	m	
168	m		m

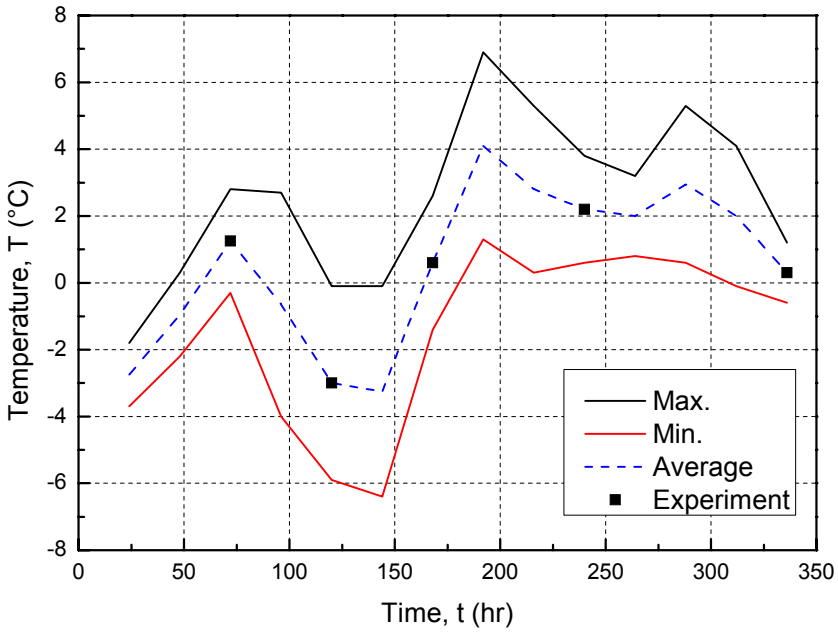

Figure 4.1 Outdoor curing procedure during winter and associated mechanical investigations (Sikadur-30)

4.2.2 Investigation of physical properties

DSC experiments were performed for curing procedure B according to the alternative method discussed in Section 3.2.1 for curing procedure A. Pre-conditioning of samples took place in the climate chamber (accuracy of ±1°C) according to cyclic temperatures and during the time periods listed in *Tables 4.2*. Three samples were investigated for each combination of T_{cure} and t_{cure}.

4.2.3 Investigation of mechanical properties

Tensile specimens were fabricated in an aluminum mold according to ASTM D638-08 with the dimensions shown in *Figure 4.2a*. The mold was placed in a climate chamber where specimens were cured according to the curing procedures A) and B) and time periods listed in *Tables 4.1* and *4.2*. Again, the relative humidity was kept constant at 50%±2% (above 5°C) in order to eliminate any effects of humidity on the results. Another set of specimens was subjected to curing procedure C) according to *Figure 4.1*.

Quasi-static tensile experiments were performed according to ASTM D638-08 using an MTS Landmark 25-kN servo-hydraulic load unit calibrated to 20% of its load capacity. Specimens were loaded under displacement control at a loading rate of 5mm/min. For determination of the Young's modulus, *E*, longitudinal strains were measured using an MTS clip-on extensometer, as shown in *Figure 4.2b*. The extensometer had a gage length of 25±0.05 mm and a minimum accuracy of ±0.5% of the measured strain. A data acquisition system was used to record the time, machine displacement, strain and corresponding load. Five specimens were investigated for each curing combination of T_{cure} and t_{cure}. Specimens with voids or other defects in the failure section were not taken into account in the analysis. However, a minimum of three specimens per curing combination was considered in each case.

The whole experimental program was performed according to a standard operational procedure, which had been previously established to ensure the quality and consistency of the results.

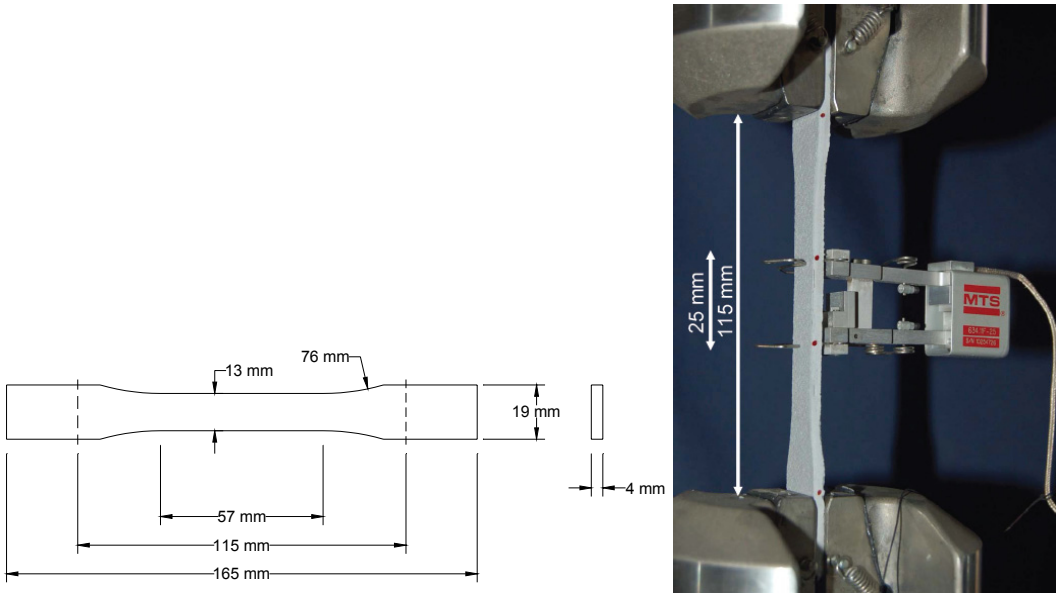

Figure 4.2 a) Specimen dimensions according to ASTM-D638; b) Experimental set-up

4.3 Experimental results and discussion

4.3.1 Physical properties

The development of α and T_g at different isothermal temperatures (5, 10, 25 and 70°C) and cyclic temperatures (0-10°C and 5-15°C) are shown in *Figures 4.3* and *4.4* respectively. The development of both during the cyclic profiles (curing procedure B in Section 4.2.1) showed a similar behavior to that of the isothermal temperatures (see Chapter 3 – Sections 3.3 and 3.4) where the curing process was decelerated due to material vitrification. Moreover, the T_g development at cyclic temperatures (0-10°C and 5-15°C) approached that of the corresponding average isothermal temperatures (5 and 10°C respectively), as shown in *Figure 4.4*.

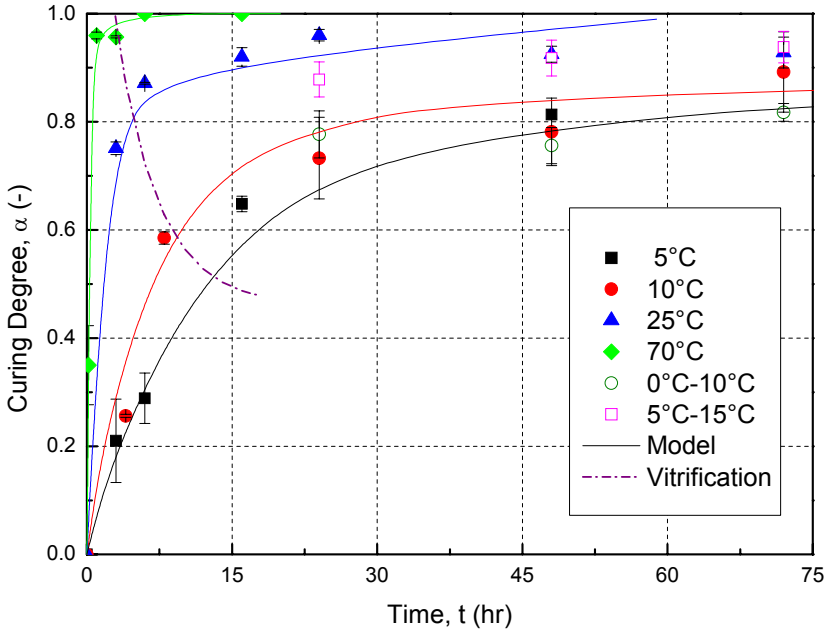

Figure 4.3 Curing degree vs. time of partially cured samples at different isothermal and cyclic temperatures (Sikadur-30)

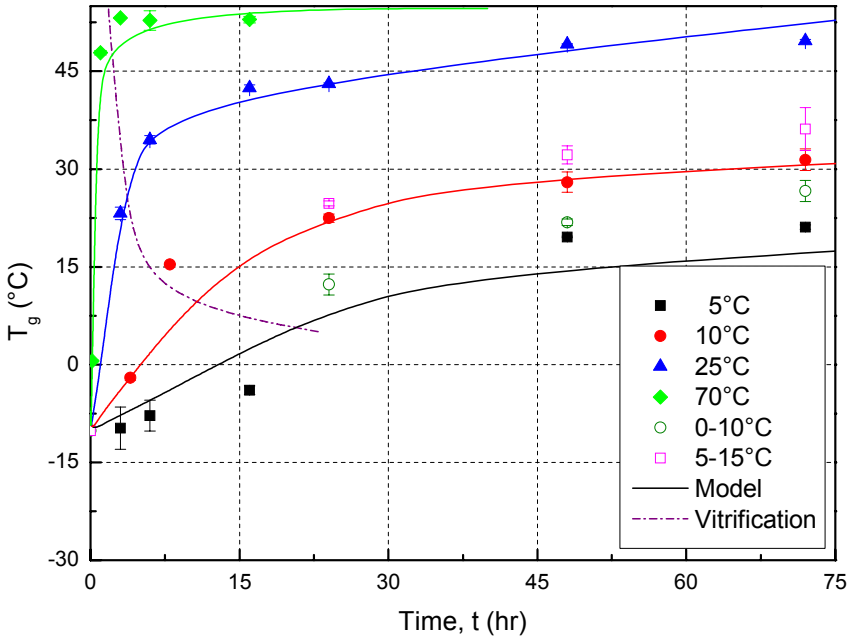

Figure 4.4 Glass transition temperature vs. time of partially cured samples at different isothermal and cyclic temperatures (Sikadur-30)

The relationship between α and T_g for both isothermal and cyclic curing is shown in *Figure 4.5*. The results of cyclic curing confirmed the curing temperature dependence discussed in Section 3.4 due to early vitrification at low curing temperatures, which leads to a deviation from the proposed models [8-9]. This also confirms the importance of the proposed modification of the modeling parameter λ in Eq. (3.13) when curing temperature is lowered (see *Figure 3.12*).

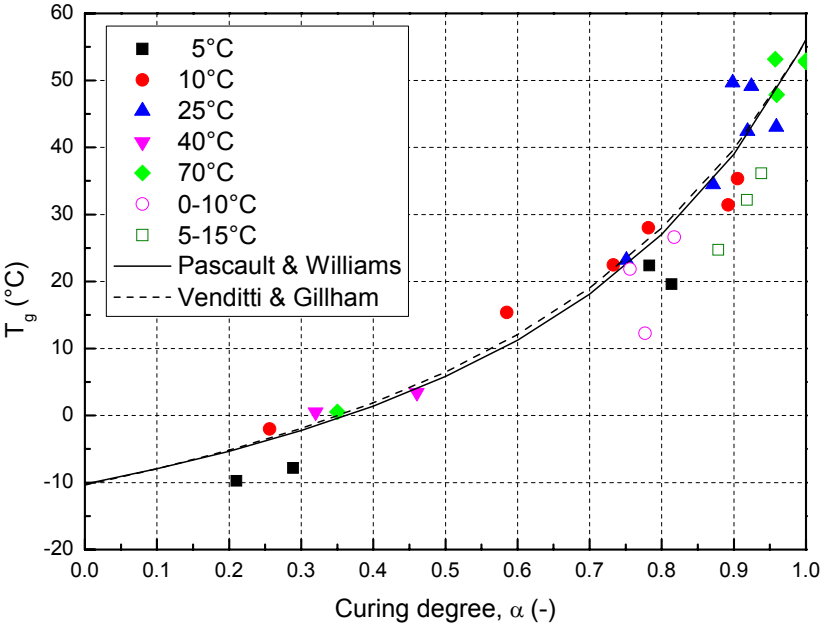

Figure 4.5 Glass transition temperature vs. curing degree of partially cured samples at different isothermal and cyclic temperatures (Sikadur-30)

4.3.2 Mechanical properties

The development of tensile strength, f_t, and stiffness (Young's modulus, E) vs. time, t, (up to two weeks) during isothermal curing is shown in *Figures 4.6a* and *b* respectively. Both properties rapidly increased at high curing temperatures, while a delay in the process was observed particularly during the initial curing stage at low curing temperatures. *Figures*

4.6a and *b* also show the curves when vitrification started and significant increases in mechanical properties only occurred after that point, particularly at lower curing temperatures. Since vitrification was delayed at low curing temperatures, the development of mechanical properties was also delayed. Furthermore strength, compared to stiffness development, was delayed at low curing temperatures – after 240 hours maximum stiffness was reached at all curing temperatures while maximum strength had not yet been reached at the lowest curing temperature of 5°C. Also, maximum stiffness values were lower at 70°C curing temperature than those at 25°C. This was due to the increase in randomness of network cross-linking at high curing temperatures as previously found in [3]. By prolonging the curing period at 10°C to 720 hours (1 month), a slight increase in mechanical properties (around 6% in stiffness and 10% in strength) was achieved compared to those reached after 240 hours.

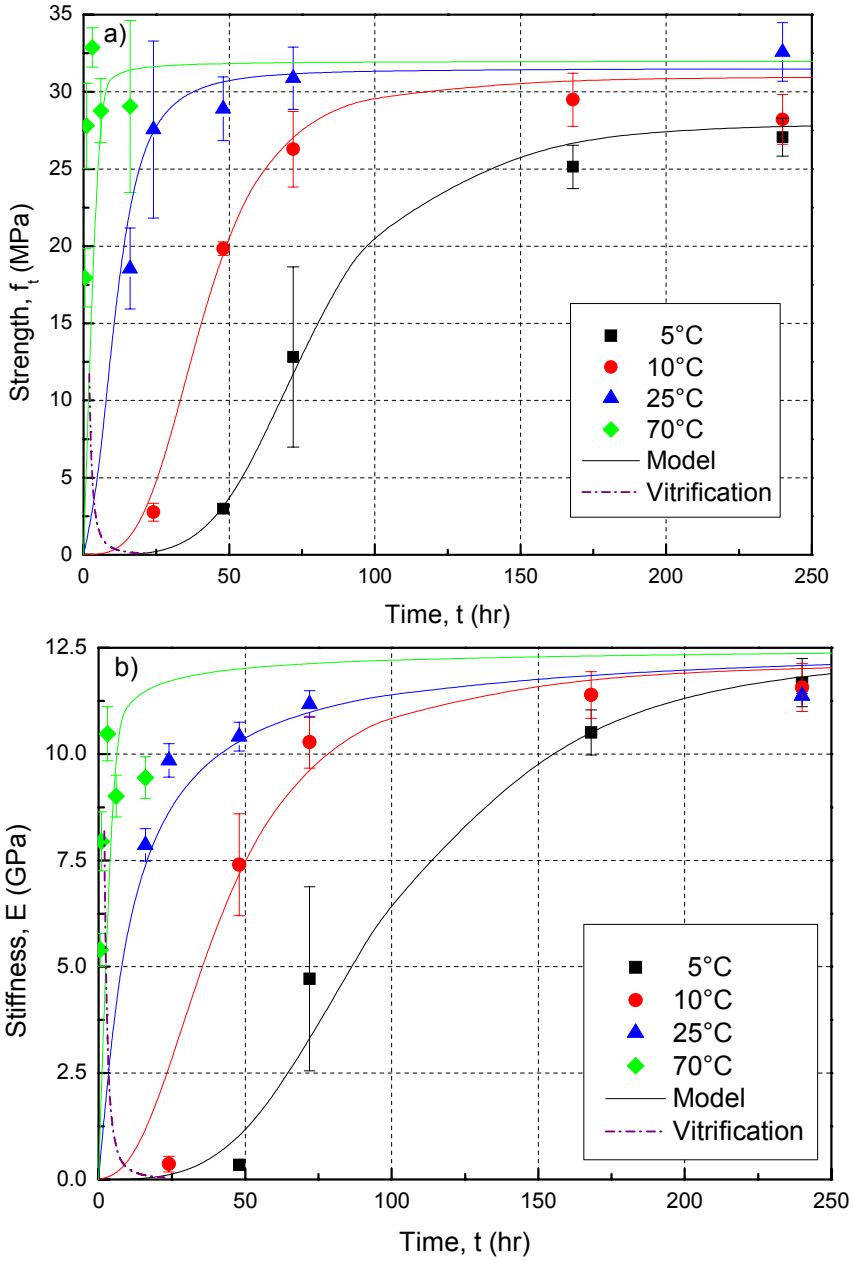

Figure 4.6 Mechanical property development at different isothermal temperatures and early stages of curing: a) strength; b) stiffness (Sikadur-30)

Figure 4.7 shows that strength and stiffness relationship was linear, but dependent on curing temperature at later curing stages. The lower the curing temperature, the more strength development was delayed compared to stiffness development. The delay in

strength development may be attributed to a delay in the development of the bond quality, which depends on curing temperature (see next Section 4.5). A potential dependence of stiffness development on curing temperature may have been masked by the high filler content. The results also show that the scatter in the measured properties tended to be highest when the slope of the curves in *Figure 4.6* was steepest and then decreased for longer durations.

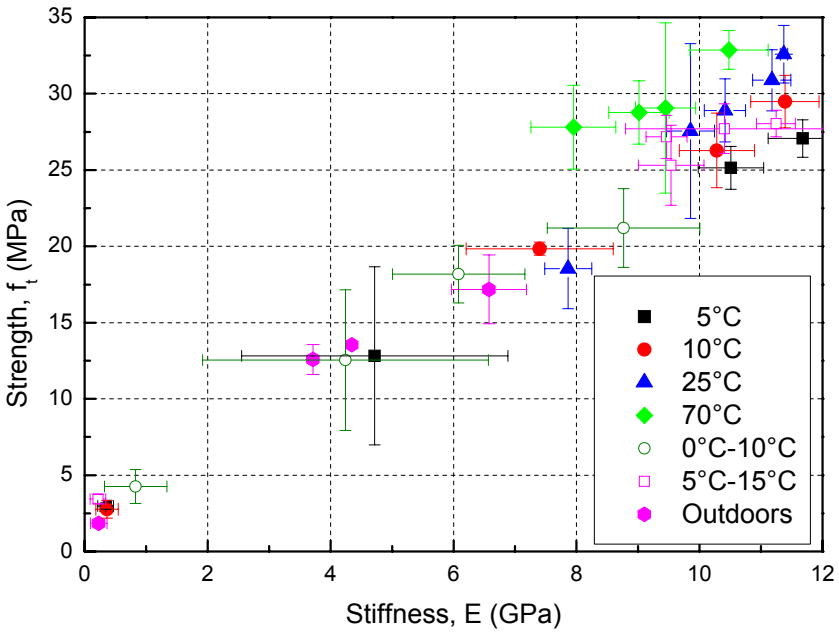

Figure 4.7 Strength vs. stiffness relationship (Sikadur-30)

The tensile strength and stiffness development under cyclic curing are shown in *Figures 4.8a* and *b* respectively. The comparison of 0-10°C and 10-0°C cycles shows that the former decelerated property development considerably, more than the 12-hour delay introduced at the 10°C level, and that this difference increased (up to approximately 50 hours after 150 hours of cure) with further curing. An average increase in mechanical properties of more than 40% was obtained after 72 hours when the adhesive curing cycle started by 10°C instead of 0°C. Therefore beginning with the 0°C cycle had a negative effect on the initial cross-linking and continued to have an increasingly negative effect as curing progressed. After around 200 hours, however, this was no longer the case since the two curves approached each other. The results also fitted well with the results from isothermal curing shown in *Figure 4.7*. During the 5-15°C cycles, mechanical properties developed more rapidly as compared to the other two cycles. In addition and similar to the T_g results (shown in *Figure 4.4*), results of the 5-15°C cycles and 10°C isothermal temperature (average temperature of 5 and 15°C) agreed well, particularly after 72 hours and above.

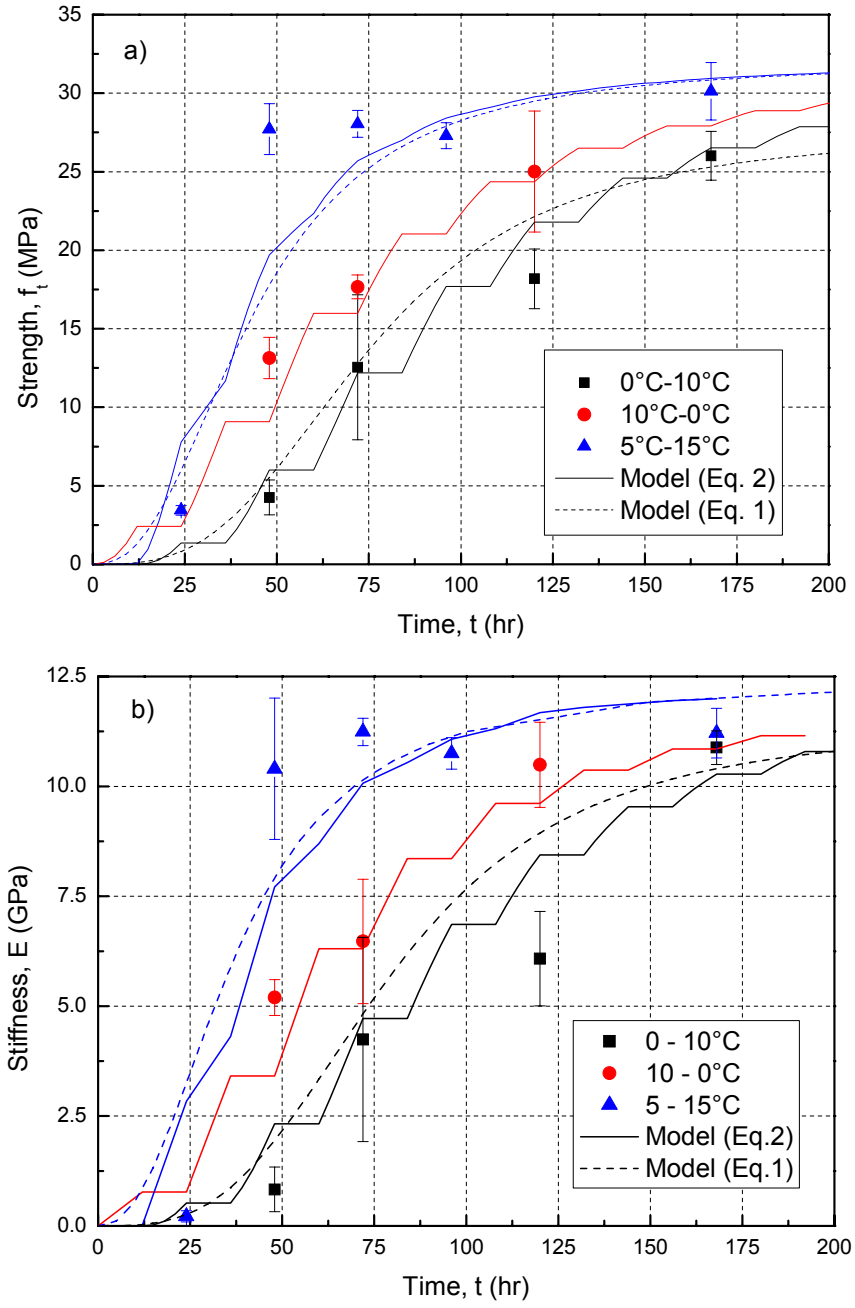

Figure 4.8 Mechanical property development at cyclic temperatures and early stages of curing: a) strength; b) stiffness (Sikadur-30)

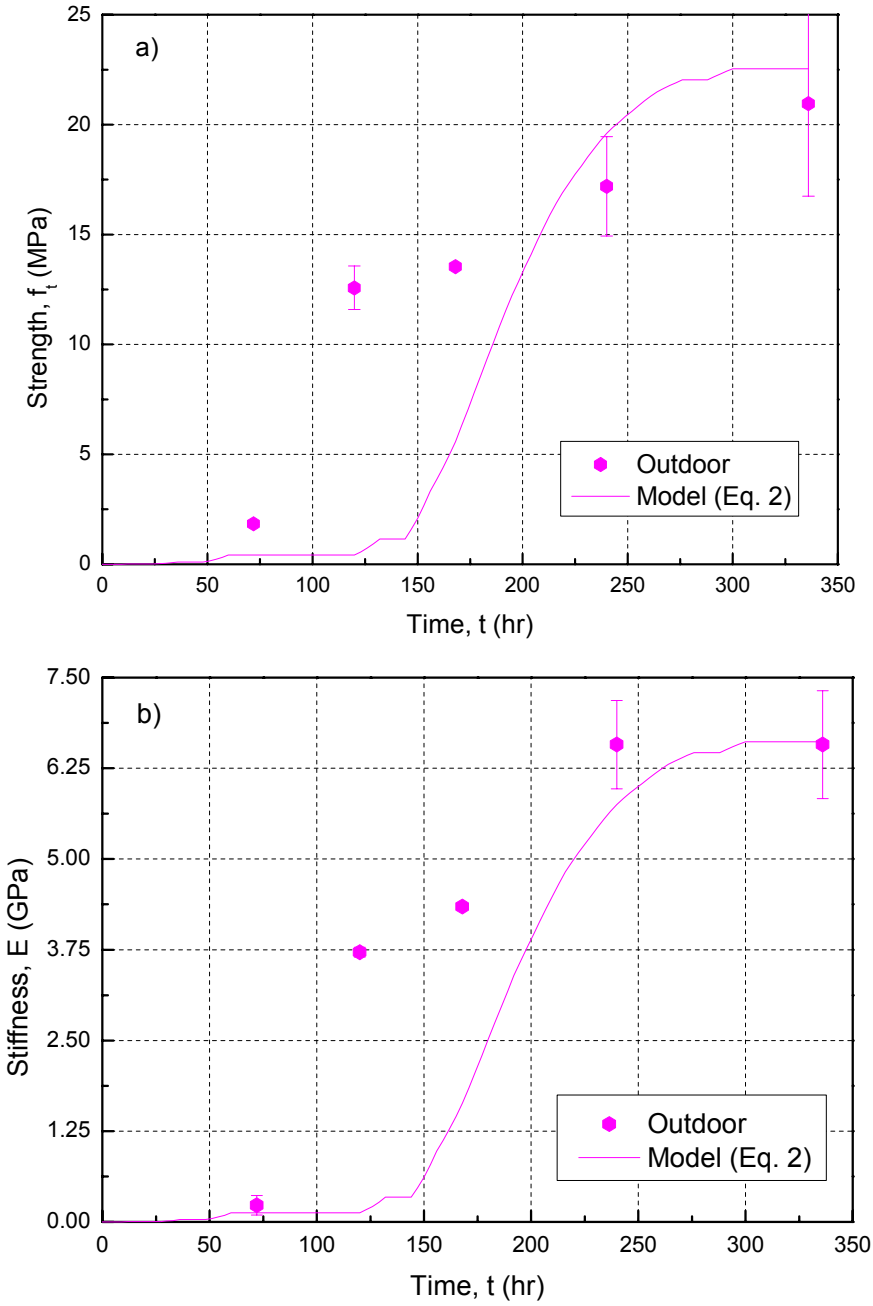

Figure 4.9 Mechanical property development during outdoor curing in winter: a) strength; b) stiffness (Sikadur-30)

The outdoor curing results are shown in *Figures 4.9a* and *b*. Property development started only after 72 hours, when the maximum temperature rose from below 0°C to almost 3°C. During the subsequent drop of maximum temperature to 0°C, the development almost stopped and then restarted when the maximum temperature rose above 0°C again. When the maximum temperature fell again (but remained around 4°C), the strength development still continued while stiffness development ceased. As a conclusion of the cyclic and outdoor curing results, 0°C seems to be the critical temperature at which curing stops or does not start. At slightly higher temperatures (3-5°C) curing does start, but at a very low rate.

4.4 Relationship between physical and mechanical properties

The development of mechanical properties directly depended on changes in the physical state, as shown in *Figure 4.10*, which illustrates the relationship between mechanical

properties (strength and stiffness) and physical properties (T_g) for the different curing procedures. *Figure 4.10* also shows the points at which vitrification started. In the first curing phase, T_g developed significantly in contrast to the mechanical properties, which did not develop at all. The mechanical properties particularly developed after vitrification started, as already discussed in relation to *Figure 4.6*. During this phase, T_g development dropped behind strength and stiffness development. It seems that the development of the molecular network by cross-linking, expressed by T_g, and the development of the mechanical bond quality of the cross-links did not proceed in parallel. The former process seemed to particularly occur before and the latter particularly after the onset of vitrification. Furthermore – or as an alternative explanation – the decrease in the rate of cross-linking during vitrification of an already strongly cross-linked network was able to over proportionally increase the mechanical properties.

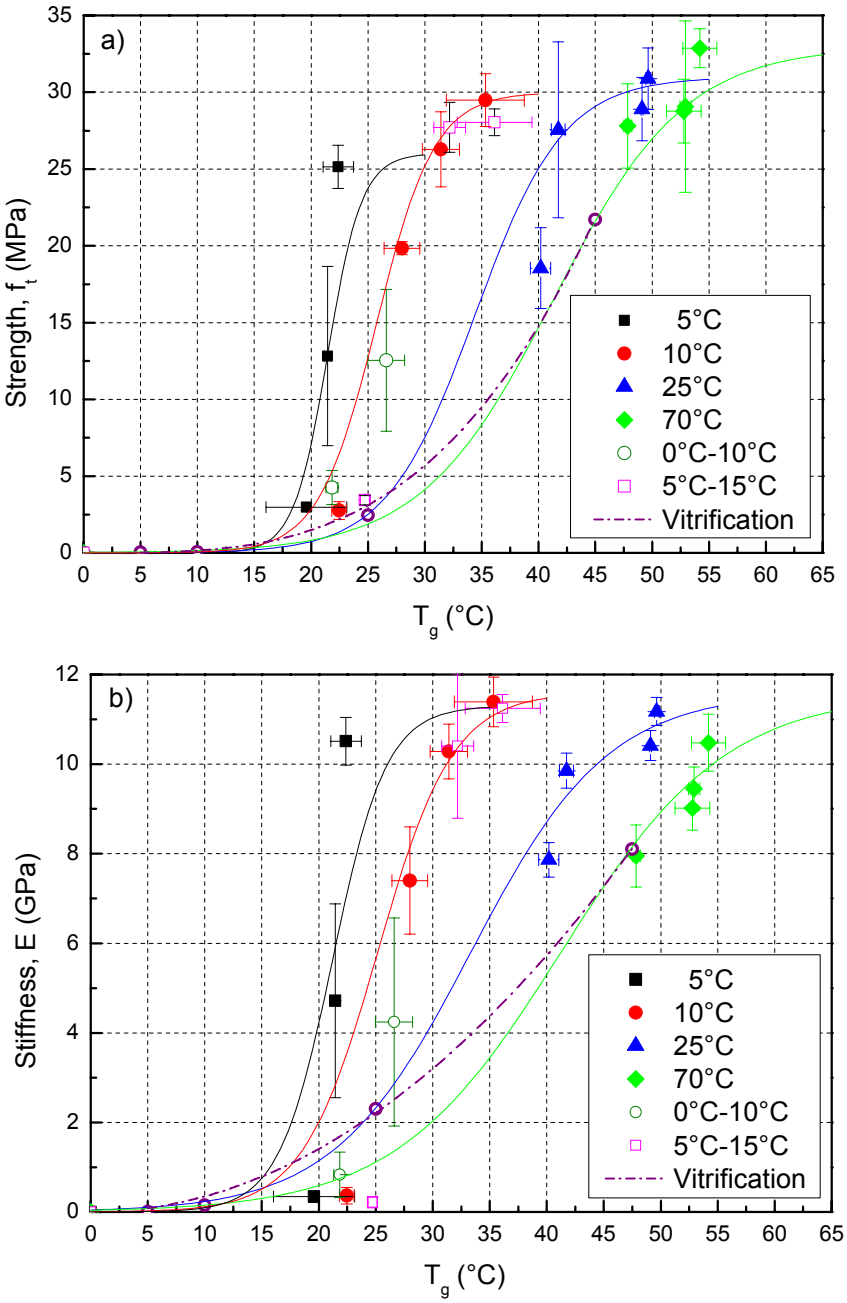

Figure 4.10 Mechanical properties vs. T_g during different curing procedures: a) strength; b) stiffness (Sikadur-30)

The slope of the curves in *Figure 4.10* increased with decreasing the curing temperature, i.e. a smaller T_g increase produced a larger increase of mechanical properties. However,

this effect occurred during a much longer time period – it has to be noted that the required curing time is not shown in *Figure 4.10*. Results from cyclic curing fell within same ranges between corresponding isothermal temperatures as in the T_g vs. time relationship (shown in *Figure 4.4*). Furthermore, *Figure 4.10* again shows that strength development was behind stiffness development at lower temperatures during the observed early-age period.

4.5 Modeling and discussion

A model describing the early-age development of mechanical properties as a function of T_g, as shown in *Figure 4.6*, was established. A logistic equation according to [10] was used to describe mechanical behavior since the curing behavior of the epoxy material was autocatalytic (see [7]) and this equation was employed for establishing autocatalytic reaction models. The model takes into consideration the curing temperature-dependent delay at the beginning of property development as well as a plateau at a maximum property value that can be specified. The equation takes the following form:

$$P(t) = \frac{P_0 - P_\infty}{1 + (t / t_m)^s} + P_\infty \tag{4.1}$$

where $P(t)$, P_0 and P_∞ are the property values at a given time, t, at the beginning (t=0) and at the end of the curing process, respectively. The parameter t_m represents the time required to attain a value of $P_\infty/2$ and s is the power of the curve (governing the slope of the curve or rate of development). The value P_0 (at the beginning of the curing process) is zero for freshly mixed material while the property end value, P_∞, was assumed at 240 hours of curing. Accordingly, stiffness was identical for all curing temperatures (~11.4 GPa) while strength at lower curing temperatures was delayed, as previously discussed and shown in *Figure 4.6a*. The relationships of curing temperature, T_{cure}, vs. t_m, s and P_∞ (for strength only) are presented in *Figures 4.11a*, *b* and *c* respectively. A similar behavior for both strength and stiffness was obtained from the first two relationships. The time required to attain $P_\infty/2$ was found to be very similar for strength and stiffness, as shown in *Figure 4.11a)*, and the rate of development changed similarly from one curing temperature to another (almost parallel curves). It is obvious from *Figures 4.11a* and *b* that at temperatures approaching 0°C, t_m and s tend to infinity, meaning that curing would almost cease at these temperatures, a result that has been confirmed experimentally, as previously shown.

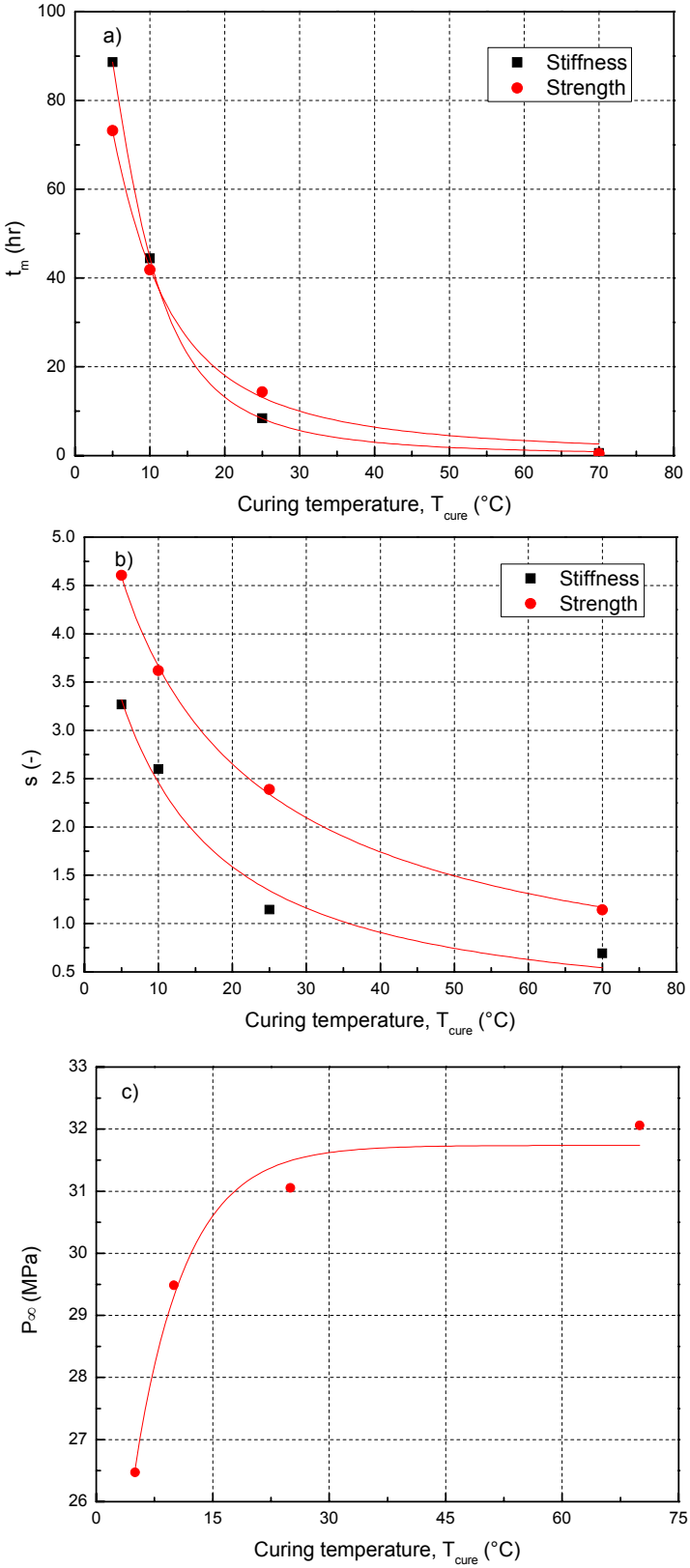

Figure 4.11 Model parameters as a function of curing temperature: a) t_m; b) s; c) P_∞ (Sikadur-30)

The tensile strength and stiffness at different isothermal temperatures were calculated according to Eq. (4.1) based on the relationships shown in *Figure 4.11*. A good agreement between experimental and modeling results was found as shown in *Figures 4.6a* and *b*. In order to predict the results at cyclic temperatures, an extended procedure

was used taking the variation of curing temperature and the period during which each temperature was sustained into account. According to this procedure, Eq. (4.1) can be rewritten as:

$$P(t) = \underbrace{\left[\frac{P_0 - P_{\infty_1}}{1+(t_1/t_{m_1})^{s_1}} + P_{\infty_1}\right]}_{P_1} + \underbrace{\left[\frac{P_1 - P_{\infty_2}}{1+(t_2/t_{m_2})^{s_2}} + P_{\infty_2}\right]}_{P_2} + \ldots + \left[\frac{P_{n-1} - P_{\infty_n}}{1+(t_n/t_{m_n})^{s_n}} + P_{\infty_n}\right] \quad (4.2)$$

with each of the terms of Eq. (4.2) referring to a single history profile (as a function of curing temperature and curing time) as shown in *Figures. 4.6* and *4.11*. It was assumed that no curing occurred at 0°C, as mentioned in the above discussion. The modeling results according to Eq. (4.2), shown in *Figures 4.8a* and *b*, agree well with the experimental results.

Alternatively, Eq. (4.1) was applied to also predict mechanical property development under cyclic temperatures by assuming an equivalent curing temperature at the intersection of the T_g and vitrification curves in *Figure 4.4* (resulting in a T_g of 7.4 and 10.1°C for 0-10 and 5-15 cycles respectively). The parameters corresponding to the equivalent curing temperatures were again selected from *Figure 4.11*. A good agreement with the experimental results and the results of Eq. (4.2) was obtained, see *Figure 4.8* (model Eq. (4.1)).

The model Eq. (4.2) was also applied to predict the behavior of outdoor specimens during early-age curing; Fig. 4.9 shows the strength and stiffness results. The development after a period of around 150 hours was well predicted, while the effect of the first low temperature peak between approximately 50 and 100 hours, see *Figure 4.1*, was underestimated. Although the maximum temperature during this period was below 3°C, this level already produced a significant increase of the mechanical properties. It should be noted that the available data only comprised the highest and lowest temperatures of a given day, excluding details concerning the change of temperature during the same day. Furthermore, other potential effects, such as humidity, were unknown. This may also explain the deviations of the predictions.

Based on the derived models, the tensile strength and stiffness of the adhesive used in this study as a function of curing temperature and curing time can be determined as shown in *Figure 4.12*. The mechanical properties were calculated as a percentage of maximum (100%) properties at 240 hours according to *Figure 4.6*.

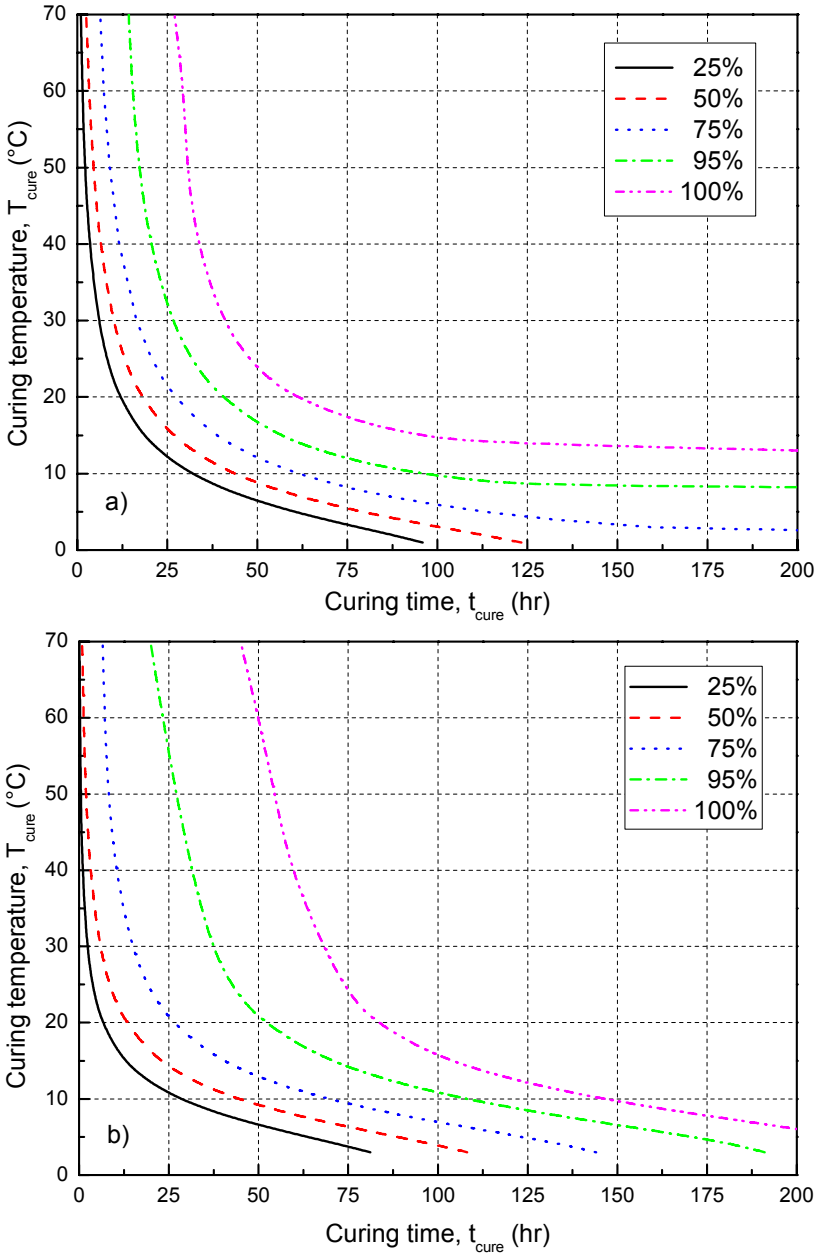

Figure 4.12 Mechanical property levels as a function of curing conditions: a) strength; b) stiffness (Sikadur-30)

4.6 Conclusions

Experimental and analytical investigations concerning the early-age development of mechanical tensile properties of a structural epoxy adhesive were performed. The effects of different curing procedures and the associated physical material states on the mechanical properties were investigated. The following conclusions can be drawn:

1) The mechanical properties started developing significantly only after the onset of material vitrification. This was in contrast to the development of the glass transition temperature, which particularly increased before vitrification and leveled off during vitrification.
2) The mechanical property development strongly depended on the curing temperature. Lower curing temperatures significantly decelerated the process. At 0°C curing was inhibited or did not start at all.
3) Strength and stiffness developed at the same rate. Strength development, however, was slightly delayed at later stages of cure compared to stiffness development at low curing temperatures.

4) An analytical model is proposed that can predict the development of mechanical properties under isothermal and cyclic curing conditions. Modeling and experimental results compared well.
5) Based on the analytical model, design curves for early-age mechanical properties as a function of curing temperature and time can be established.

4.7 References

C. Jordan, J. Galy and J.P. Pascault, "*Measurement of the extent of reaction of an epoxy-cycloaliphatic amine system and influence of the extent of reaction on its dynamic and static mechanical properties*", J. Appl. Polym. Sci., 1992; 46(11-12): 859-871. [1]

G. Wisanrakkit and J.K. Gillham,"*Glass transition temperature (T_g) as an index of chemical conversion for high-T_g amine/epoxy system: chemical and diffusion-controlled reaction kinetics*", J. Appl. Polym. Sci., 1990; 41(5): 2885-2929. [2]

E. Sancaktar, J. Hooshang and R.M. Klein, "*The effects of cure temperature and time on the bulk tensile properties of a structural adhesive*", J. Adhes., 1983; 15(3-4): 241-264. [3]

S.J. Shaw and D.A. Tod, "*The effect of cure conditions on a rubber-modified epoxy adhesive*", J. Adhes., 1989; 28(4): 231-246. [4]

J.W. Sinclair, "*Effect of cure temperature on epoxy resin properties*", J. Adhes., 1992; 38: 219-234. [5]

F. Lapique and K. Redford, "*Curing effects on viscosity and mechanical properties of commercial epoxy resin adhesive*", Intl. J. Adhs. Adhs., 2002; 22(4): 337-346. [6]

O. Moussa, A. Vassilopoulos and T. Keller, "*Effects of low temperature curing on physical properties of structural epoxy adhesive joints in bridge construction*", Int. J. Adhes. Adhes., 2011; 32(1): 15-22. [7]

G. W. Ehrenstein and S. Pongratz, "*Beständigkeit von Kunststoffen*", Carl Hanser Verlag, München 2007. [8]

R. S. Bauer, "*Epoxy Resins, ACS Symp. Ser. 285, Applied Polymers Science"*, II Edition, ACS, Washington 1985. [9]

N. A. Gershenfeld, "*The Nature of Mathematical Modeling*", Cambridge University Press, 1999. [10]

5 Thermomechanical recovery

5.1 Overview

Low-temperature curing of adhesives leads to incompletely cured systems and may therefore delay the development of physical and mechanical properties. Full properties can only be attained after significantly longer curing periods compared to curing during summer [1-5].

During the long curing periods at low temperatures, the development of the glass transition temperature, T_g, is decelerated and the latter, still of a low value, may be exceeded by the environmental temperature or temperature increases caused by sun radiation at the location of certain joints during certain periods. In this case the secondary bonds of the adhesive are broken and the material behavior changes from glassy to rubbery. This may result in a significant drop in the mechanical properties, which may affect serviceability and structural safety if the joint is not properly designed, i.e., if these potential effects are not taken into account. After cooling from a temperature that exceeded T_g, the question arises as to whether the secondary bonds are fully or partially reformed and, correspondingly, whether the mechanical properties can recover and the material can revert to the glassy state.

The temperature-dependent variation of the mechanical properties of bulk adhesives, adhesively-bonded joints and polymer composites is widely discussed in the literature. The effect of elevated temperatures on mechanical properties has been investigated for different types of polymers such as thermosets (cross-linked) and thermoplastics (amorphous, linear, semi-crystalline) [6-10]. The results consistently demonstrate the sensitivity of these materials to elevated temperatures, particularly when T_g is exceeded. Engineering relationships between mechanical properties and temperature have been established in order to model the phenomena [7, 9-10]. These relationships demonstrated their applicability over a vast range of polymers and polymer composites.

The effect of cooling the materials from temperatures above to temperatures below T_g on the physical and mechanical properties, i.e. on the recovery capacity, is investigated in only a few studies [11-12]. The reversibility/reformation of hydrogen bonds during cooling and the effect of the thermal history on T_g during heating/cooling were investigated. Results showed the reformation of hydrogen bonds during cooling and also a dependency of T_g on the cooling rate. These studies mainly focused on physical changes in the polymeric structure however. The effect of the physical changes on the mechanical properties during recovery has not yet been addressed. As yet no models to predict the thermomechanical recovery behavior of adhesives during cooling from temperatures exceeding T_g to temperatures below T_g exist.

The aim of the work presented in this section is to fill this gap. The physical and mechanical behaviors of a commercial epoxy adhesive during heating/cooling across T_g were examined. The relationships between the curing degree, α, the glass transition temperature, T_g, and the mechanical properties (tensile stiffness and strength) during thermomechanical recovery were experimentally investigated. Based on these results, an existing model for predicting temperature-dependent mechanical properties was extended to also predict the thermomechanical recovery behavior of the examined adhesive.

5.2 Thermophysical and mechanical background

The behavior of inter- and intra-molecular bonds during polymer material exposure to an increasing temperature has been extensively discussed [6-7]. The bonds can be divided into two major categories: the first consists of the strong covalent (primary) intra-molecular bonds. These bonds form the backbone of the polymer chain with high dissociation energy. The second category groups different types of weaker secondary

bonds (e.g. hydrogen bonds, dipole and Van der Waals interactions). Polymer chains are bonded to each other by these secondary bonds that have low dissociation energy.

During the heating process, from the glassy state up to the initiation of decomposition, primary bonds remain intact. The secondary bonds, however, are altered by molecular motions during relaxation or are broken. The mechanical response of thermosets, i.e. epoxy adhesives as examined in this study, if exposed to an increasing temperature, can be generally divided into three different phases, as shown in *Figure 5.1*. During Phase 1, commonly referred to as the glassy state, mechanical properties remain almost constant and most of the secondary bonds stretch without breaking. However, in the case of some polymers, the thermal energy is sufficiently high to allow the rotation of side groups, which is linked to the breakage of some secondary bonds. Accordingly, one or more secondary relaxations can occur (designated *β*-transition and *γ*-transition, the latter in the case of two transitions), characterized by a slight drop in properties at temperatures T_β and T_γ. Phase 2, also referred to as glass transition (*α*-transition or primary relaxation), usually results in a dramatic drop in mechanical properties at a temperature range characterized by the T_g value. In this phase, the polymer chains start sliding against each other and the remaining secondary bonds are broken. The glass transition phase usually terminates in a plateau during the property response, denominated as the rubbery state of the material. Unlike thermoplastics, the polymeric structure of thermosets is usually heavily cross-linked which at this stage prevents viscous flow and a direct transition to decomposition occurs at higher temperatures. Decomposition represents the last of the three phases in the response of thermosets to an increasing temperature.

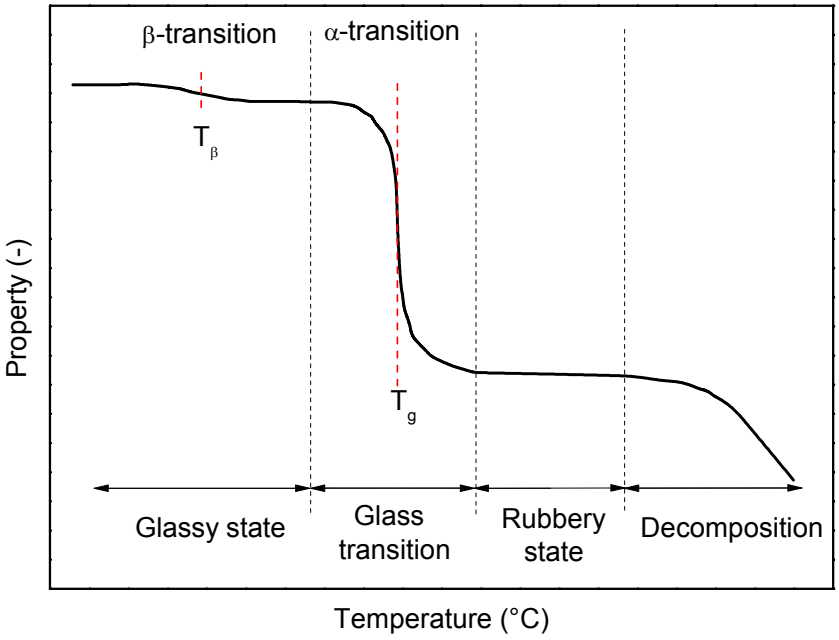

Figure 5.1 Thermoset adhesive properties vs. increasing temperature

Among the different existing models to describe this process, those proposed by Mahieux et al. [12] and Gibson et al. [15] demonstrated good applicability to different types of composite materials. The first model relates the number of polymer chain segments involved in each of the relaxations (which increases with temperature due to bond breakage) to Weibull distributions, i.e. for each relaxation a Weibull modulus is obtained. The equation of this model is as follows:

$$P(T) = (P_1 - P_2)\exp(-(\frac{T}{T_1})^{m_1}) + (P_2 - P_3)\exp(-(\frac{T}{T_2})^{m_2}) \tag{5.1}$$

where *P(T)* is the material property (strength or stiffness) at a given temperature *T*; T_1 and T_2 are the temperatures at which secondary relaxation and glass transition take

place (T_β and T_g in *Figure 5.1*, in degrees Kelvin); P_1 and P_2 are the instantaneous material properties preceding the secondary and primary relaxations respectively, i.e. the upper and lower plateau values before and after the secondary relaxation; P_3 is the property at the rubbery plateau. The model was derived from DMA and, accordingly, T_g is based on the peak of the tan-δ curve (a curve which is also obtained from DMA measurements). Parameters m_1 *and* m_2 are the Weibull moduli, which are also dependent on the degree of impediment of the molecular motion (by cross-linking, molecular weight, fillers, etc.). If the movement of the molecular chains is restricted, the Weibull moduli tend to decrease.

The second model by Gibson et al. [10] is semi-empirical, derived from fitting the regular antisymmetrical shape of the property distribution along the glass transition as follows:

$$P(T) = \left(\frac{P_U + P_R}{2} - \frac{P_U - P_R}{2} \tanh(k(T - T_k)) \right) \tag{5.2}$$

where *P(T)* is the material property (strength or stiffness) at a given temperature, P_u and P_R are the property values of the unrelaxed material (i.e. glassy at low temperature) and relaxed material (i.e. rubbery at high temperature) respectively; *k* is a constant obtained by fitting the model to the experimental data and T_k is the glass transition temperature obtained as the temperature corresponding to 50% remaining property (between the glassy and rubbery states).

The above models are proposed to predict mechanical properties at elevated temperatures. The question now arises - and will be discussed in the following – as to whether they are also applicable for describing the thermomechanical recovery after the cooling process.

5.3 Experimental investigation

5.3.1 Thermophysical experiments

The aim of the thermophysical experiments was to evaluate the effect of different temperature histories (combinations of temperature and time) on the curing degree and the corresponding glass transition temperature. DSC experiments were performed following the alternative method discussed in Section 3.2 (see also *Figure 3.3*).

Samples of 5-10 mg weight were placed in steel pans covered with lids and sealed with a manual press. After preparation, the samples were cured at laboratory temperature (~20°C) for two weeks. Three samples were directly scanned in order to obtain the glass transition temperature of samples cured under laboratory conditions, T_{gL}. The resulting value was 45.6±2.8°C at a curing degree of α_L=94.3±0.03%. The experimental program further comprised nine different time-temperature conditions. Experiments were performed on three sets of samples subjected to three different temperatures above T_{gL}: 60°C (just above T_{gL}), 100°C (rubbery state), and 150°C (close to onset of decomposition). Samples of each set were exposed during three time periods (0.5, 2.0, and 4.0 hours). These time periods were selected in view of different structural applications, e.g. bridge deck joints during asphalt application where the asphalt temperature on the bridge surface is within the range of 90 - 120°C and drops below T_g in few hours hours. Following exposure to each condition in a climate chamber (Instron SFL regulated by a Eurotherm 2704 controller), samples were quenched in liquid nitrogen to stop the reaction. The curing degree and the corresponding glass transition temperature were then obtained based on a dynamic scan between -50 and 250°C at a heating rate of 5°C/min. A minimum number of three samples were scanned for each time-temperature condition; a total of 30 samples were used.

5.3.2 Thermomechanical experiments

Experimental set-up and procedure

Tension experiments were performed according to the procedure described in Section 4.2.3 (for dimensions see *Figure 4.2a*). Specimens were fabricated in aluminum molds and left to cure under laboratory conditions for two weeks thus assuring a high curing degree (~ 94% see Section 5.3.2). Experiments were performed under displacement control at a loading rate of 5mm/min. Wooden tabs were glued onto each side of the specimen (contact zones with the machine's metal wedges, as shown in *Figure 5.2*) to minimize any temperature change at the location of the grips (particularly at high temperatures) thus ensuring a uniform temperature distribution along the full length of the specimen.

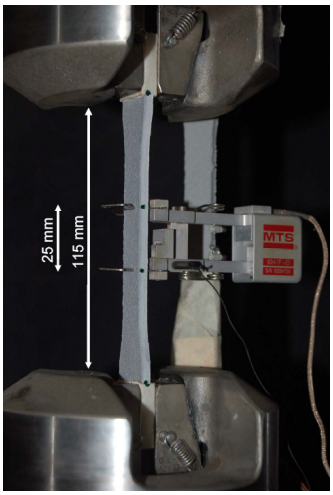

Figure 5.2 Experimental set-up

All experiments were performed in a climate chamber (ATS 3710) connected to a liquid nitrogen cooling system. The accuracy of the chamber was ± 0.5°C during heating and ± 3°C during cooling (using liquid nitrogen). A reference specimen (for temperature measurement) was placed close to the loaded specimen with a thermal gage (Pt-100) embedded in the middle. *Figure 5.3* illustrates the temperature profile obtained from one of the reference specimens.

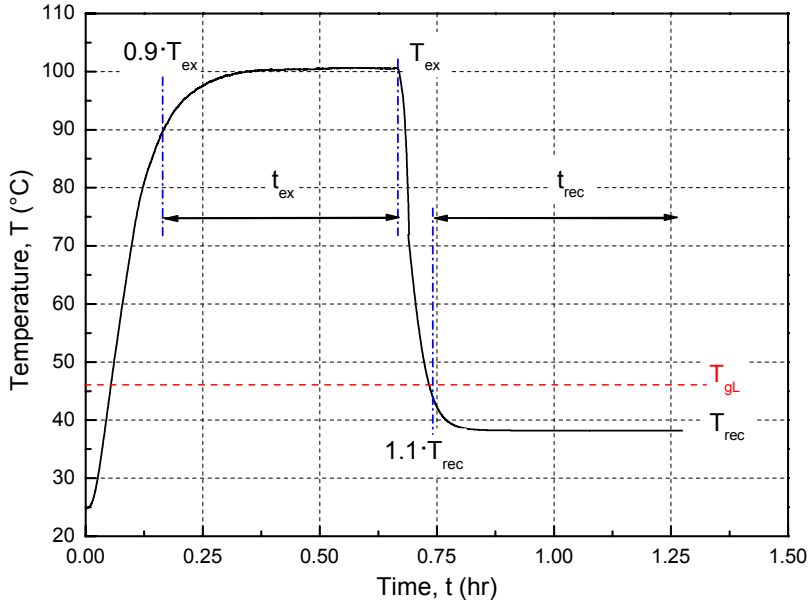

Figure 5.3 Thermal history of one T_g–exceeding cycle investigations (T_{ex}=100°C, t_{ex}=0.5 hour, T_{rec}= 40°C and t_{rec}=0.5 hour) (Sikadur-30)

Experimental program

The thermomechanical response of the adhesive to different constant temperatures and time periods was first investigated. The effect of cooling from temperatures, T_{ex}, which exceeded T_{gL} ($T_{ex} > T_{gL}$), to recovery temperatures, T_{rec} ($T_{rec} < T_{gL}$), on tensile strength and stiffness was then studied as well as the effect of varying the time periods at both T_{ex} and T_{rec}. Lastly, the effect of more than one cycle across the glass transition range was investigated, simulating outdoor conditions where the adhesive is subjected to varying heating/cooling cycles. Accordingly, the experimental program was divided into three experimental categories as follows:

The first category, denominated ″low/high temperature″, included exposing specimens to different temperatures ranging from -35 to 100°C for 0.5 hours and performing the experiments at the same temperature according to *Table 5.1*. Additional exposure time periods (two and four hours) were considered for two temperatures, 40 and 50°C, below and above T_{gL}.

Table 5.1 Thermal exposures for constant temperature investigations

T (°C) / t (hr)	-35	0	20	30	40	50	60	100
0.5	▨	▨	▨	▨	▨	▨	▨	▨
2					▨	▨	▨	
4						▨	▨	

The second category, denominated ″one T_g-exceeding cycle″, involved experiments on specimens exposed to $T_g$exceeding temperatures, T_{ex}, of 60, 100 and 150°C (see previous section) subsequently cooled to recovery temperatures, T_{rec}, according to *Table 2*. The effects of the exposure time at T_{ex}, t_{ex}, and the time allowed for the specimen to recover, t_{rec}, on the thermomechanical behavior were also investigated.

The third category, denominated ″eight T_g–exceeding cycles″, involved exposure of specimens to eight heating/cooling cycles between 30 and 60°C, across the glass transition range. During each cycle, the specimen was kept at each temperature for 0.5 hour. At the end of the eight cycles, specimens were kept at three different temperatures (30, 50 and 60°C) for 0.5 hour, at which the tensile experiments were performed.

Table 5.2 Thermal exposures for one T_g–exceeding cycle investigations

T_{ex} (°C) / t_{ex} (hr)	60			100			150			
0.5	▨	▨	▨	▨	▨	▨	▨	▨	▨	▨
2			▨			▨			▨	▨
T_{rec} (°C) / t_{rec} (hr)	20	40	50	20	40	50	60	50	60	70
0					▨					
0.25					▨					
0.5	▨	▨	▨	▨	▨	▨	▨	▨	▨	▨
2						▨				▨
6						▨				

The heating and cooling rates were around 6°C/min and 5°C/min respectively. All time periods were recorded as from the moment when 90% of the target temperature when heating ($0.9 \cdot T_{ex}$) and 110% of the target temperature when cooling ($1.1 \cdot T_{rec}$) were attained, see *Figure 5.3*. A minimum number of three specimens were used for each

time-temperature combination except for exposures of t_{ex}= 2 hours where a minimum of two specimens were examined.

5.4. Experimental results and discussion

5.4.1 Thermophysical properties

The effects of T_g–exceeding temperature and time on the curing degree, α, and T_g are shown in *Figures 5.4* and *5.5* respectively. The curing degree increased with time and temperature from 94.3 to 100%. The effect of the exposure time, t_{ex}, between 0.5 and 4.0 hours, on α was significant up to around T_{ex}=90°C but then almost disappeared at higher temperatures. The time dependence was much more significant in the case of T_g. When subjected to T_{ex}=150°C, T_g increased from 45.6°C to 62°C at 0.5 hour and to a maximum of 72°C at 4.0 hours exposure. The parabolic trend of the increase also changed: the increase was delayed at shorter exposure times.

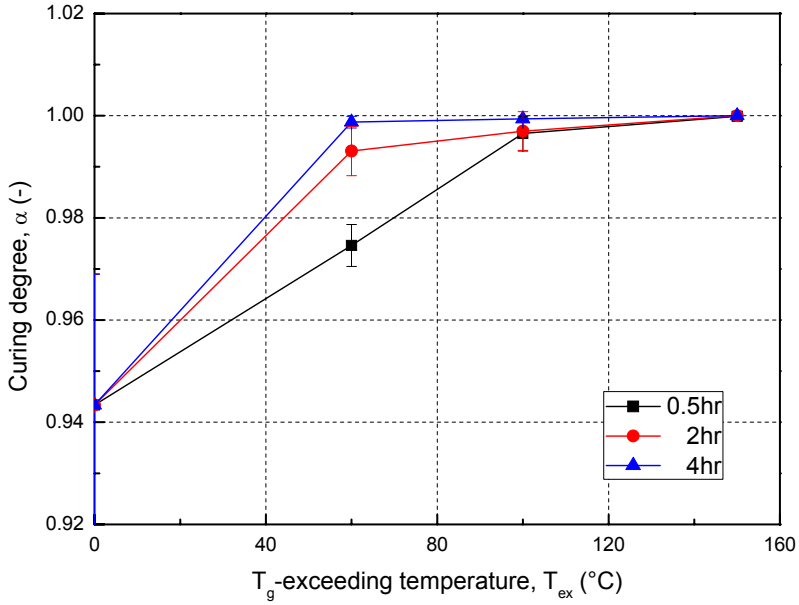

Figure 5.4 Effect of T_g–exceeding temperature, T_{ex}, and exposure time, t_{ex}, on curing degree (Sikadur-30)

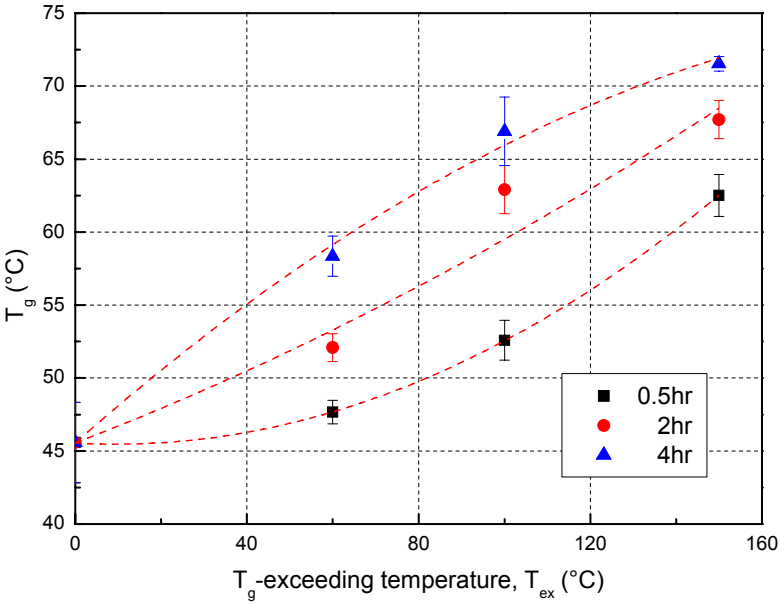

Figure 5.5 Effect of T_g–exceeding temperature, T_{ex}, and exposure time, t_{ex}, on T_g (Sikadur-30)

As more thermal energy was supplied to the system, the curing reaction was accelerated due to increased chain motion and a higher degree of cross-linking was achieved compared to the preceding curing at ambient temperature. The cross-linking of polymer groups that react very slowly at low-curing temperatures (such as secondary amino groups or sterical hindered amino groups) was accelerated in particular. In addition, stresses induced in the material during cure (due to the difference between glass transition temperature and room temperature [13-14]) were expected to decrease, which increased mobility of the chains and again led to a higher cross-linking and consequently T_g.

5.4.2 Thermomechanical properties

Low/high temperature exposure

The nominal stress-strain responses at temperatures between -35°C and 60°C are shown in *Figure 5.6*. A change in the basic adhesive behavior was noticed at 40°C, i.e. when approaching T_{gL}. Specimens examined below this temperature exhibited a stiff and almost linear-elastic behavior while specimens examined above this temperature showed a viscoelastic non-linear response. Tensile stiffness and strength were reduced from 14.1±0.3 GPa and 45.0±4.4 MPa at -35°C to 0.16±0.01 GPa and 5.27±0.13 MPa at 60°C respectively, which emphasizes the dependence of mechanical properties on temperature. At 100°C, results were not reliable due to the high material viscosity and tab failure. The change in tensile stiffness and strength vs. temperature are shown in *Figures 5.7a* and *b* (results denominated "low/high"). A secondary relaxation was noticed below laboratory temperature (~20°C), while glass transition initiated just above laboratory temperature accompanied by a pronounced drop in mechanical properties.

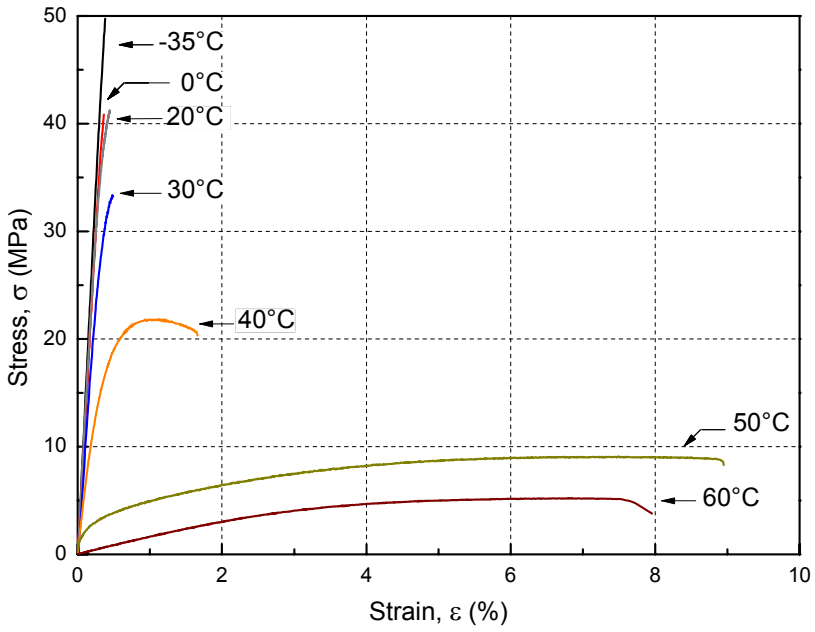

Figure 5.6 Effect of temperature on stress-strain response (Sikadur-30)

The stress-strain responses at 40 and 50°C after exposure during different time periods are shown in *Figure 5.8*. The responses at 40°C (which was below T_{gL}) were almost linear-elastic and insensitive to the exposure duration. At 50°C (above T_{gL}), however, the responses were strongly dependent on exposure duration. For a short duration (0.5 hour), the behavior was viscoelastic, as also shown in *Figure 5.6*. Prolonging the duration led to additional curing and an increase of T_g to above 50°C (see *Figure 5.5*). The response changed accordingly to almost linear-elastic and the specimens exhibited a stiff behavior.

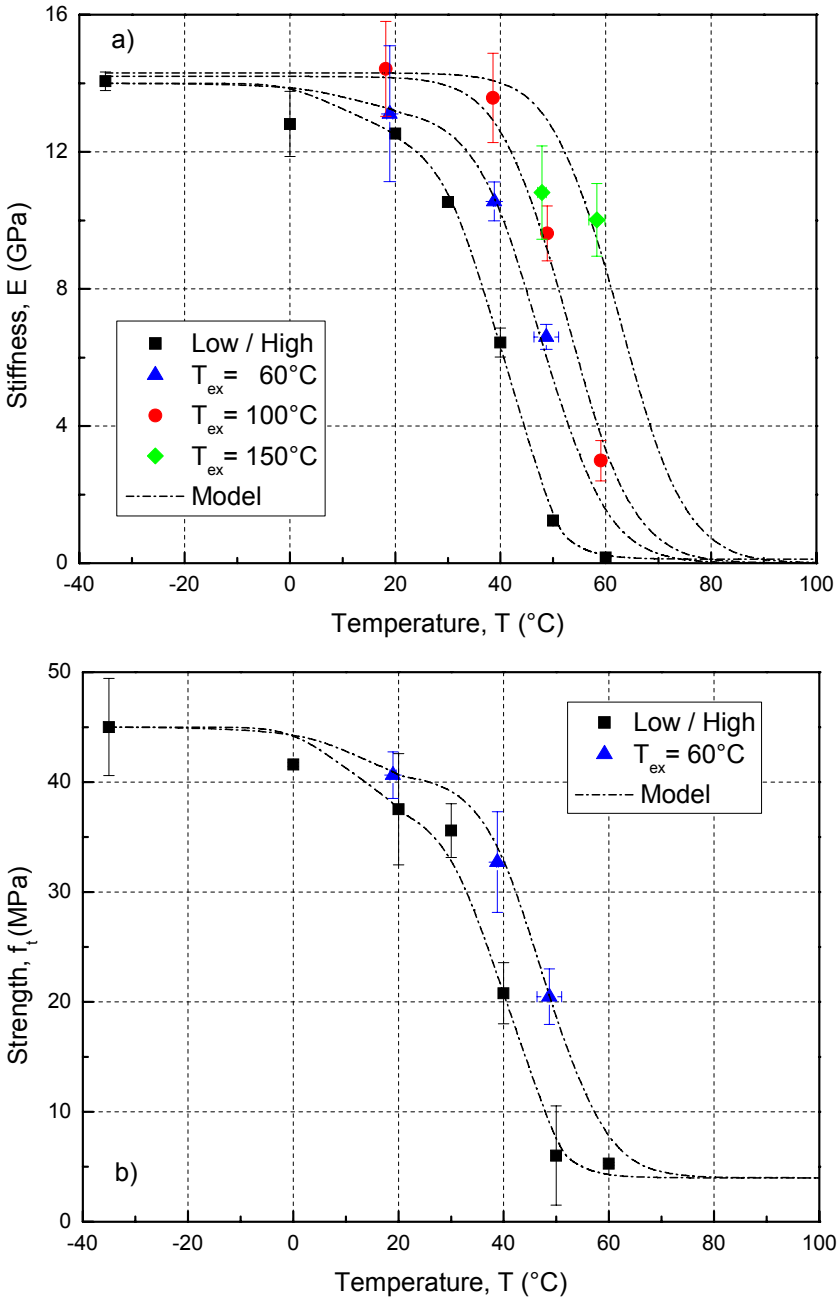

Figure 5.7 Effect of T_g–exceeding temperature, T_{ex}, during t_{ex}=0.5 hour on a) stiffness; b) strength (t_{rec}=0.5 hour) (Sikadur-30)

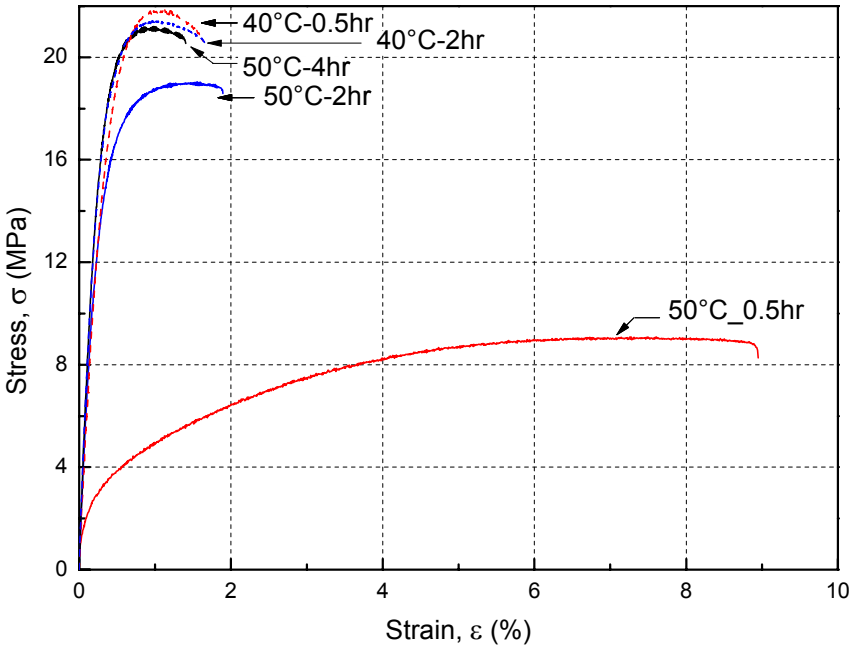

Figure 5.8 Effect of time on stress-strain response at 40°C and 50°C (Sikadur-30)

One T_g–exceeding cycle

The thermomechanical recovery behavior of tensile stiffness and strength after exposing the specimens to T_g-exceeding temperatures (T_{ex}) of 60, 100 and 150°C during 0.5 hour (t_{ex}) and cooling to the recovery temperatures (T_{rec}) according to *Table 5.2* (t_{rec}=0.5 hour) is shown in *Figures 5.7a* and *b*. Compared to the "low/high" temperature results, the stiffness responses up to T_{ex}=100°C and strength responses up to T_{ex}=60°C showed a similar sigmoid shape and shift towards higher temperatures. An increase of stiffness and strength with increasing T_g-exceeding temperature was therefore observed. This increase was attributed to the completion of cure as discussed in Section 5.4.1 (see *Figure 5.4*). The secondary relaxation furthermore disappeared with increasing T_g-exceeding temperature (see stiffness values at 20°C in *Figure 5.7a*). Similar results were found in [2-3] and attributed to an initially low cross-link density.

The stiffness of specimens cooled from 150°C to 50°C was lower than expected from the trend shown by the results. This might have been caused by initiating material decomposition and this assumption is confirmed by changes in the specimen color, as shown in *Figure 5.9*. Strength values at T_g-exceeding temperatures of 100 and 150°C were affected by tab failure (see *Figure 5.9*) and are therefore not included in *Figure 5.7b*.

Figure 5.9 Specimen color changes and tab failure at elevated temperatures (Sikadur-30)

In addition to the recovery behavior at t_{ex}=0.5 hour, an extension to 2.0 hours was also investigated. The corresponding stiffness results, shown in *Figures 5.10* and *5.11*, do not exhibit a clear trend at first glance. At T_{ex}-T_{rec} of 60-50°C and 100-60°C a stiffness increase occurred – in contrast to 100-50°C and 150-60°C, where in the first case a slight

and in the second case a significant decrease resulted. The results can be explained by comparing T_{rec} to the T_g obtained at 0.5 and 2.0 hours exposure according to *Figure 5.5*. In the 60-50°C case, T_g increased from 48°C ($T_g<T_{rec}$) to 52°C ($T_g>T_{rec}$). Similarly in the 100-60°C case, T_g increased from 52°C (<60°C) to 63°C (>60°C), i.e. the material was fully in the glassy state at 2.0 hours while it was still in the glass transition range at 0.5 hour. In the 100-50°C case, the material was already in the glassy state at 0.5 hour (T_g=52°C > T_{rec}=50°C), which explains why stiffness did not significantly change from 0.5 to 2 hours.

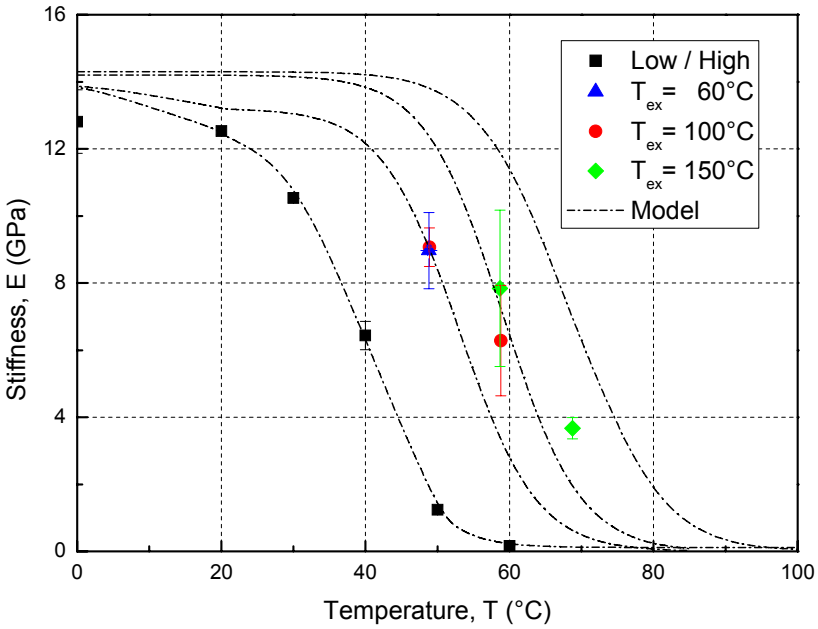

Figure 5.10 Effect of T_g–exceeding temperature, T_{ex}, during t_{ex}=2.0 hours on stiffness (t_{rec}=0.5 hour) (Sikadur-30)

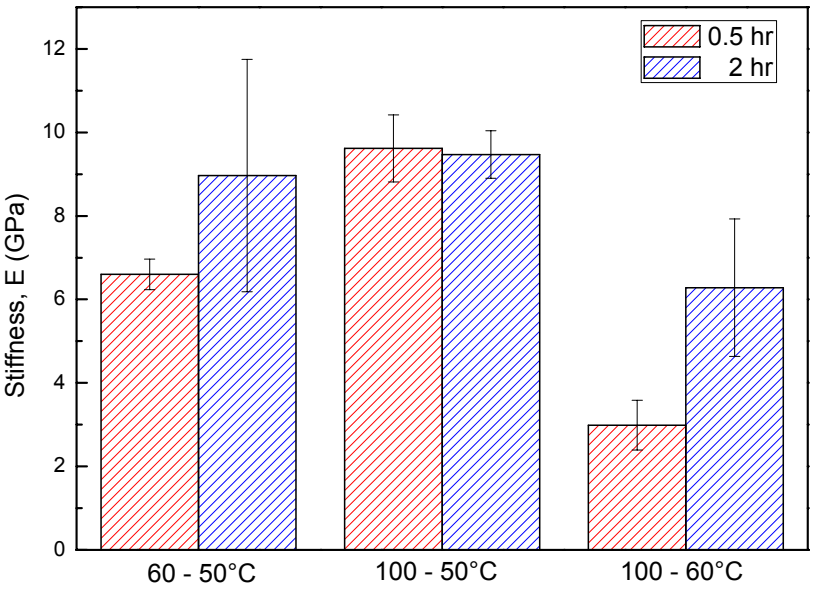

Figure 5.11 Effect of T_g–exceeding duration, t_{ex},on stiffness (T_{ex}-T_{rec} combinations are indicated, t_{rec}=0.5 hour) (Sikadur-30)

The stiffness values of specimens exposed to a temperature of 100°C for 2.0 hours and examined at 50°C did not follow the expected trend, see *Figure 5.10* (values were too low). Since no material degradation was assumed at this temperature, an effect of the recovery duration was hypothesized. The effect of the extension of the recovery time, t_{rec}, on stiffness is shown in *Figure 5.12* for different experimental conditions. In all cases,

extending the recovery time resulted in increased stiffness. This increase was attributed to providing sufficient time for reformation of the secondary bonds between the polymer chains.

Eight T_g–exceeding cycles

The specimen stiffness at 30, 50 and 60°C, obtained after eight successive cycles between 30 and 60°C is shown in *Figure 5.13*. Specimens exhibited full recovery with no observed degradation effect resulting from cyclic thermal loading. Since specimens were subjected to a total time of four hours (8·0.5) at 60°C, an increase in stiffness was observed compared to specimens examined after 0.5 and 2 hours' exposure at 60°C (curves also shown in *Figure 5.13*).

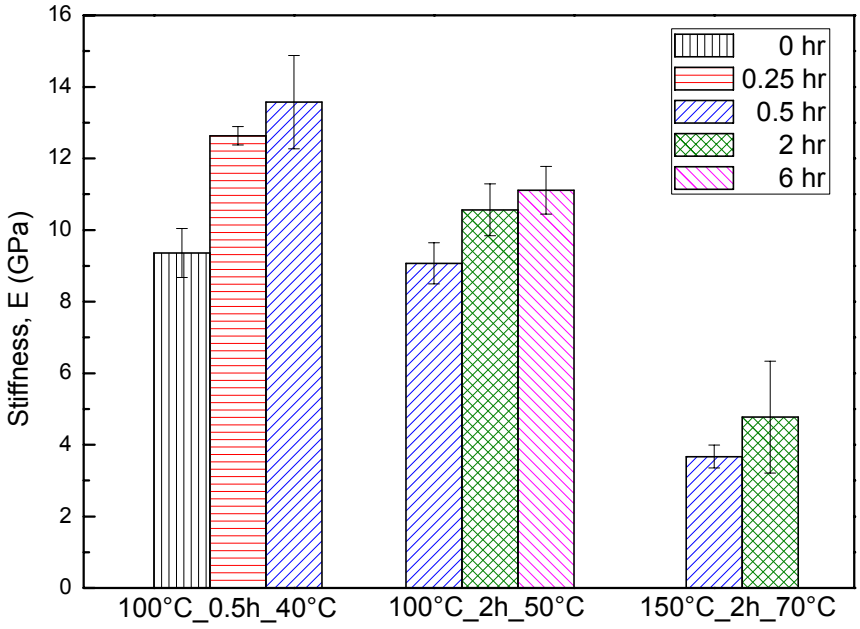

Figure 5.12 Effect of recovery duration, t_{rec}, on stiffness for different cases T_{ex}-t_{ex}-T_{rec} (Sikadur-30)

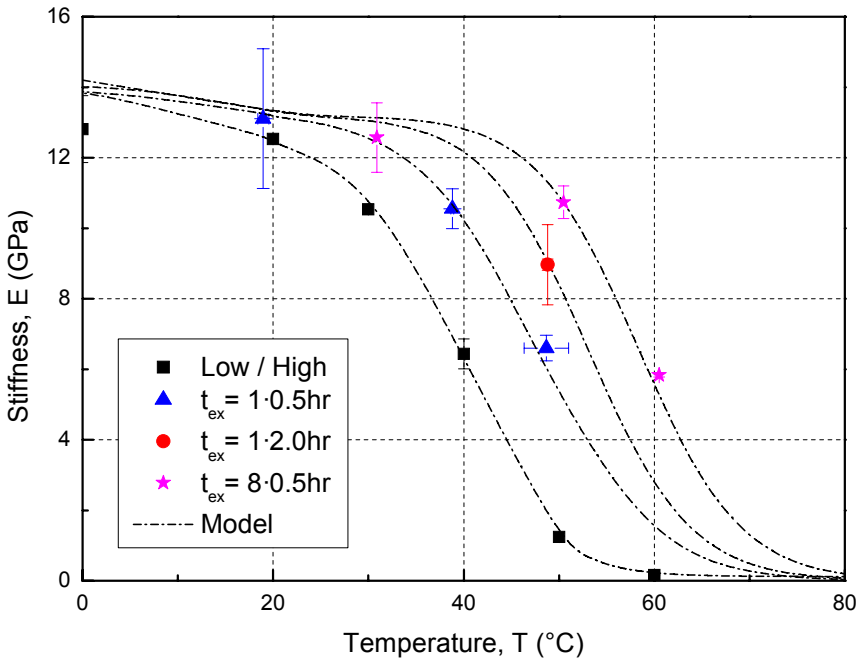

Figure 5.13 Effect of eight T_g-exceeding cycles (T_{ex}=60°C) on stiffness, comparison to one-cycle curves at t_{ex}=0.5/2.0 hours (Sikadur-30)

5.5 Modeling of experimental results

5.5.1 Glass transition temperature

The two models presented in Section 5.2 were fitted to the stiffness and strength results of ″low/high″ temperature and ″one T_g–exceeding cycle″ investigations shown in *Figures 5.7a* and *b* in order to compare the resulting T_g values to those obtained from DSC. The values of the Weibull modulus m_2 and constant k, resulting from the fitting, varied for each case, as shown in *Table 5.3*. Average values of m_2 = 5.0 (corresponding to glass transition – Phase 2) and k = 0.083 were considered for the T_g prediction. The value of m_2 = 5.0 agreed with the result obtained by Mahieux for filled polymers (same filler content of ~55% by weight as for the adhesive used in this study) compared to a value of 20 for unfilled polymers [12]. The average T_g difference between the two models was ~4°C. Compared to the DSC values, Gibson's model provided more accurate results (T_k), as shown in *Table 5.3*. The more significant differences resulting from Mahieux's model (T_2 results) could be attributed to the T_g measurement method. The model is based on the tan-δ peak from DMA, which usually provides higher T_g values than DSC [15-16].

Table 5.3 T_g resulting from modeling and DSC experiments (t_{ex}=0.5 hour)

Condition	Mahieux			Gibson			DSC
	m_2	T_2	R^2	k	T_k	R^2	T_g
low/high	4.15	46.2	0.957	0.082	43.9	0.989	45.6 ± 2.75
T_{ex} = 60°C	5.25	52.4	0.999	0.077	47.2	0.989	47.7 ± 0.80
T_{ex} = 100°C	5.64	56.5	0.974	0.089	52.4	0.979	52.6 ± 1.37
T_{ex} = 150°C	5.52	66.0	0.923	0.062	62.6	0.932	62.5 ± 1.43

5.5.2 Thermomechanical properties

To model the thermomechanical recovery behavior, Gibson's model (Eq. (5.2)) was modified by implementing the change in the glass transition temperature due to the additional curing at T_{ex}. The effect of T_{ex} and t_{ex} on T_g, as shown in *Figure 5.5*, can be described as follows:

$$T_g = \left(T_{gL} + (0.079 t_{ex} - 0.0516) T_{ex} - (4.08.10^{-4} t_{ex} - 0.0011) T_{ex}^{\ 2} \right) \tag{5.3}$$

Furthermore, Eq. (5.2) was also used to model the secondary relaxation by replacing P_u, P_R and T_k (T_g) by P_1, P_2 and T_1 (see definitions from Mahieux's model) and using a k value of 0.12.

The modeling results, shown in *Figures 5.7a, b* and *5.10* showed good agreement with the experimental results across glass transition up to T_{ex} = 100°C. The secondary relaxation modeling was less accurate due to the predefined descending trend of the model, which could not exhibit a plateau. The differences at 150°C occurred due to the initiation of decomposition, as previously explained. Degradation of the material could have also been taken into account by Gibson's model by taking the resin decomposition into account (adding a residual resin content parameter) [6].

The same modified model was used to describe the results of the cyclic experiments. Equivalent to the total time at 60°C, a t_{ex} of 4 hours was selected (8·0.5 hour). The results are shown in *Figure 5.13* and agree well with experimental values. The cooling phases apparently did not influence the results; the total T_g–exceeding duration was the driving parameter.

5.6 Conclusions

The thermomechanical recovery behavior of a commercial cold-curing structural epoxy adhesive was experimentally investigated and modeled. The material was pre-cured for 2

weeks at laboratory temperatures of approximately 20°C, resulting in a T_{gL}=45.6° at a curing degree of around 94%. The following conclusions were drawn:

1) Exposing the adhesive to temperatures T_{ex} above the glass transition temperature T_{gL} increased the latter by 58% for the longest exposure duration of t_{ex}=4 hours though the curing degree increased by only 6%. A model was established by fitting the experimental results that predicts T_g as a function of exposure temperature $T_{ex} > T_{gL}$ and time t_{ex}.
2) Cooling the adhesive from temperatures $T_{ex} > T_{gL}$ to recovery temperatures $T_{rec} < T_{gL}$ led to full recovery of the mechanical properties (tensile stiffness and strength). The secondary bonds between the polymer chains obviously fully reformed after cooling. A temporary exceeding of T_g, therefore, did not result in any degradation of the material (as long as the temperature remained below the initiation of decomposition). On the contrary, the mechanical properties significantly improved due to post-curing of the material.
3) In addition to the temperature level T_{ex}, the duration of exposure at this level, t_{ex}, and the recovery duration, t_{rec}, also significantly influenced the mechanical properties.
4) Simulating temperature fluctuations by eight consecutive cycles across glass transition also improved the mechanical properties and did not lead to any degradation.
5) An existing model for predicting temperature-dependent mechanical properties was extended to also describe the recovery behavior. The simulations agreed well with the experimental results.

5.7 References

B. Ellis, *"Chemistry and technology of epoxy resins"*, Blackie academic professional, an imprint of Chapman & Hall, 1993. [1]

W.K. Goertzen and M.R. Kessler, *"Thermal and mechanical evaluation of cyanate ester composites with low-temperature processability"*, Compos. Pt. A-Appl. Sci. Manuf., 2007; 38(3): 779–784. [2]

J.K. Lee and J.K. Gillham, *"Evolution of properties with increasing cure of a thermosetting epoxy/aromatic amine system: physical ageing"*, J. Appl. Polym. Sci., 2003; 90(10): 2665–2675. [3]

I. Stewart, A. Chambers and T. Gordon, *"The cohesive mechanical properties of a toughened epoxy adhesive as function of cure level"*, Int. J. Adhes. Adhes., 2007; 27(4): 277–287. [4]

O. Moussa, A. Vassilopoulos and T. Keller, "*Effects of low temperature curing on physical properties of structural epoxy adhesive joints in bridge construction"*, Int. J. Adhes. Adhes., 2011; 32(1): 15-22. [5]

M.F. Ashby and D.R.H. Jones *"Engineering materials 2: an introduction to microstructures, processing and design"*, Oxford: Pergamon Press, 1997. [6]

C.A. Mahieux and K.L. Reifsnider, *"Property modeling across transition temperatures in polymers: a robust stiffness-temperature model"*, Polymer, 2001; 42(7): 3281–3291. [7]

L.F.M. Da Silva. and R.D. Adams, *"Measurement of the mechanical properties of structural adhesives in tension and shear over a wide range of temperatures"*, J. Adhesion Sci. Technol., 2005; 19(2): 109–141. [8]

C.A. Mahieux, K.L. Reifsnider and S.W. Case, *"Property modeling across transition temperatures in PMC's: part I. tensile properties"*, Appl. Compos. Mater., 2001; 8(4): 217–234. [9]

A.G. Gibson, Y.-S. Wu, J.T. Evans and A.P. Mouritz, *"Laminate theory analysis of composites under load in fire"*, J. Compos. Mater., 2006; 40(7): 639–658. [10]

C.B. St. Pourcain and A.C. Griffin, *"Thermoreversible supramolecular networks with polymeric properties"*, Macromolecules., 1995; 28(12): 4116–4121. [11]

C.T. Vijayakumar and H. Kothandarman, *"A comparative study of the kinetic and thermodynamic approaches to the glass transition phenomenon in high polymers"*, Thermochim. Acta, 1987; 118(C): 159–181. [12]

M. Shimbo, M. Ochi and A. Katsumasa, *"Internal stress of cured epoxide resin coatings having different network chains"*, J. Coat. Technol., 1984; 56(713): 45–51. [13]

Y. Nakamura, M. Yamaguchi, K. Iko, M. Okubo and T. Matsumoto, *"Internal stress of epoxy resin modified with acrylic polymers containing functional groups produced by in situ u.v. radiation polymerization"*, Polymer, 1990; 31(11): 2066–2070. [14]

R.E. Wetton, in: B.J. Hunt and M.I. James (Eds.), *"Polymer characterization"*, Blackie, London, 1993, P.178. [15]

J.J. Aklonis and W.J. MacKnight, "*Introduction to polymer viscoelasticity*", 2nd ed., New York, 1983, P. 60. [16]

6 Long-term performance

6.1 Overview

As shown in Chapter 3, low-temperature curing leads to an incompletely cured adhesive system as it greatly decelerates the development of full physical and mechanical properties, which can only be achieved after significantly longer curing periods. Therefore, mechanical properties are expected to change over the long term (several years) as curing of the adhesive will still be taking place [1-2].

The long-term behavior of structural adhesives is usually influenced by different factors, e.g. environmental effects and creep. These effects normally have a negative influence on the mechanical performance of the adhesive, leading to a reduction in the mechanical properties. On the other hand, an increase in cure level with time leads to the formation of a more densely branched polymeric network that improves the mechanical behavior of adhesives. In the case of well-sealed adhesive joints, the effect of environmental conditions (such as humidity and salinity) can be much reduced or even eliminated and therefore the positive effect of the increase in cure level prevails.

The long-term curing behavior of a cold-curing structural adhesive is investigated in this chapter. An accelerated experimental method based on post-curing of the adhesive at different temperatures is used to simulate the long-term improvement in physical and mechanical properties up to full cure. A model previously developed for predicting the long-term properties of concrete is modified to predict the long-term mechanical properties of cold-curing structural adhesives.

6.2 Experimental investigation

6.2.1 Experimental set-up and procedure

Physical experiments
A total of 52 DSC samples, each weighing 5 -10 mg, were examined during this study. After curing under laboratory conditions (T=23±5°C and RH=50±10%), post-curing at different temperatures and during different time periods according to *Tables 6.1* and *6.2* was performed either outdoors, under laboratory conditions or in a climate chamber (details are given in Section 6.2.2). Post-cured samples were then cooled under laboratory conditions during 24 hours. DSC scans were performed according to the procedure described in Section 3.2.1. The curing degree (as function of residual cure) and the corresponding T_g were obtained.

Mechanical experiments
A total of 55 tension specimens of Sikadur-330 were fabricated and examined according to ASTM D 638, as described in Section 4.2.3 and shown in *Figure 4.2*. Specimens were cured under laboratory conditions for one week (T=23±5°C and RH=50±10%). Post-curing of specimens was then carried out under different conditions (temperature and time as presented in *Table 6.2*) and then cooled for 24 hours at laboratory temperature. Five specimens were examined for each condition and the results for a minimum of three specimens were analyzed after discarding specimens with flaws or voids and those exhibiting a tab failure.

6.2.2 Experimental program

In order to investigate the long-term change in T_g, DSC samples were prepared from adhesive material cured under laboratory conditions during different time periods, t, of between 1 and 7 years as shown in *Table 6.1*. Similar samples were prepared from material exposed to outdoor curing (in Lausanne) between 2003-2010 for comparison of results with samples cured at laboratory temperature. A minimum of two samples was examined for each curing condition.

Furthermore, several sets of tensile specimens and DSC samples were examined according to the conditions shown in *Table 6.2*. The long-term development was simulated by accelerating the reactions by post-curing at elevated temperatures.

Table 6.1 Experimental program for DSC samples cured during several years

Curing Condition	**Laboratory**						**Outdoors**	
***t* (yr)**	1	2	3	4	5	6.75	6.75	7.25
Physical								

Table 6.2 Experimental program for post-curing of DSC samples and tensile specimens

	Procedure			**Verification (1)**			**Verification (2)**			**Verification (3)**	
T_{pc} **(°C)**	**Reference**	**60°C**					**40°C**			**~ 23°C**	
t_{pc} **(hr)**	0	4	8	24	72	168	24	48	168	2160	17520
Physical											
Mechanical											

The tensile specimens and DSC samples from one set, denominated the reference set, were examined immediately after curing (no post-curing involved). The obtained strength and stiffness values and the corresponding glass transition temperature, T_{gL}, were used as reference values during the analysis in order to observe the changes in properties after subjecting the material to various post-curing conditions. Post-curing of several sets was then performed in the climate chamber under different conditions as shown in *Table 6.2*. Four experimental groups can be characterized as follows:

Group 1, designated as the procedure group in *Table 6.2*, consists of the reference set in addition to two sets of tensile specimens and DSC samples post-cured at 60°C during four and eight hours to establish the model.

Group 2, designated as verification 1, consists of three sets of tensile specimens and DSC samples post-cured at 60°C during 24, 72 and 168 hours. Results from this group are used to verify the applicability of the model when extrapolated.

Group 3, designated as verification 2, consists of three sets of tensile specimens and DSC samples post-cured at 40°C during 24, 48 and 168 hours. Results from this group are used to investigate the effect of post-curing temperatures below T_g.

Group 4, designated as verification 3, consists of two sets of tensile specimens only cured under laboratory conditions (~ 23°C) during 3 months and two years. Results from this group are used to verify the applicability of the experimental method (accelerated curing procedure) and further verify the developed model.

Moreover, an additional verification of the ultimate T_g of the adhesive was carried out by post-curing DSC samples at 100°C during 24 and 72 hours.

6.3 Experimental results and discussion

6.3.1 Physical behavior

The change in T_g over a long-term period of up to seven years is presented in *Figure 6.1*. An almost bi-linear increase in T_g took place.. After one year, T_g increased by approximately 29% while the increase after 7 years was 42%. Samples cured outdoors showed a supplementary increase in T_g values due to their exposure to higher temperatures (> 30°C during certain summers) compared to samples cured in the laboratory. It was not possible to precisely measure the curing degree corresponding to

these high T_g values due to the difficulty in precisely monitoring the small residual cure that took place during the later stages of the curing process. However, it could be concluded that a curing degree exceeding 98 % was achieved by all samples.

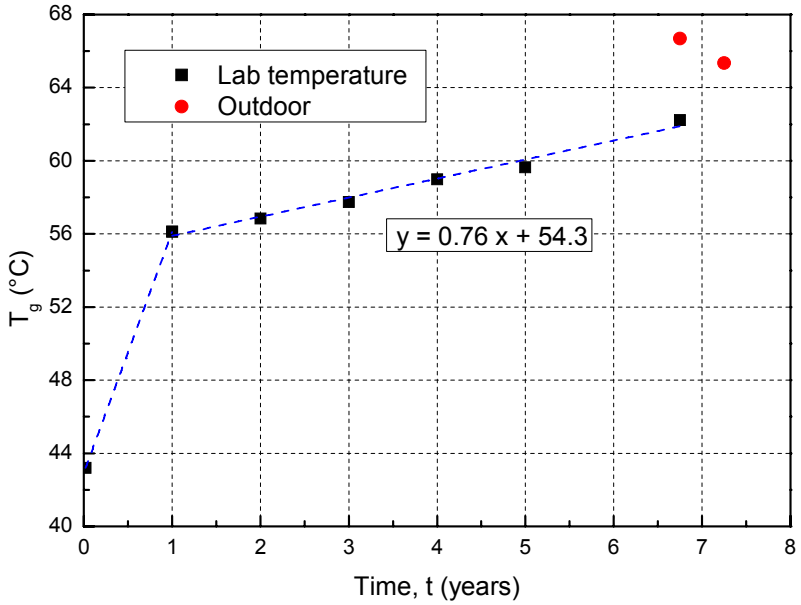

Figure 6.1 Measured T_g vs. time for samples cured for up to seven years (Sikadur-330)

The development of curing degree, α, and T_g vs. post-curing time, t_{pc}, is presented in *Figures 6.2* and *6.3* during the post-curing of samples at 40 and 60°C (results from all experimental sets are shown). The curing degree increased from an average of 96.5% (reference set cured for two weeks under laboratory conditions) to above 98% and 99% for samples post-cured at 40 and 60°C respectively. This increase was attributed to the increase in thermal energy supplied to the system, leading to an acceleration of curing reactions and resulting in a higher degree of cross-linking (that of those reactive groups that react very slowly at low-curing temperatures such as secondary amino groups or sterical hindered amino groups was particularly accelerated). An increase in T_g of around 63% and 41% was observed when samples were post-cured for one week at 60 and 40°C respectively.

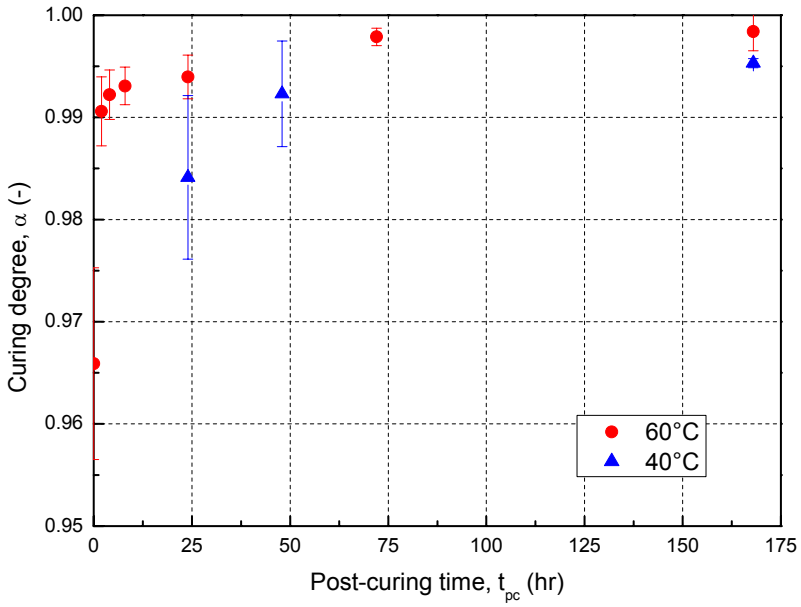

Figure 6.2 Curing degree vs. time for samples post-cured under different conditions (Sikadur-330)

The maximum attainable T_g (denominated ultimate T_g in Section 6.2.2) was obtained by post-curing samples at 100°C for 24 and 72 hours (73°C±1.26), as shown in *Figure 6.3*. Similar results were achieved at 60°C for 72 and 168 hours respectively. Therefore the maximum attainable T_g of the adhesive can be assumed as being approximately 73°C.

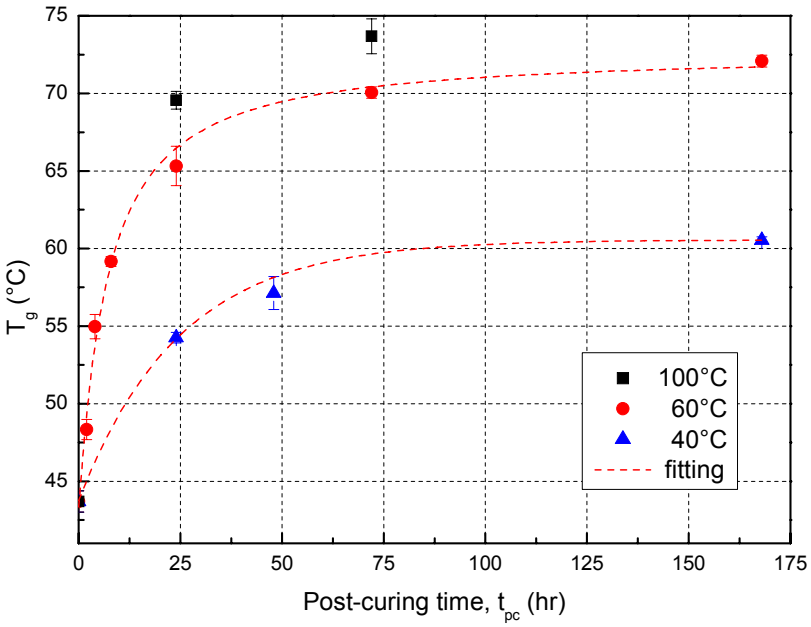

Figure 6.3 T_g vs. post-curing time for samples post-cured at different temperatures (Sikadur-330)

Approaching the bi-linear increase of T_g with time, shown in *Figure 6.1*, by a logarithmic fitting up to the ultimate T_g, the equivalent time, t_{eq}, required to achieve the same T_g values when the adhesive is cured under laboratory conditions was determined, as shown in *Figure 6.4*.

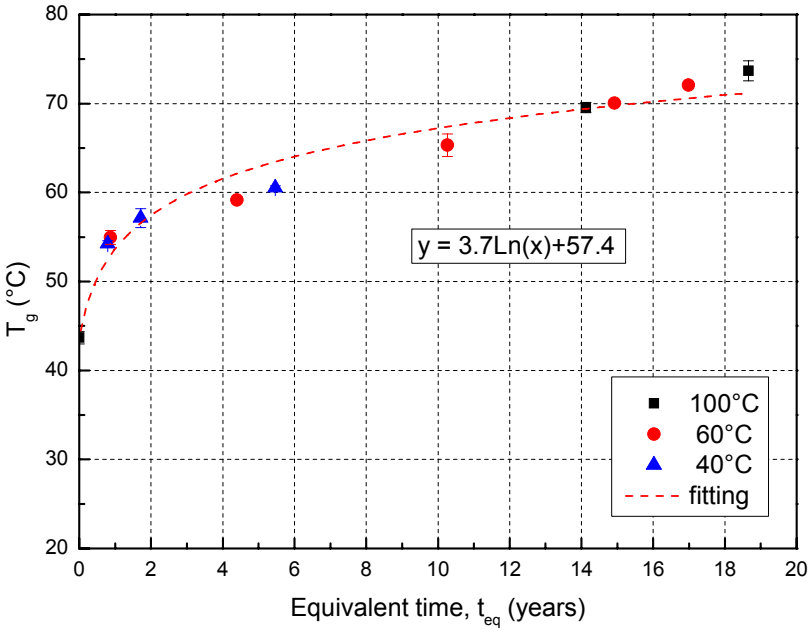

Figure 6.4 T_g vs. equivalent time under laboratory conditions for samples post-cured under different conditions (Sikadur-330)

A relationship between the post-curing time and the equivalent curing time required at laboratory temperature can then be obtained as shown in *Figure 6.5*. A dependence on the post-curing temperature was observed. The rate of increase in T_g was higher when

the post-curing temperature is increased above T_{gL} (at 60°C). Post-curing below T_{gL} (at 40°C) also exhibited an increase in T_g but at a lower rate. For instance, a post-curing time of 72 hours at 60°C would result in a T_g equivalent to that obtained during 14.8 years at laboratory temperature or almost two years at 40°C.

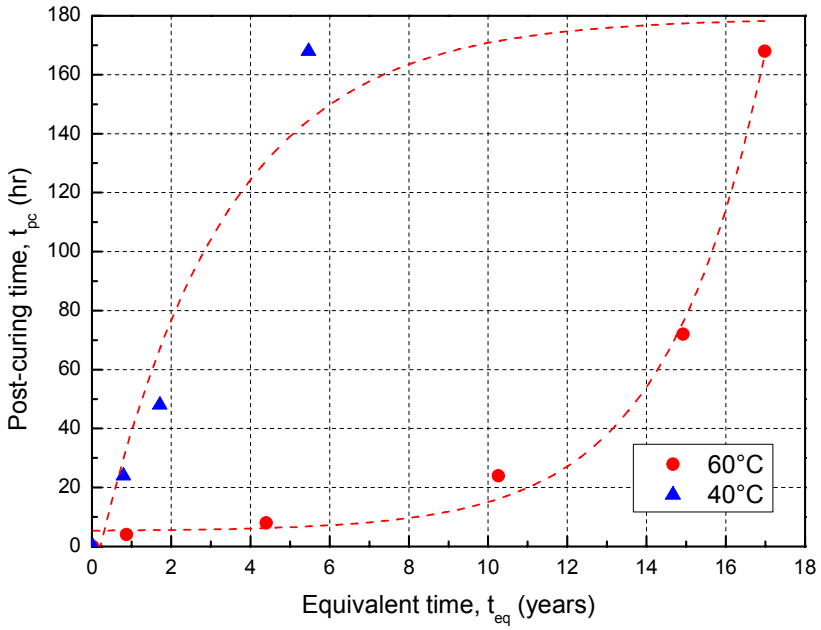

Figure 6.5 Equivalent time required for curing of samples at laboratory temperature compared to post-cured samples (Sikadur-330)

6.3.2 Mechanical behavior

The development of tensile strength and stiffness for specimens post-cured at 60 and 40°C is shown in *Figures 6.6a* and *b* respectively. By knowing the corresponding T_g, the equivalent time required to achieve a certain property level under laboratory conditions was derived from *Figure 6.4*. An increase of 48% and 15% was attained for tensile strength and stiffness respectively by post-curing at 60°C for one week (168 hours), which is equivalent to approximately 17 years.

The increase in tensile strength was more significant than that in stiffness for two possible reasons: firstly, strength is more dependent on changes in polymeric structure in terms of increase in chain branching and molecular bond strength, which is also demonstrated by the increase of strain at failure after post-curing, as shown in *Figure 6.7*. In addition, the fillers comprised in the material contribute more to the stiffness than to the strength and therefore the change in stiffness due to changes in the polymeric structure is smaller than the change in strength. An increase in mechanical property values for specimens post-cured at 40°C (verification 2) was also observed albeit at a slower rate than those post-cured at 60°C during the same post-curing periods (verification 1). Specimens cured at laboratory temperature for longer periods (verification 3) were found to follow the same trend. Of all the experimental groups, the results of the specimens of group 2 (verification 1) showed the biggest scatter, which could be attributed to an insufficiently long cooling period (24 hours).

The relationship between tensile strength and stiffness is shown in *Figure 6.8*. The quasi-linear relationship between both properties found during curing at early age in Chapter 4 was not confirmed at high curing degrees. A deviation in the long-term relationship between tensile strength and stiffness was observed, which can be attributed to the more significant increase in strength than stiffness.

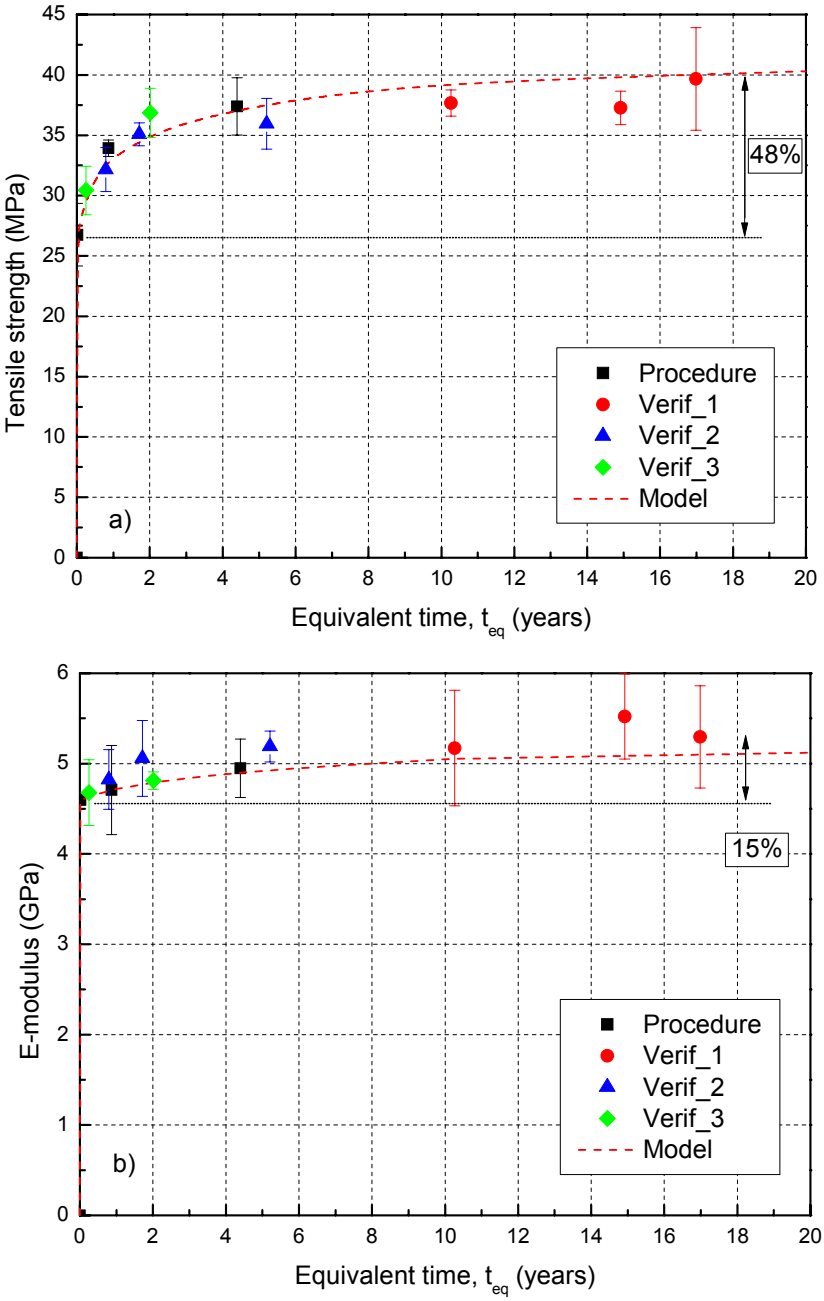

Figure 6.6 Mechanical property development due to post-curing for predicting long-term material behavior - a) Strength b) Stiffness (Sikadur-330)

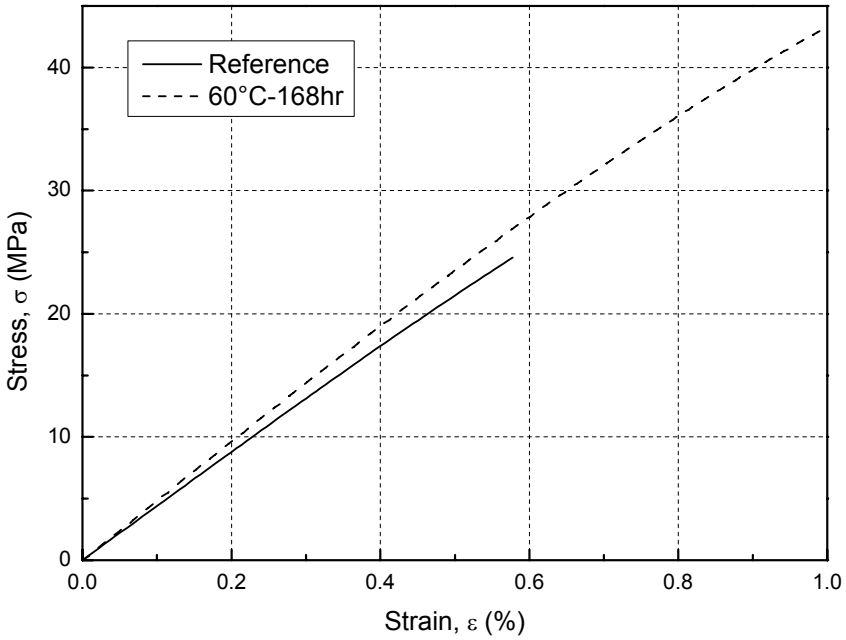

Figure 6.7 Change in stress-strain behavior due to post-curing for selected specimens (Sikadur-330)

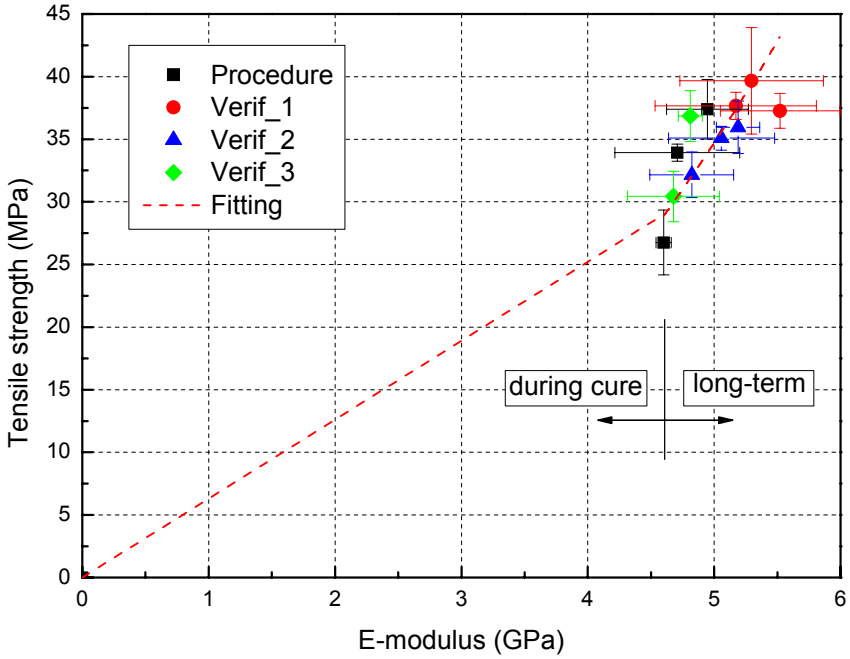

Figure 6.8 Tensile strength vs. stiffness relationship (Sikadur-330)

6.4 Modeling

6.4.1 Existing models for concrete curing

The curing behavior of both structural adhesives and concrete (setting of cement) is characterized by an exothermic reaction. The mechanical properties of both materials at young age are dependent on the curing reaction, and an increase in mechanical properties occurs over the long term [3-6]. Therefore, a model presented in [7] for concrete is adopted in order to predict the long-term development of adhesive properties. The concrete model assumes that the rate at which concrete compressive strength increases with time depends on a variety of parameters, in particular the type and strength class of the cement, the type and amount of admixtures and additions, the

water/cement ratio and environmental conditions. The development of compressive strength with time is estimated as follows [7]:

$$f_{cm}(t) = \beta_{cc}(t) f_{cm} \tag{6.1}$$

with

$$\beta_{cc}(t) = \exp\left\{ s\left[1 - \frac{28}{t} \right]^{0.5} \right\} \tag{6.2}$$

where $f_{cm}(t)$ is the mean compressive strength at a concrete age of t in days, f_{cm} is the mean compressive strength at a concrete age of 28 days, $\beta_{cc}(t)$ is a function describing the development of compressive strength with time, t is the concrete age in days and s is a coefficient which depends on the strength class of the cement. These equations are valid for a concrete temperature of 20°C. For temperatures deviating from 20°C, a temperature-adjusted concrete age should be used.

The development of the tensile strength of concrete with time is much more difficult to predict because it is significantly influenced by the development of shrinkage stresses, which in turn depend on structural member size and curing conditions. Therefore, only for a concrete age exceeding 28 days, it may be assumed that the development of tensile strength with time is similar to that of concrete compressive strength [7].

The modulus of elasticity of concrete develops more rapidly than does the compressive strength. $E_c(t)$ is to a large extent controlled by the modulus of elasticity of the aggregates, which in turn is independent of concrete age. This is taken into account in the following equations:

$$E_{ci}(t) = \beta_E(t) E_{ci} \tag{6.3}$$

with

$$\beta_E(t) = \left[\beta_{cc}(t) \right]^{0.5} \tag{6.4}$$

where $E_{ci}(t)$ is the tangent modulus of elasticity at a concrete age of t in days, E_{ci} is the tangent modulus of elasticity at a concrete age of 28 days, and $\beta_E(t)$ is a function that describes the development of the modulus of elasticity with time.

6.4.2 New model for cold-curing adhesives

The model for concrete compressive strength development was adopted to predict the long-term change in the strength and stiffness of structural adhesives as follows:

$$P(t) = \beta_P(t) P_7 \tag{6.5}$$

where P_7 is the value of the mechanical property after seven days curing at laboratory conditions, usually given in the datasheets provided by most manufacturers of commercial adhesives. Assuming that the mechanical properties are governed by the physical state of the adhesive, the s factor in Eq. (6.2) was replaced by a term, $\beta_p(t)$, expressing the change in T_g with time as follows:

$$\beta_P(t) = \exp\left\{ \left(1 - \frac{7}{t} \right)^{0.5} \left[\frac{T_g(t) - T_{g,7}}{T_{g,7}} \right]^n \right\} \tag{6.6}$$

where $T_g(t)$ is the glass transition temperature of the adhesive at time t measured as the midpoint of the T_g step in DSC or at the peak point of the tan-δ curve during DMA, $T_{g,7}$ is the glass transition temperature of the adhesive after seven days curing at 23°C (laboratory conditions) and n is a property-dependent parameter describing long-term property development. Due to the negligible influence of shrinkage in the curing of adhesives, the compressive and tensile strengths can be described by the same model. Stiffness can also be described using the same model as applied for concrete stiffness in Eq. (6.3). Moreover, the development of adhesive strength and stiffness are similar regardless of the rate of development, as demonstrated in Chapter 4.

6.4.3 Modeling results

The values of n for tensile strength and stiffness were obtained by fitting Eq. (6.6) to the experimental results (the procedure points in *Table 6.2*) and applying the corresponding T_g values shown in *Figure 6.4*. Values of 1.06 and 2.62 for tensile strength and stiffness were obtained respectively. The value of n resulting from the fitting of strength results (~1) indicated that the rate of change in strength and T_g is somewhat similar, on the other hand the rate of change in stiffness was lower than that of T_g and consequently strength, yielding to an n value > 1. The rate of change of mechanical properties with respect to T_g is also confirmed by the experimental results, as shown in *Figure 6.9*. A steeper slope was obtained in the case of strength.

Three sets of verifications were performed as previously mentioned. Firstly, the model was extrapolated (using the same n values obtained from the fitting) and the modeling curve was compared to results for specimens post-cured at 60°C for longer periods (verification 1). A good agreement was found. Moreover, the results for specimens post-cured at 40°C (verification 2) compared well to the modeling curve and therefore confirmed the possibility of post-curing at temperatures below T_g, regardless of the rate of increase in properties. The third verification was performed using specimens cured under laboratory conditions for long periods (verification 3). The model also compared well to these experimental results, therefore confirming the applicability of the accelerated curing method and the validity of the model.

According to the new model, the values of tensile strength and stiffness after 50 years (an average bridge service life) would be 44.0 MPa and 5.5 GPa respectively. These values show an increase of 11% and 3 % in tensile strength and stiffness respectively compared to the maximum experimental results achieved (equivalent to approximately 17 years of ambient curing).

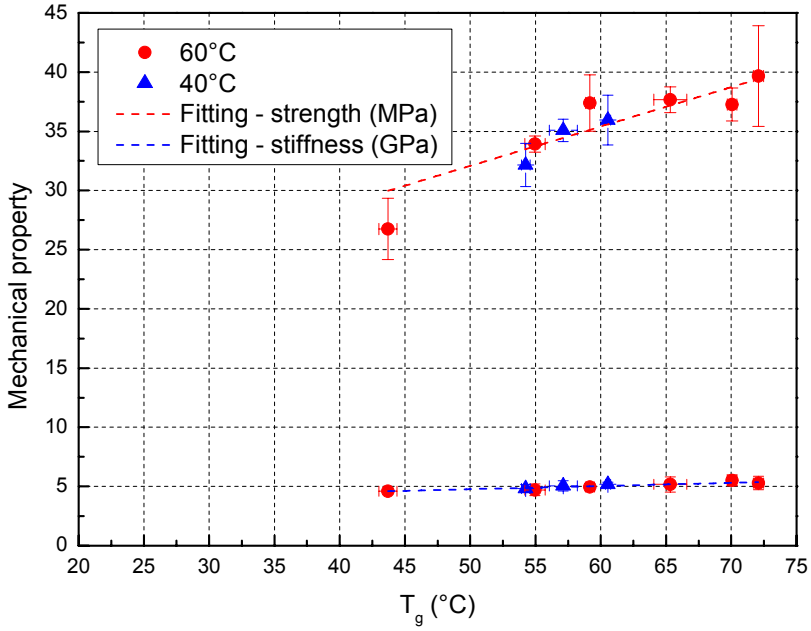

Figure 6.9 Change in strength and stiffness vs. T_g after post-curing (Sikadur-330)

6.5 Conclusions

The long-term changes in physical and mechanical properties were investigated by accelerating the curing reaction by post-curing at different temperatures above and below T_g during different periods. Also, a new model was established to predict the change in mechanical properties of structural adhesives by taking into account the change in the adhesive's physical state. The following conclusions were drawn:

1) The experimental data available concerning the glass transition temperature, T_g, for periods of up to 7 years could be extrapolated up to 17 years by accelerating the curing reaction by post-curing at elevated temperatures (slightly above and below T_g).
2) Based on this extrapolation procedure, tensile strength and stiffness measurements could also be extrapolated up to 17 years.
3) An existing model for the long-term development of concrete properties was modified for the prediction of the long-term mechanical properties of adhesives. The applicability of the acceleration procedure and the new model was confirmed by several verification procedures.
4) Structural adhesives exhibit significant increases in T_g, strength and stiffness over the long term provided that joints are adequately sealed and protected from environmental impact, particularly humidity and UV radiation.

6.6 References

J.K. Lee and J.K. Gillham, *"Evolution of properties with increasing cure of a thermosetting epoxy/aromatic amine system: physical ageing"*, J. Appl. Polym. Sci., 2003; 90(10): 2665–2675. [1]

I. Stewart, A. Chambers and T. Gordon, *"The cohesive mechanical properties of a toughened epoxy adhesive as function of cure level"*, Int. J. Adhes. Adhes., 2007; 27(4): 277–287. [2]

E. Sancaktar, J. Hooshang and R.M. Klein, "*The effects of cure temperature and time on the bulk tensile properties of a structural adhesive*", J. Adhes., 1983; 15(3-4): 241-264. [3]

S.J. Shaw and D.A. Tod, "*The effect of cure conditions on a rubber-modified epoxy adhesive*", J. Adhes., 1989; 28(4): 231-246. [4]

R.N. Tolbert, R.M. Hackett, M.H. Baluch, "*Parameter testing of epoxy polymer concrete*", Polym. Eng. Sci., 1976; 16(8): 575-578. [5]

G.S. Wojcik, "*Effects of atmospheric and construction conditions on concrete equivalent ages*", ACI Mater. J., 2004; 101(5): 376-384. [6]

H. Müller and M. Haist, *"Effects of time upon strength deformation"*, fib Bulletin 51: structural concrete – Text book on behaviour, design and performance, vol. 1, 2009: 53-71. [7]

7 Application in bridge construction

7.1 Overview

As previously mentioned, bridge construction continues throughout the year and is not interrupted during winter because of the unacceptable traffic obstructions this would cause. To obtain the benefits of structural adhesive bonding and enable a widespread application of this technique, rapid bonding during wintertime - at relatively low temperatures - must thus be possible. The results of this investigation show, however, that curing at low temperatures, i.e. at around 5-10°C, develops very slowly. At 5°C, for example, a curing time of several days is required to obtain around 80% cure and consequently the development of mechanical properties at low curing temperatures is greatly decelerated, as discussed in Chapter 4. In most cases, however, time intervals of this length are not acceptable for bonding only. To accelerate curing and the development of mechanical properties, the joint must therefore be conceived in such a way that it can either be heated or that the curing heat cannot easily dissipate. In the case of steel adherends, with relatively high thermal conductivity, the first method seems more suitable while in concrete construction the second method seems more adequate due to the lower thermal conductivity.

Together with curing degree and mechanical properties, the glass transition temperature also develops very slowly. This latter delay however is not as critical as the former because temperatures are low during winter and the T_g will not be exceeded in most cases. Subsequently, during spring, the T_g will develop rapidly with increasing temperature. According to *Figure 3.10*, 3 to 4 days at 25°C suffice for the maximum value to be reached.

On the one hand, curing and the associated mechanical properties already develop at temperatures slightly above 0°C albeit slowly. On the other hand, bridge construction, in most cases, occurs in different stages and during the construction stages full mechanical properties are often not required. The models developed above allow the required curing time to be estimated as a function of curing temperature and, based on the required level of full mechanical properties, can serve as a useful tool for establishing the time schedule for construction stages as discussed concerning *Figure 4.12.*

7.2 Potential bonded joints

In the framework of this project, various types of bonded joints can be executed in bridge construction. Potential applications are listed in *Table 7.1,* which summarizes the details concerning each type of joint, including the expected loads and other considerations. The degrading effects of humidity are not included assuming that joints are properly sealed.

Three joint types (A, C and F in *Table 7.1*) have been selected to demonstrate how the models developed in Chapters 3 and 4 can be applied to estimate either temperature-dependent mechanical properties or waiting periods for achieving a certain property level. The selection concerns primary structural joints in new constructions (types A and C) or joints required for the rehabilitation and strengthening of existing bridges (type F). However, the same verification procedure can be applied for any of the joint types listed in *Table 7.1*.

Table 7.1 Overview of potential bonded bridge joints

Joint	Type	Loads	Specific effects	Notes
A	Steel girder – concrete deck	Shear - tension	Fatigue - creep	Structural
B	Parapet joints	Shear	Impact - temperature	Semi-structural
C	Transverse deck or girder joints (segmental bridging)	Shear - compression	Fatigue - creep - temperature	Structural
D	Guard rail fixation	Tension (peeling) - shear	Impact - temperature	Structural
E	Expansion joints	Tension (peeling)	Impact - fatigue - temperature	Semi-structural
F	Steel rebars in concrete	Shear	Temperature	Structural
G	Strengthening with CFRP strips	Shear - transverse tension	Temperature	Structural

7.3 Study parameters

7.3.1 Exposure conditions

The curing of cold-curing adhesives and the corresponding development of mechanical properties in outdoor applications are affected by many parameters, primarily weather conditions during and after joint fabrication, type of adhesive and adherends and geometrical joint configuration. The latter two mainly influence the amount of reaction heat trapped in the joint and if this amount is significant, the drawback of low environmental temperature can be at least partially compensated.

Bridge joints are subjected to temperature variations during the whole year. In the central alpine region of Europe, low temperatures during winter vary as shown in *Figure 7.1*. Daily average temperature and humidity variations between 1961-1990, recorded in Switzerland at selected weather stations in regions experiencing low, medium and high temperatures are shown in *Figure 7.2* [1]. The lowest values vary between approximately -5°C (Zermatt) and 3°C (Lugano) while the highest values do not exceed 26°C (Lugano).

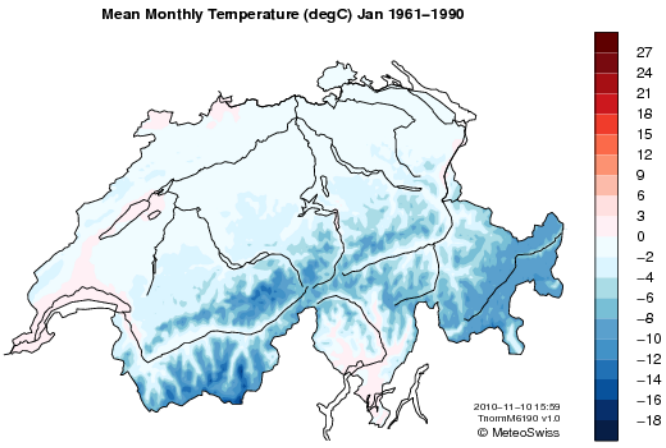

Figure 7.1 Average monthly temperature during January recorded in Switzerland between 1961 and 1990 [1]

In addition to temperature, bridges are exposed to humidity and salinity. Water, in both liquid and vapor form, has proved to be the most hostile environment for adhesives and adhesively-bonded joints [2-5]. Therefore, proper sealing of the joints is essential and, if this is ensured, only the effect of temperature on the short- and long-term mechanical properties has to be taken into account.

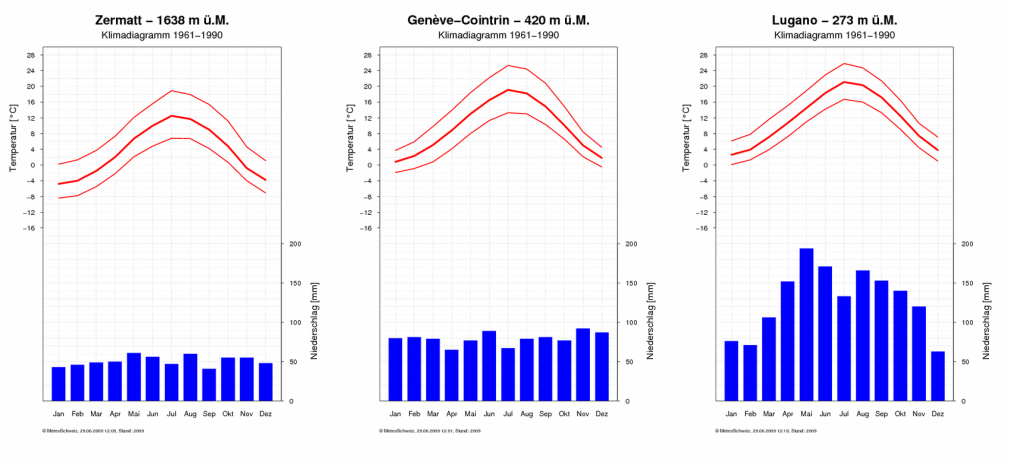

Figure 7.2 Average daily temperature and humidity variations recorded at different stations in Switzerland between 1961 and 1990 [1]

It is well known that the bridge surface temperature differs from the surrounding air temperature and mainly depends on heat transfer by radiation and convection. Direct solar radiation, radiation from the atmosphere and radiation from surrounding surfaces can all impact the surface temperature. Convection is the heat transfer from bulk fluid movement caused by the wind.

The temperature in the joint layer differs again from the surrounding air and surface temperature and depends mainly on its depth inside the construction, i.e. the adherend thickness, the adherends' thermal conductivity and the surface temperature [6-7]. This complex heat transfer behavior can either be modeled by complex analytical models or numerical modeling taking into account all boundary conditions and parameters affecting the temperature changes. Since the determination of the exact joint temperature was not the objective of this research, the ambient air temperature is considered as the curing temperature of the adhesive in the following.

7.3.2 Temperature-dependent property development

The development of adhesive properties as a function of curing temperature can be expressed by the model presented in Section 4.6. This model developed for tensile properties can be generalized for shear and compressive properties if the material satisfies the isotropy criterion:

$$G = \left[\frac{E}{2(1+\nu)} \right] \tag{7.1}$$

where E and G are the tensile and shear moduli and ν is the Poisson's ratio. Experiments performed on Sikadur-30 specimens cured at laboratory temperature for 14 days resulted in an average tensile stiffness, E, and average shear stiffness, G, of 12.5±0.11 and 5.0±0.06 respectively. Applying Eq. (7.1) results in a Poisson's ratio value of 0.26, which almost coincides with a value of 0.28 for epoxies with 55% filler content according to [8]. Since the isotropic criterion can therefore be assumed as being satisfied, it can be further supposed that all material properties develop at the same rate in all directions during cure. The same model developed for the tensile properties can therefore be used for predicting the development of shear and compressive properties when the short-term "end" value of the property (P_∞ according to Chapter 4) is known. These values can be

either extracted from manufacturers' datasheets or determined experimentally using specimens cured under laboratory conditions for a period of seven days. Based on Chapter 4, the normalized development of mechanical properties (strength and stiffness) at different isothermal temperatures is shown in *Figures.7.3a* and *b* respectively.

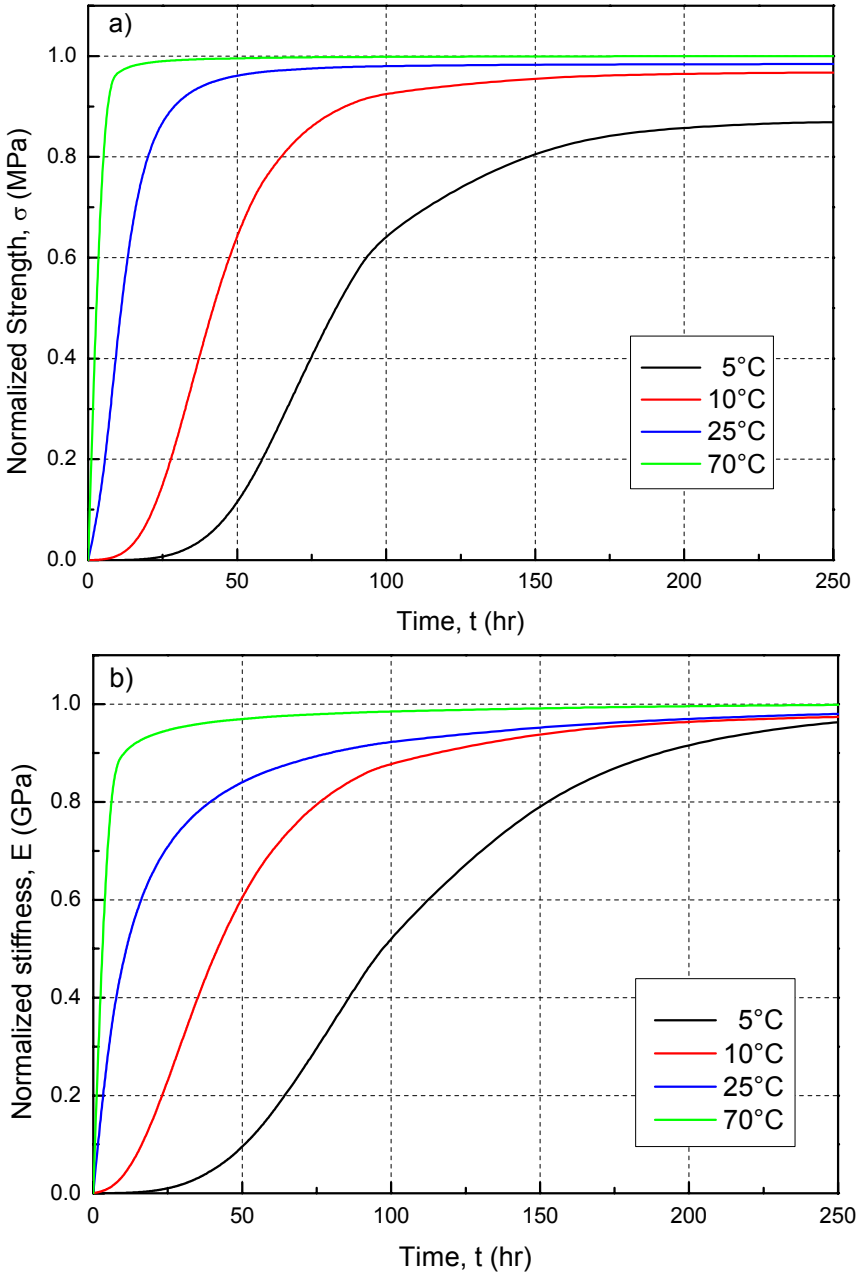

Figure 7.3 Normalized property development at different isothermal curing temperatures, a) strength, b) stiffness

7.3.3 Selection of temperature scenarios and effect on mechanical properties

The average daily air temperature was selected to examine the effect of specific curing scenarios on the development of mechanical properties. Three two-week periods were selected from the daily average air temperatures recorded at the Geneva weather station between the 07.06.2010 and 06.06.2011, as shown in *Figure 7.4*. The first two scenarios, SC1 and SC2, were selected on the basis of fixing a minimum fabrication temperature of 5°C (designated by most manufacturers as the minimum temperature at which the curing reaction can take place) with a continuous decrease to 3°C (SC1: mid to end November) or increase to 7°C (SC2: mid to end March). The third scenario, SC3, was selected at the

lowest temperature of the year (beginning to mid January) with an almost constant temperature of 1.5 °C. *Figure 7.5* shows the three scenarios in detail.

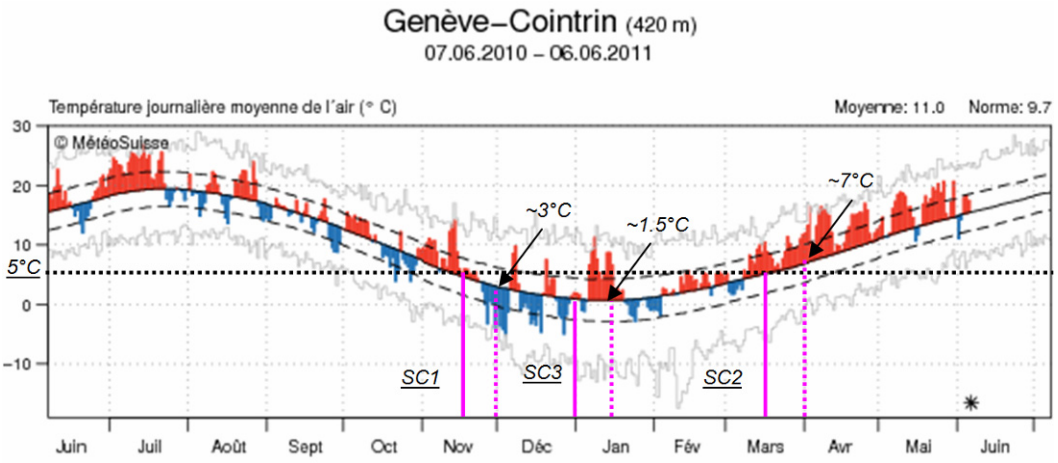

Figure 7.4 Daily average air temperature in Geneva between 07.06.2010 and 06.06.2011 [1]

The normalized strength development according to the model presented in Section 4.5 for the three scenarios is shown in *Figure 7.6*. Comparing the results after around 3 days (75 hours) for example, shows how small temperature differences can have a significant effect on mechanical property development. The temperature difference between SC1 and SC2 after 3 days is only around 1°C, while the normalized strength varies between 20% (SC1) and 40% (SC2). Curing far below 5°C in SC3 leads to a value of only 5%. After the two weeks (336 hours), however, the difference between the three scenarios decreases and is less significant (between 69 and 87%).

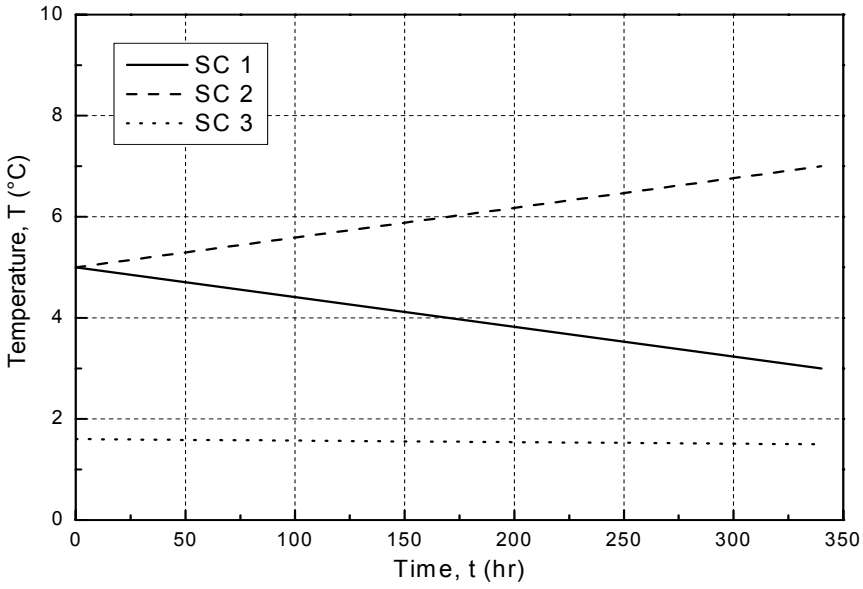

Figure 7.5 Temperature change during the selected curing scenarios

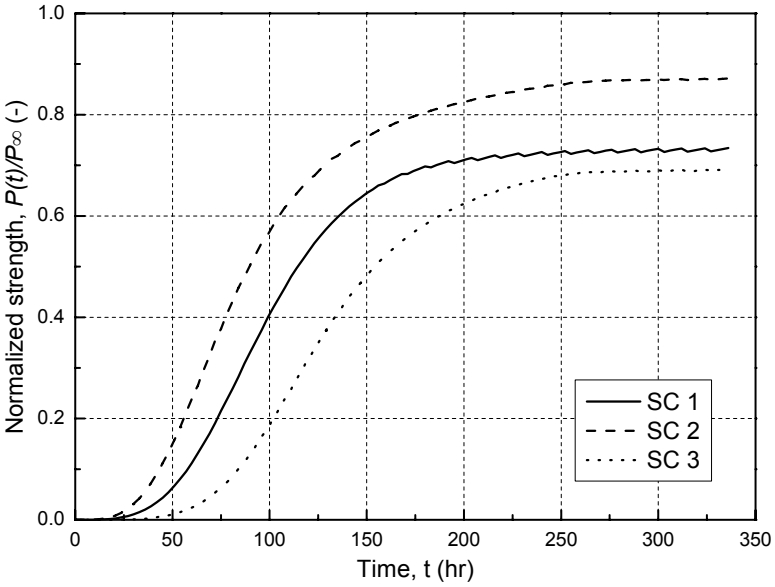

Figure 7.6 Normalized strength development during the selected curing scenarios

7.3.4 Partial safety factors and design values

According to current design concepts, the characteristic (5%-fractile) properties are reduced by partial safety factors. The EUROCOMP design code [9] specifies partial safety factors, γ_m, for adhesives based on the effect of different parameters as follows:

$$\gamma_m = \gamma_{m1} \cdot \gamma_{m2} \cdot \gamma_{m3} \cdot \gamma_{m4} \tag{7.2}$$

where γ_{m1} to γ_{m4} are the partial safety factors according to the source of the adhesive properties, method of adhesive application, type of loading and environmental conditions respectively. They can be selected as 1.25 for values obtained by tests, 1.25 for manual application with controlled adhesive thickness, 1.5 for long-term loading and 1.0 for outdoor curing and low temperature. Substituting the selected values into Eq. (7.2) results in a total partial safety factor of 2.35. In the following case studies, this value is applied to the experimental results which, however, represent mean values and not characteristic values. The case studies, furthermore, are limited to a discussion of strength development and therefore stiffness development can be estimated in an analogue way.

7.4 Case studies

7.4.1 Girder-deck joints

Overview

The adhesive joining of concrete slabs to steel girders was initiated in the late sixties in Germany where several bridges were built over a period of 25 years. The deck was bonded to the upper flanges of the steel girders using an epoxy adhesive (as schematically shown in *Figure 7.7*). The main reasons for such bonding were the fast erection and optimal stress transfer between the deck and steel girders [10-11].

Girder-deck joints are structural joints of prime importance, as they connect the two main load-bearing members of the bridge superstructure - the deck and the girder. Any failure of these joints would alter the serviceability behavior of the bridge (leading to larger deflections due to the loss of composite action) or in some cases might even lead to the collapse of the structure. These joints are primarily subjected to flexural and shear stresses mainly due to the dead load (depending on the construction method), traffic loading and temperature (provided a correct sealing exists, as mentioned above). However, as shown in [12], the shear stresses, in particular, are small due to the large

bonding surfaces and therefore creep and fatigue are normally not critical. Also, the temperature variations are relatively small because the joint is not exposed to direct radiation. The area and thickness of the joint can be easily adjusted to meet design requirements.

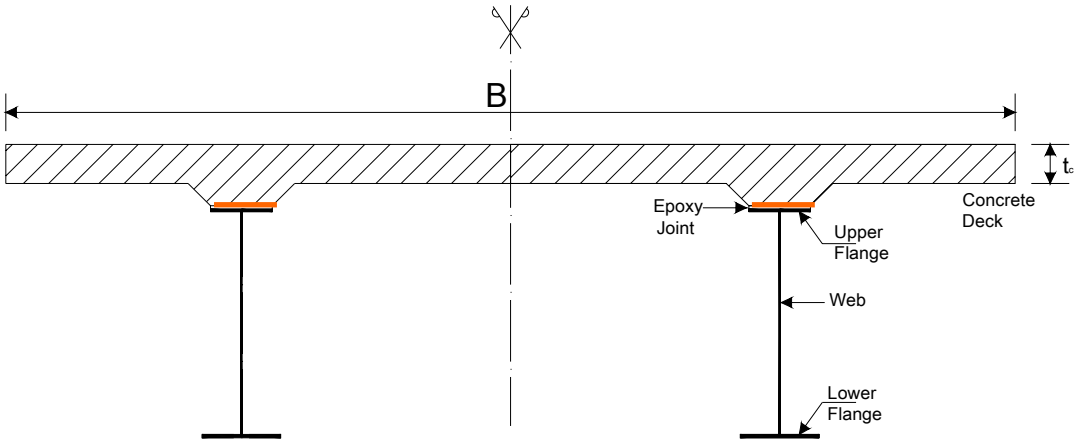

Figure 7.7 Schematic cross section of a typical bonded composite bridge girder

Numerical example

A simple span bridge with a typical cross section, as shown in *Figure 7.7*, and the dimensions listed in *Table 7.2* was selected. The bridge height was adjusted to keep the slenderness of the beams at around 16. The dimensions of the steel girder components were adjusted in such a way that the ratio of areas was 2:2:1 for web, lower flange and upper flange respectively. The total slab width, *B*, was selected as being 9 m with the two steel girders spaced at 53% of *B* and overhangs of 24% of *B*.

The bridge was loaded as shown in *Figure 7.8* according to SIA 261 [13] in addition to its own weight. The loads were increased by load factors specified in SIA 261. A transformed area elastic analysis was carried out to determine the bending stresses in the adhesive layer, σ_a, as shown in *Figure 7.9a*.

Table 7.2 Bridge dimensions considered in the case study

Dimension	Range
Bridge span, *L* (m)	10 ÷ 40
Slab thickness, t_s (mm)	150 ÷ 350
Web height, h_w (mm)	800 ÷ 2500
Web thickness, t_w (mm)	8 ÷ 18
Upper flange thickness, t_{uf} (mm)	15 ÷ 40
Upper flange width, b_{uf} (mm)	300 ÷ 600
Lower flange thickness, t_{lf} (mm)	20 ÷ 60
Lower flange width, b_{lf} (mm)	400 ÷ 900
Adhesive bond thickness, t_a (mm)	15 ÷ 25

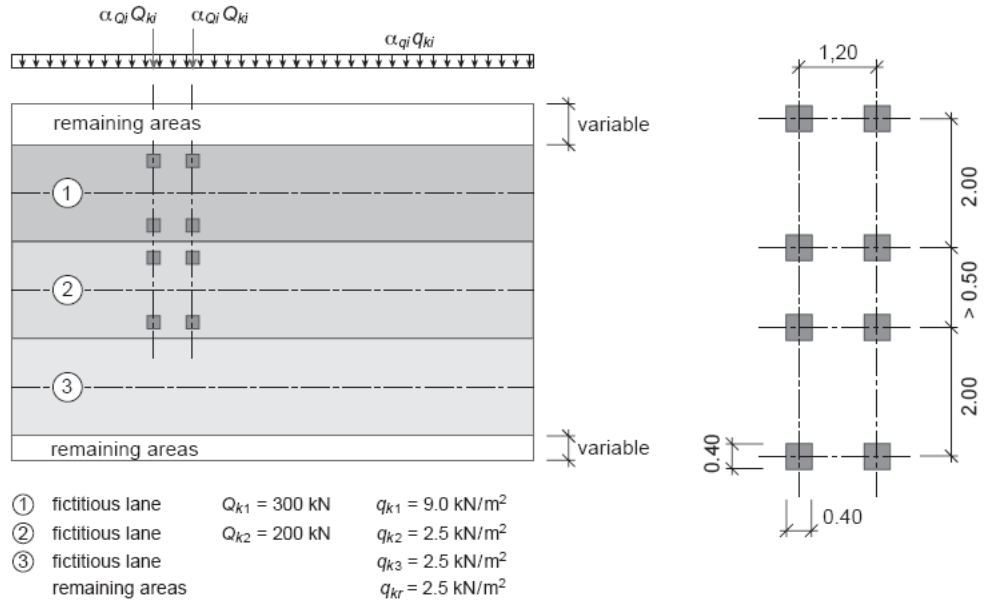

Figure 7.8 Bridge load model (1) according to SIA 261

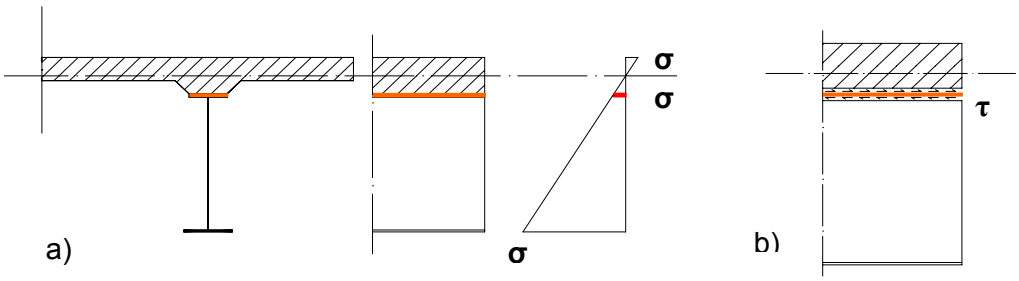

Figure 7.9 Schematic drawing of stresses induced in transformed composite section, a) bending stress distribution, b) shear stresses

Assuming full composite action (i.e. no slip between deck and girder) up to adhesive bond thicknesses of 4 cm, as stated in [12], the shear stresses shown in *Figure 7.9b)* were calculated by an elastic analysis as follows:

$$\tau_a = \frac{VS_c}{nI_b b_{eff}} \tag{7.3}$$

where V is the shear force in the considered section (at support), S_c is the static moment of the concrete slab of effective width b_{eff} (selected according to [14-15]), and I_b is the moment of inertia of the composite section.

The changes in tensile and shear stresses in the adhesive layer due to varying bridge dimensions are shown in *Figures 7.10* and *7.11*. A significant decrease in tension stresses was observed by increasing the bridge span. This was due to increasing the cross section of the steel girders, which led to a lowering of the neutral axis (approaching the adhesive bond layer). On the other hand, the influence of varying bridge span and slab thickness was less pronounced for the already low shear stresses.

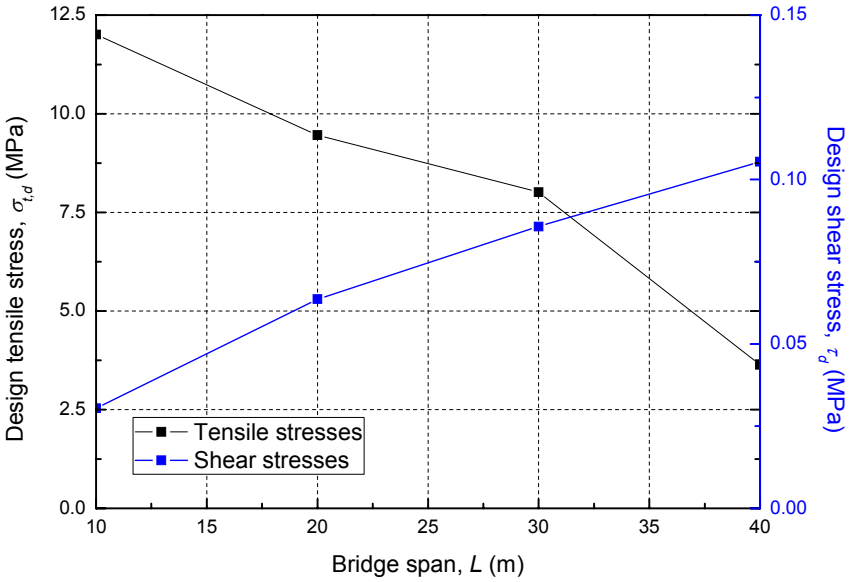

Figure 7.10 Change in adhesive design stresses due to variation of bridge span (for t_s=300mm)

The comparison between the possible resulting tensile and shear stress ranges (based on adjusting all bridge dimensions including span and slab thickness at the same time) and the developed material strength on the design level for the three curing scenarios is shown in *Figures 7.12* and *7.13*. The tensile stresses are much more critical than the shear stresses. In the worst case (short bridge and scenario SC3) the waiting period until sufficient adhesive strength is attained is around 6 days, while in the best case (long bridge, scenario SC2) this period decreases to 2 days.

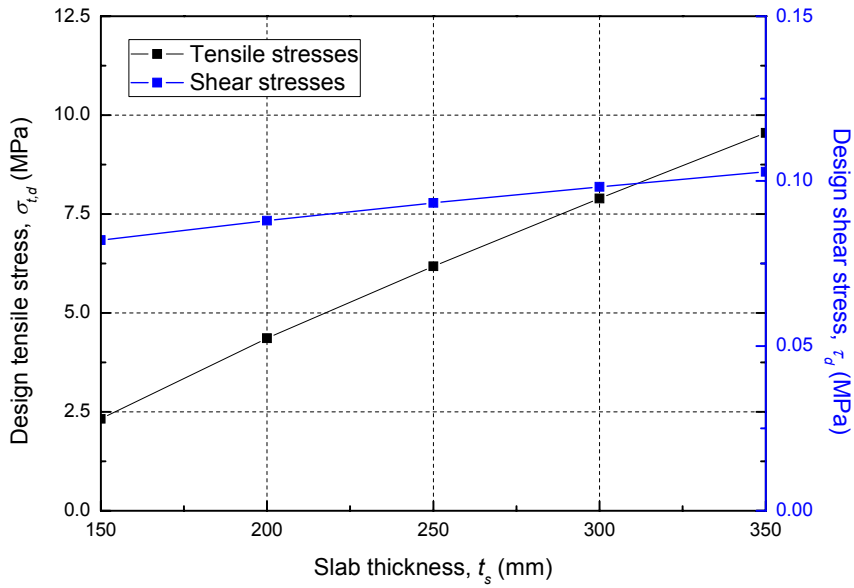

Figure 7.11 Change in adhesive design stresses due to variation of concrete slab thickness (for L=30m)

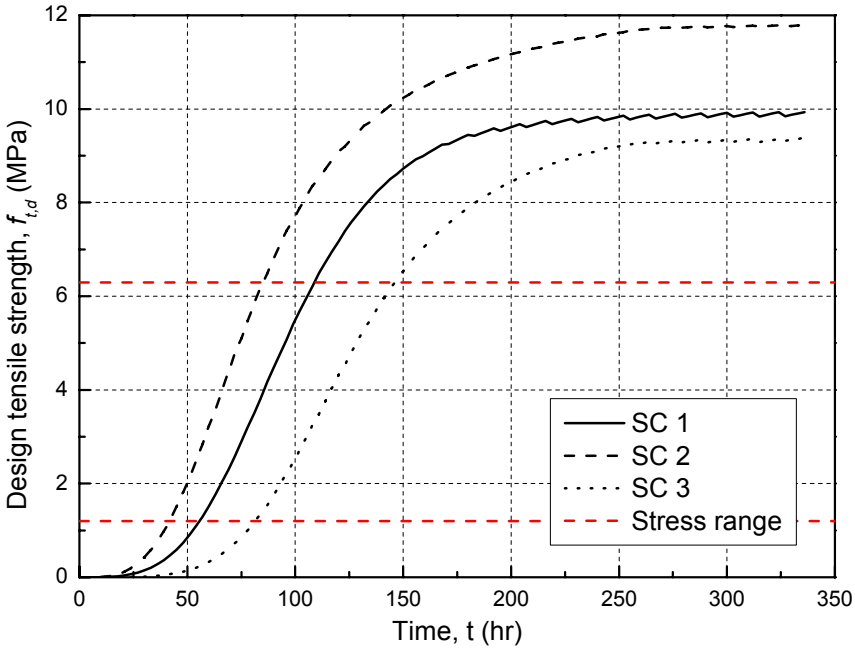

Figure 7.12 Comparison between design tensile stress range (dashed red lines) and developed design tensile strength in adhesive layer (curves SC1-3) for three curing scenarios

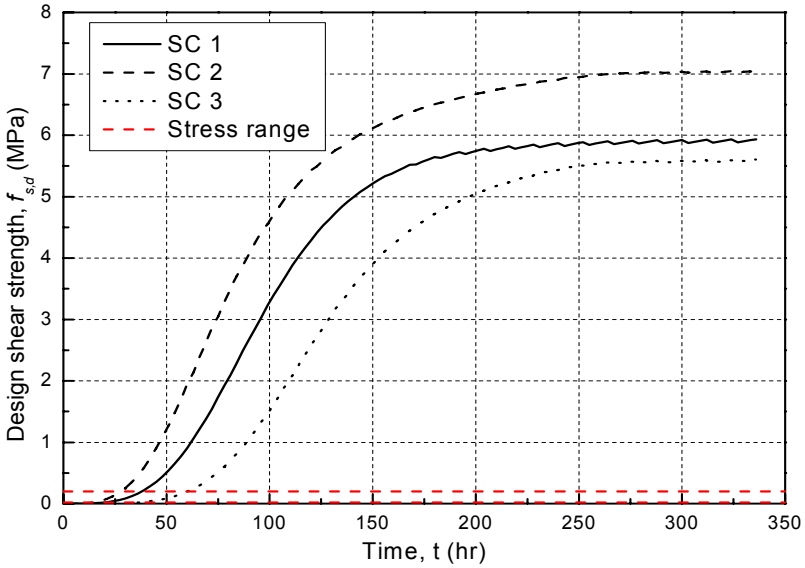

Figure 7.13 Comparison between design shear stress range (dashed red lines) and developed design shear strength in adhesive layer (curves SC1-3) for three curing scenarios

7.4.2 Shear joints in precast-prestressed segmental bridges

Overview

In precast concrete segmental bridges, the girder consists of short precast concrete segments that are assembled and prestressed to form the complete superstructure, as shown in *Figure 7.14*. The joints between the segments require special attention in design and construction. These joints introduce discontinuity in the bridge but must nonetheless transmit compressive and shear stresses [16-20]. The shear strength of these joints is significantly increased by increasing the prestressing forces.

The joints between the segments can be adhesively bonded using a thin layer of epoxy or without epoxy (dry joints). In addition, shear keys are used in both the webs and the slabs, as shown in *Figure 7.15*. Although adhesives are mostly used to seal the joints, they can increase the strength of shear key joints up to 25-60% compared to dry joints (depending on the prestressing level [19]). The curing of the epoxy in the joints fabricated on site is controlled by the surrounding environmental conditions (solar radiation, ambient temperature and wind speed fluctuations), bridge material properties, surface characteristics and section geometry, as schematically shown in *Figure 7.15*. The resulting curing temperature distribution along the joint is normally not uniform, a difference up to 10°C being observed along the web between top and bottom surfaces of a box girder [20].

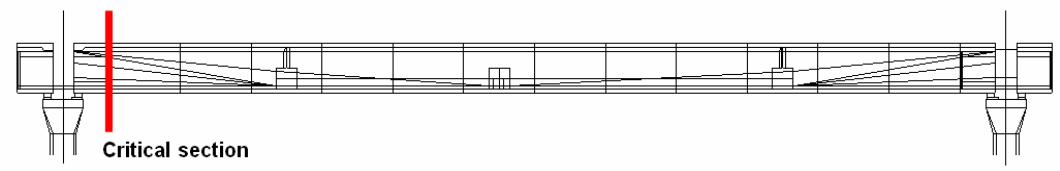

Figure 7.14 Schematic elevation of segmental precast-prestressed simply supported bridge [16]

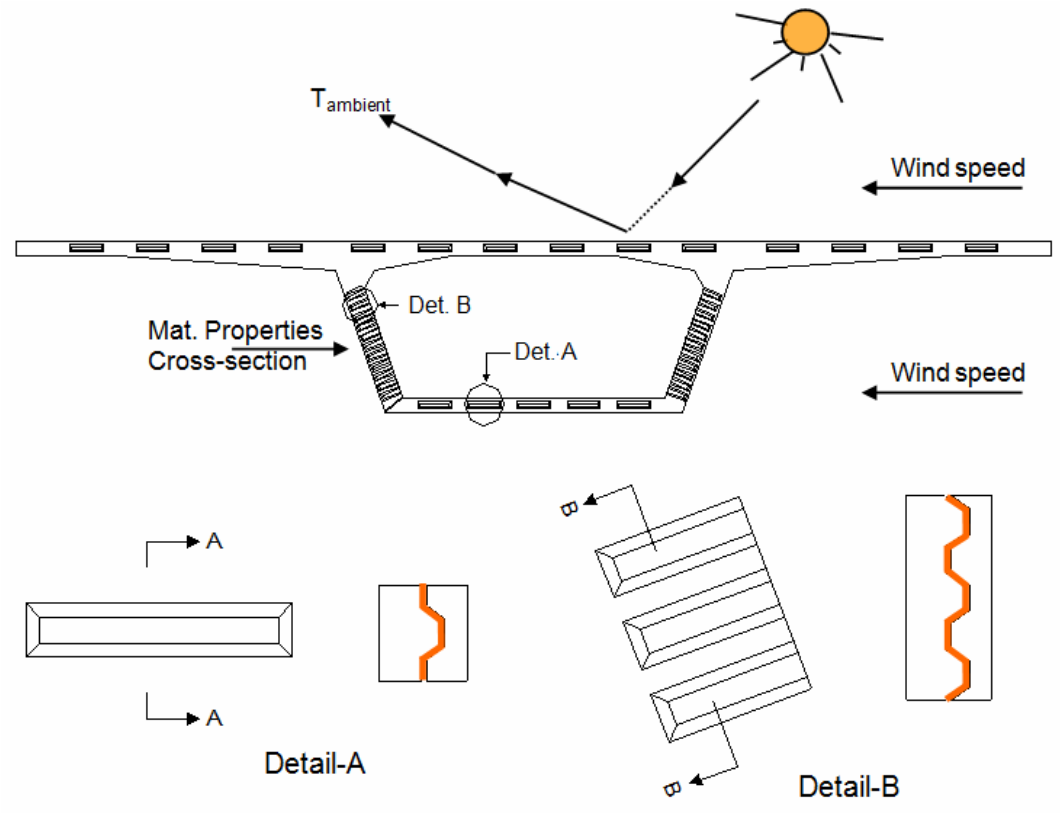

Figure 7.15 Schematic drawing of cross section of segmental precast-prestressed bridge with shear keys

Design codes like AASHTO and ACI provide empirical relationships for the design of dry joints in particular. Data for epoxy-bonded joints are reported in research publications. Push-off experiments were carried out in [18-19] to assess the shear strength and deformation behavior of precast segmental bridge joints. Investigated parameters included flat and keyed joints, with and without epoxy, the level of prestressing, and the epoxy layer thickness. It was found that the strength of epoxy-bonded flat or shear key joints is consistently higher than that of dry joints. In [18] the experimental data was fitted

to predict the shear strength of epoxy-bonded joints and the following equation was proposed:

$$V_j = A_j \sqrt{f_c'}(0.53 + 0.17\sigma_n) \tag{7.4}$$

where V_j is the ultimate joint load, f_c' is the concrete strength, A_j is the area of the joint surface between segments and σ_n is the average compressive stress across the joint due to prestressing (SI units are used). In [19], Eq. (7.5) is proposed for flat epoxy joints and Eq. (7.6) for keyed epoxy joints (in SI units):

$$V_j = A_j(45.6\sqrt{f_c'} + 4.36\sigma_n) \tag{7.5}$$

$$V_j = A_j(49.4\sqrt{f_c'} + 5.34\sigma_n) \tag{7.6}$$

Numerical example
A simple span box girder concrete bridge with the same dimensions as in [16] and as shown in *Figure 7.16* was selected. The bridge span was varied between 10 and 60 m in order to capture the possible shear stress range acting on the epoxy joint. In addition to the dead load, the bridge was loaded by the load model shown in *Figure 7.8*.

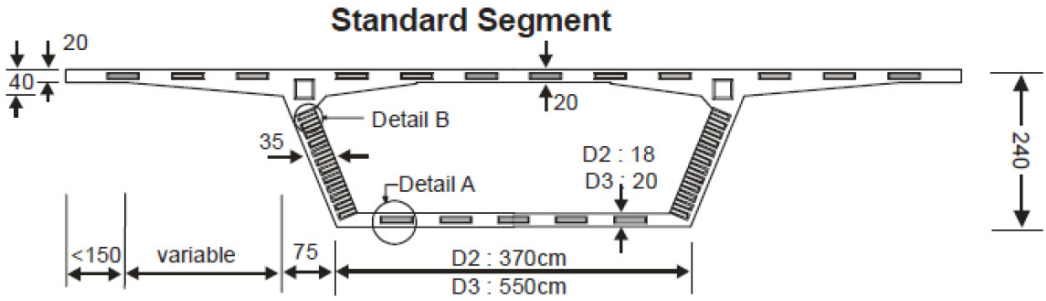

Figure 7.16 Cross section of bridge used in this case study [16]

Figure 7.17 shows the resulting joint shear strength as a function of the compressive stress (due to prestressing) according to Eqs. (7.4) to (7.6) (assuming f_c'= 40 MPa and A_j=6.48 m^2). Keyed epoxy joints provided higher strength than flat epoxy joints in [19] while results in [18] gave lower values for flat epoxy joints than in [19]. This result also suggests that a minimum compressive stress of around 1 MPa is required in order to obtain a shear strength exceeding the shear stress developed in the joint in the most unfavorable case.

Assuming a similar effect of the prestressing force during the curing of the adhesive, the development of the shear strength according to Eqs. (7.4) to (7.6) leads to the result shown in *Figure 7.18* (selected parameters: worst case scenario SC3, σ_n = 1.0 MPa and f_c'= 40 MPa). This result can again serve as a basis for selecting construction stages or time durations before a bridge is brought into service.

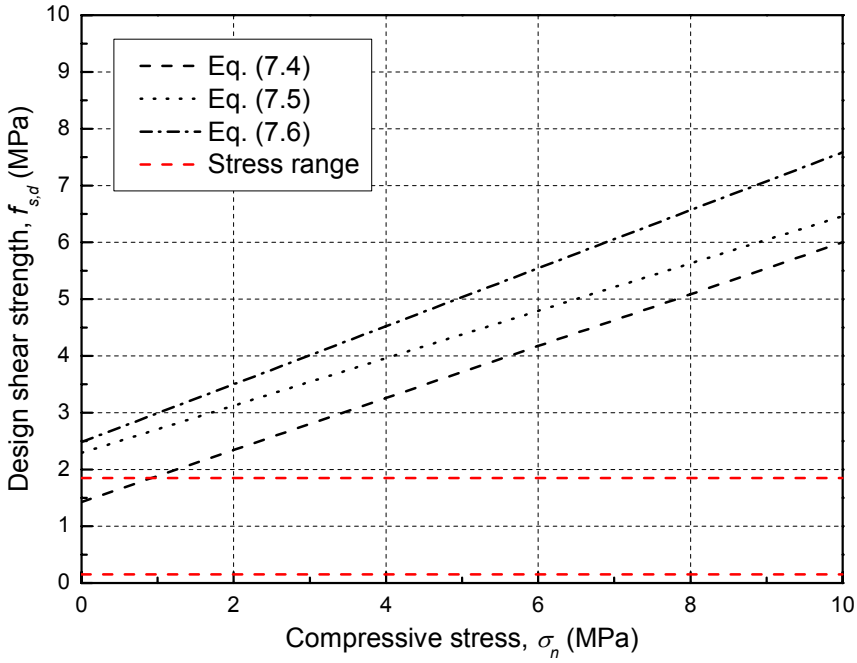

Figure 7.17 Relationship between design shear strength and design compressive stress due to prestressing

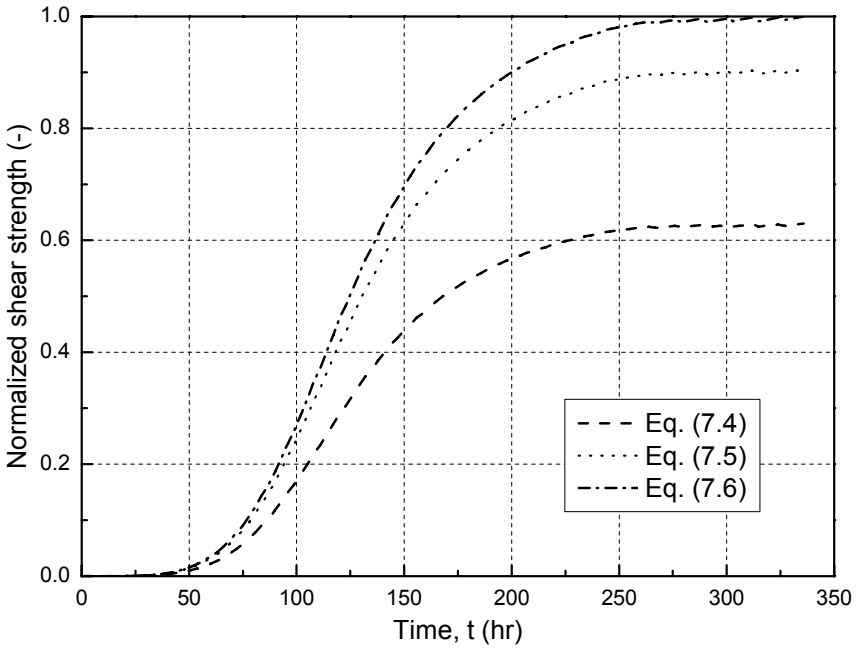

Figure 7.18 Development of shear strength under 1MPa compressive stress and curing according to scenario SC3

7.4.3 Bonded steel rebars in concrete

Overview

In order to meet rapidly increasing user demand, bridge strengthening and widening projects are carried out more and more frequently, thus improving both the serviceability and load-bearing capacity of structures. In these projects, bonded steel rebars are being used for joining new and old structural components, thus assuring the continuity of steel reinforcement and the performance of the bridge structure [21].

Numerical example

The general expression that defines the pull-out strength of an adhesively-bonded steel rebar, as shown in *Figure 7.19*, is given in [22] as follows:

$$P_{td} = \left[\left(\pi f_{s,d} d^{1.5}\right)/\lambda'\right]\tanh\left(\lambda' L_e/\sqrt{d}\right) \tag{7.8}$$

and

$$\lambda' = \sqrt{4G/tE} \tag{7.9}$$

where P_{td} is the design tension capacity (N), $f_{s,d}$ is the required design shear strength of the adhesive (MPa), d is the diameter of the drilled hole (mm), G is the shear modulus of the adhesive (MPa), t is the thickness of the adhesive layer in (mm), E is the elastic modulus of the steel rebar (MPa), and L_e is the embedment length (bonded portion) (mm).

As failure in the steel rebar is targeted in the case of this joint, P_{td} was selected according to the Swiss standard for concrete construction, SIA 262 [23]. Steel rebars of class B500B and 20- mm diameter were considered with a design yielding strength of 435 MPa. Based on this value $\tau_{d,max}$ was determined from Eq. (7.8) after assuming the embedment length according to SIA 262. Assuming the bond strength between the adhesive and the concrete is at least equal to the bond strength between the concrete and steel rebar, the embedment length is determined as:

$$L_e = \frac{d_b f_{sd}}{4 f_{bd}} \tag{7.10}$$

where d_b is the nominal diameter of the bar (mm), f_{sd} is the design strength of the rebar (MPa) and f_{bd} is the design bond strength based on the concrete grade (selected as 3.3 MPa for C40/50).

The required design shear strength of the adhesive vs. the design shear strength developed during the three curing scenarios is shown in *Figure 7.20*. Below the required shear strength, failure in the adhesive is expected. Results show an extension of the curing period of up to five days is required for the least favorable curing scenario (SC3) in order to obtain a tensile failure in the steel rebar. On the other hand, a period of 3 days is sufficient for the other two scenarios (SC1 and SC2) to develop the required adhesive strength.

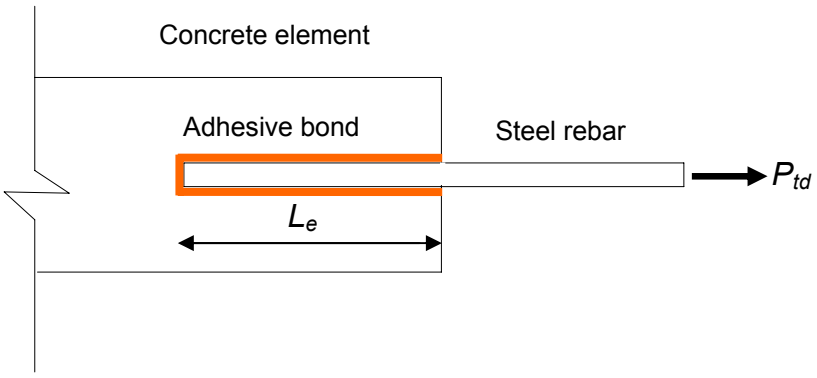

Figure 7.19 Schematic drawing of adhesively-bonded steel rebar in concrete element

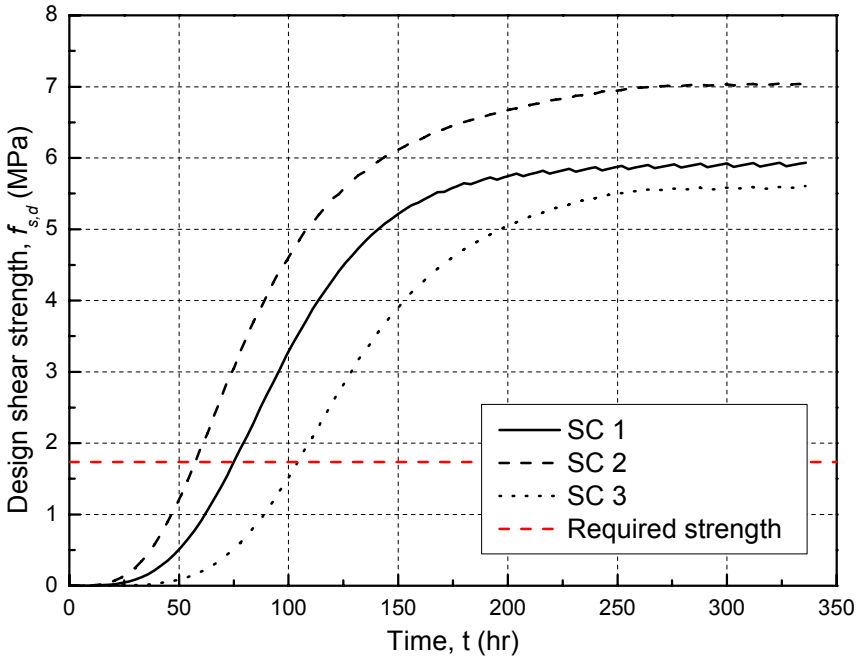

Figure 7.20 Comparison between required design shear strength and developed design shear strength for three curing scenarios

7.5 Conclusions

The implementation of the research results obtained from experimental and analytical investigations of the design of adhesively-bonded bridge joints was demonstrated. The discussion focused on the critical low-temperature curing during wintertime. Three typical bridge joints were selected and the strength development during different curing scenarios was compared to the possible stress ranges of each joint type. The following conclusions were drawn:

1) Adhesives in bridge joints are usually subjected to shear stresses. Shear stresses in bridge joints are normally low compared to the adhesive shear strength of fully cured adhesives. Because of this, although strength development is slow at low temperatures, reasonable curing periods can be achieved during wintertime.
2) A period of 3 to 7 days is sufficient in many cases to develop the required adhesive strength during wintertime. This period is similar to the waiting periods applicable to concrete. It can be decreased if the reaction heat is trapped in the joint or if the joint is heated during one day.

7.6 References

http://www.meteoswiss.admin.ch "*Federal office of meteorology and climatology meteoswiss".* [1]

G.C. Mays and A.R. Hutchinson, "*Adhesives in civil engineering*", Cambridge university press, 1992. [2]

J. Comyn, "*Developments in adhesives - 2*", (Ed. Kinloch, A.J.), Applied science publishers, London, 1981, Chapter 8. [3]

A.J. Kinloch, "*Durability of structural adhesives*", Applied science publishers, London, 1983. [4]

A.J. Kinloch, *"Interfacial fracture mechanical aspects of adhesive bonded joints – a review"*, J. Adhes., 1979; 10(3): 193–219. [5]

A.C. Carden and G.E. Ramey. "*Weather exposure and its effects on bridge deck curing in Alabama*". Practice Periodical on Structural Design and Construction., 1999; 4(4): 139–146. [6]

K.A. Riding, J.L. Poole, A.K. Schindler, M.C.G Juenger and K.J. Folliard, "*Temperature boundary condition models for concrete bridge members*". ACI Mat. J., 2007; 104(4): 379-387. [7]

D.E. Cuche, *"Determination of the Poisson's ratio of filled epoxy and composite materials"*. Proceedings of SPIE - The International Society for Optical Engineering, 1990; 1212: 315-324. [8]

J.L. Clarke (Ed.), *"Structural Design of Polymer Composites: Eurocomp Design Code and Background Document"*, Taylor and Francis (1st edn.), 1996. [9]

H. Hänsch and W. Krämer, "*Experiments with bonded composite structures"*. The road, 1968; 3: 137-141. [10]

E. Fiedler, "*The development of the steel bridge in the GDR until the turn of a retrospective*". Stahlbau, 2001; 70(5): 317-328. [11]

H.W Gürtler, *"Composite action of FRP bridge decks adhesively bonded to steel main girders"* PhD thesis No.3135, Ecole Polytechnique Fédérale de Lausanne (EPFL), 2004. [12]

SIA 261, *"Actions on structures "*. SIA Swiss soceity of engineers and architects, Zurich, 2003. [13]

M.A Hirt and R. Bez, *"Construction métallique: notions fondamentales et méthodes de dimensionnement"* Traité de génie civil Vol. 10, Ecole Polytechnique Fédérale de Lausanne (EPFL), 1994. [14]

M.A Hirt and M. Crisinel, *"Charpentes métallique: conception et dimensionnement des halles et bâtiments"* Traité de génie civil Vol. 11, Ecole Polytechnique Fédérale de Lausanne (EPFL), 2004. [15]

G. Rombach, *"Bangkok Expressway – Segmentbrückenbau contra Verkehrchaos, aus: Aus dem Massivbau und seinem Umfeld",* Schriftenreihe des Institutes für Massivbau und Baustofftechnologie, University of Karlsruhe, 1995, 645 – 656. [16]

Deutscher Beton-Verein: *"Empfehlungen für Segmentfertigteilbrücken mit externen Spannglieden"*, 1999. [17]

X. Zhou, N. Mickelborough and Z. Li *"Shear strength of joints in precast segmental bridges"*, ACI Struct. J., 2005; 102(2): 3–11. [18]

O. Buyukozturk, M.M. Bakhoum and S.M. Beattie, *"Shear behavior of joints in precast concrete segmental bridges"*, J. Struct. Engrg., 1990; 116(12): 3380–3401. [19]

M. Arockiasamy, D.V. Reddy, M. Sivakumar and M. Shahwy *"Fatigue loading and temperature distribution in single cell segmental box bridges"*, Practice Periodical on Structural Design and Construction., 2008; 113(3): 118–127. [20]

T. Hassan and S. Rizkalla, *"Flexural strengthening of prestressed bridge slabs with FRP systems",* PCI J., 2002; 47(1): 76–93. [21]

A. Colak *"Parametric study of factors affecting the pull-out strength of steel rods bonded into precast concrete panels"*, Intl. J. Adhes. Adhes., 2001; 21(6): 487–493. [22]

SIA 262, *"concrete structures"*. SIA Swiss soceity of engineers and architects, Zurich, 2003. [23]

8 Conclusions and future work

8.1 Summary of conclusions

This chapter presents the principal conclusions and recommendations for future work. The conclusions are linked to the objectives of this project explained in Section 1.2, with a particular focus on implementation of the results in bridge construction.

8.1.1 Physical characterization of adhesives at low temperatures

The effect of low-temperature curing on the physical state of commercial cold-curing epoxy adhesives was experimentally investigated. The development of the curing degree, α, and glass transition temperature, T_g, during different curing periods was monitored for different curing temperatures down to 5°C. Moreover, the applicability of kinetic models - previously developed for hot-curing adhesives - to cold-curing adhesives was examined. A new practical experimental method for investigating the T_g–α relationship was developed. The main conclusions drawn are as follows:

- Curing still takes place at low temperatures but will be significantly decelerated when construction takes place during winter. A low glass transition temperature also occurs because early material vitrification occurs. Heating of the joints is therefore recommended in order to accelerate the curing process and achieve higher T_g values.
- Existing models can be used, after some modifications have been made, to predict the curing behavior (level and rate) and the development of the glass transition temperature of cold-curing adhesives during curing in winter.
- The newly proposed experimental method establishes the T_g–α relationship more efficiently than the existing isothermal method. The method proved to be applicable to various cold-curing adhesives with different formulations.

8.1.2 Development of mechanical properties at early age

The effects of low temperature curing on early-age mechanical properties were investigated. Several curing procedures (isothermal, cyclic and outdoor) were taken into account. Additionally, the relationship between physical and mechanical properties was established and an empirical model was proposed to predict the mechanical properties as a function of the curing procedure. The following main conclusions can be drawn:

- The mechanical properties of cold-curing adhesives continue to develop during winter curing, and a significant increase in mechanical properties occurs after the onset of material vitrification.
- The strength and stiffness of the adhesive develop at the same rate, except at low temperatures where strength development is slightly delayed during the later stages of cure.
- An empirical model, based on the material curing behavior, was developed and is able to predict the development of mechanical properties during early age for various curing procedures. Based on this model, design curves for early-age mechanical properties as a function of curing temperature and time were established for design purposes.

8.1.3 Time-temperature dependence during thermomechanical recovery

The thermomechanical recovery behavior of cold-curing adhesives was investigated. The changes in the thermophysical state of the adhesive and its influence on mechanical properties during recovery after cooling from temperatures above T_g were experimentally investigated. Furthermore, an existing model for predicting temperature-dependent mechanical properties was extended to also predict the thermomechanical recovery behavior of the examined adhesives. The conclusions drawn from this work are as follows:

- An increase in curing degree and more significantly in the T_g is achieved by exposing the adhesives to temperatures exceeding their T_g due to an increase in polymer network branching.
- Full recovery of thermomechanical properties occurs when the material is cooled across the T_g due to the full reformation of the secondary bonds. Moreover, an increase in thermophysical and mechanical properties is achieved as a result of post-curing.
- The time periods at exposure temperature and recovery temperature significantly influence the mechanical properties.
- The extended model successfully predicted the thermomechanical recovery behavior based on the thermophysical changes.

8.1.4 Long-term performance of structural adhesives

The long-term curing behavior of a cold-curing structural adhesive was simulated by the post-curing of the adhesive at different temperatures. The corresponding changes in physical and mechanical properties were investigated. A model for the long-term property prediction of concrete was adapted to predict the long-term mechanical properties based on the physical changes. The basic conclusions are as follows:

- A significant long-term increase in mechanical properties is achieved due to the progression of curing.
- The model provides accurate predictions of the long-term mechanical property increases based on a term describing the change in T_g over the long term.

8.1.5 Application in bridge construction

The way in which the results and models developed within this work can be applied in bridge construction is demonstrated. Critical subjects are a) the low-temperature period in winter during which adhesive bonding should also be applicable and b) the potential exceeding of the glass transition temperature during hot summer days.

For the first case, the models allow estimation of the time required to obtain full or partial adhesive properties as a function of curing temperature and derive therefore the derivation of the time intervals required before bringing a bridge into service or for construction stages during which in most cases full properties are not yet required. Depending on the joint type, 3-7 curing days are normally required during winter to obtain the necessary joint strength. During the rest of the year, this time interval is reduced to 1-2 days.

With regard to the short-term exceeding of the glass transition temperature during hot summer days, it has been shown that its value increases by more than 50% during the service life of a bridge. Similarly, the mechanical properties also increase significantly. Subsequent to the exceeding of the glass transition temperature, after cooling, the mechanical properties fully recover and even increase due to post-curing. The reduction in the mechanical properties in the glass transition range can be estimated by the provided models and joints can be designed accordingly.

8.1.6 Adhesive properties required for application of research results

Throughout this research project, difficulties were encountered due to the lack or imprecise nature of the information given in manufacturers' datasheets regarding adhesive properties under different curing/post-curing conditions. Therefore, based on the results of this research and with regard to civil engineering applications, it is recommended that manufacturers include the following information in their datasheets:

- The lowest possible curing temperature.
- To predict the short-term mechanical properties (up to 10 days of cure) after applying the fresh adhesive, according to Eqs. (4.1) and (4.2) for simple and complex curing profiles respectively, the characteristic values of tensile, shear and compressive strengths and E/G-Moduli after curing during seven days at 23°C and 50% RH are required. To determine these material properties, ASTM standards can be used

(ASTM D 638 for tensile properties, ASTM D 5379 for shear properties and ASTM D 695 for compressive properties). The values for t_m and s can be determined from Fig. 4.11.

- To predict the increase in T_g after exposure to T_{ex} during t_{ex}, according to Eq. (5.3), the value of T_{gL}, which represents the T_g after curing during 7 days at 23°C and 50% RH, is required. The T_g value can be obtained according to ASTM E2041, based on DSC experiments.
- To predict the temperature-dependent mechanical properties according to Eq. (5.2), the values of T_k (which is T_g from Eq. (5.3)), k (from Table 5.3), as well as P_U and P_R are required. P_U is the characteristic value of tensile, shear or compressive strength and E/G-modulus, after curing during seven days at 23°C and 50% RH. P_R can be assumed as being 0 (a conservative assumption).
- To predict the long-term mechanical properties, $P(t)$, according to Eqs. (6.5) and (6.6), the values of P_7, $T_{g,7}$, and n (acc. to Section 6.4.3) are required. P_7 and $T_{g,7}$ are the mechanical properties and T_g after curing during seven days at 23°C and 50% RH.

To summarize, the manufacturer's datasheet should comprise the lowest possible curing temperature, the characteristic values of mechanical properties and the glass transition temperature attained after seven days curing at 23°C and 50% RH.

8.2 Future work

This section introduces research topics that should be studied in the future to complement the present work. It proposes experimental and numerical investigations and further developments to favor the use of adhesive bonding in bridge construction.

8.2.1 Long-term durability

Bridge joints – particularly in the central Alpine region of Europe – are subjected to severe environmental conditions, particularly during winter. In the case of incorrectly executed or damaged and therefore unsealed or only partially sealed joints, the mechanical properties of a bonded joint may change upon exposure to its service environment due to physical and chemical aging. Physical aging refers to a polymer relaxation process while chemical aging comprises polymer post-curing, thermal and weathering aging. In the case of bridges, the positive effects of post-curing are normally counteracted by the negative effects of weathering aging, which leads to molecular chain scission and the corresponding deterioration of mechanical properties. The interaction of these processes is still not fully understood and needs further research.

8.2.2 Characterization of ductile adhesives

The mechanical performance of ductile polyurethanes and acrylic adhesives was investigated during previous research work at CCLab [1-2]. The superior performance in terms of structural safety and robustness of ductile adhesives in comparison with brittle epoxies was demonstrated. Further research on the behavior of this promising type of adhesives during cure and their sensitivity to temperature is recommended.

8.2.3 Investigation of joint performance

Only the cohesive properties of the adhesive were investigated and discussed in this report. Various failure modes, however, may develop in a joint. Along with the cohesive failure in the adhesive, failure may occur in the adherend (normally the case for concrete and composites) or in the adhesive-adherend interface (often with metallic adherends). The stress state in joints is complex, combining non-uniformly distributed in-plane shear and through-thickness normal stresses, and may vary during the service life due to environmental effects. Investigations of the bond strength and bonding procedure between different substrates and already cured adhesives have already been carried out (e.g. [3-5]). The adhesion between adhesives and various adherends (particularly steel and concrete) at young age during cure, however, has not yet been investigated.

8.2.4 Establishing design codes

The results of this research and future works should be implemented in a design code to provide engineers with the necessary guidelines concerning the design of adhesively-bonded joints. This design code should cover various applications and include all parameters influencing the structural behavior of bonded joints and the adhesive used.

8.3 References

J. de Castro and T. Keller, "*Ductile double-lap joints from brittle GFRP laminates and ductile adhesives. Part I: Experimental investigation"*, Compos Part B-Eng, 2008; 39(2): 271-281. [1]

J. de Castro and T. Keller, "*System ductility and redundancy of FRP beam structures with ductile adhesive joints"*, Compos Part B-Eng, 2005; 36 (8): 586-596. [2]

G.C. Mays and A.R. Hutchinson, "*Adhesives in civil engineering*", Cambridge university press, 1992. [3]

J.D.N. Shaw, *"A review of resins used in construction. Types of resin - applications - case histories"*, Int. J. Adhes. Adhes., 1982; 2(2): 77–83. [4]

W. Brockmann, "*Durability of structural adhesives*", (Ed. Kinloch, A.J.), Applied science publishers, London, 1983, P. 281. [5]

Nomenclature

Abbreviations

Concept	Signification
AGB	Arbeitsgruppe Brückenforschung
ASTM	American Society for Testing and Materials
CCLAB	Composite Construction Laboratory
CFRP	Carbon Fiber-Reinforced Polymers
DATEC	Dipartimento federale dell'ambiente, dei trasporti, dell'energia e delle comunicazioni
DETEC	Département fédéral de l'environnement, des transports, de l'énergie et de la communication
DIN	Deutsches Institut für Normung
DMA	Dynamic Mechanical Analysis
DSC	Differential Scanning Calorimetry
EPFL	Ecole Polytechnique Fédérale de Lausanne
ETH	Eidgenössische Technische Hochschule Zürich
FRP	Fiber-Reinforced Polymer
ISO	International Organization for Standardization
SOP	Standard Operational Procedure
TTT	Time Temperature Transformation
UVEK	Eidgenössisches Departement für Umwelt, Verkehr, Energie und Kommunikation

Latin upper case

Concept	Signification
A	Pre-exponential factor [min^{-1}]
A_{av}	Average pre-exponential factor [min^{-1}]
A_f	Corrected pre-exponential factor [min^{-1}]
A_j	Area of joints between segments [mm^2]
A_T	Effective shear area [mm^2]
C	Temperature-dependant constant
C_f	Correction factor for pre-exponential factor
ΔC_p	Heat capacity difference in [J/mol.g]
E	Young's Modulus [GPa]
E_a	Activation energy [kJ/mol]
E_{ci}	Tangent modulus of elasticity at concrete age of 28 days [MPa]
$E_{ci}(t)$	Tangent modulus of elasticity at concrete age t in days
G	Shear modulus [MPa]
ΔH	Heat generated by cure reaction [W/g]

Concept	Signification
ΔH_{iso}	Maximum attainable heat of reaction generated during isothermal curing process [J/g]
ΔH_T	Total heat of reaction generated during dynamic curing process [J/g]
I_b	Moment of inertia of composite section [mm^4]
K	Intercept in heating rate equation
L_e	Steel bar embedment length [mm]
$P(T)$	Property value at a given temperature T
$P(t)$	Property value at a given time t
P_0	Property value at the beginning of the curing process
P_∞	Property value at the end of the curing process
P_1	Instantaneous material property preceding secondary relaxation
P_2	Instantaneous material property preceding primary relaxation
P_3	Property value at rubbery plateau
P_7	Value of mechanical property after seven days curing
P_R	Property value of relaxed material
P_{td}	Design tension capacity of bonded steel rebar in concrete [N]
P_U	Property value of unrelaxed material
R	Universal gas constant [J/mol.K]
S_C	Static moment of concrete slab [mm^3]
T	Temperature [°C]
T_β	Temperature at which β-transition occurs [°C]
T_γ	Temperature at which γ-transition occurs [°C]
T_{g0}	Glass transition temperature of uncured sample [°C]
$T_{g\infty}$	Glass transition temperature of fully cured sample [°C]
T_1	Temperature at which secondary relaxation occurs [°C]
T_2	Temperature at which glass transition occurs [°C]
T_{cure}	Curing temperature [°C]
T_{ex}	Exposure temperature > T_g [°C]
T_g	Glass transition temperature [°C]
$T_{g,7}$	Glass transition temperature after seven days curing at 23°C [°C]
$T_g(t)$	Glass transition temperature of adhesive at time t [°C]
T_{gL}	Glass transition temperature of samples cured under lab conditions [°C]
$T_{h\text{-}l}$	60-min half-life temperature [°C]
T_k	Glass transition temperature in Eq. 6.2 [°C]
T_{onset}	Onset of cure [°C]
T_p	Peak temperature of exotherm [°C]
T_{pc}	Post-curing temperature [°C]
T_{rec}	Recovery temperature < T_g [°C]
V	Shear force [N]
V_j	Shear bearing capacity of adhesive bond layer in concrete segmental bridging [MPa]

Latin lower case

Concept	Signification
c	Segmental mobility
d	Diameter of drilled hole [mm]
d_b	Nominal diameter of steel rebar [mm]
dT/dt	Heating rate [°C/min]

Concept	Signification
$d\alpha / dt$	Curing rate [min^{-1}]
$(d\alpha / dt)_p$	Curing rate at peak temperature [min^{-1}]
k	Rate constant [min^{-1}] (Chapter 3)
k	Model fitting constant (Chapter 6)
m	Reaction order
m_1, m_2	Weibull moduli (Chapter 5)
$m+n$	Overall reaction order
n	Reaction order (Chapter 3)
n	Property-dependent parameter describing property development (Chapter 6)
$f(\alpha)$	Concentration of reactants
f_{bd}	Design bond strength [MPa]
f_c'	Concrete compressive strength [MPa]
$f_{cm}(t)$	Mean compressive strength at concrete age t in days [MPa]
f_{cm}	Mean compressive strength at concrete age of 28 days [MPa]
$f_{s,d}$	Design shear strength
f_{sd}	Design stress in bonded steel rebar [MPa]
f_t	Tensile strength [MPa]
$f_{t,d}$	Design tensile strength
s	Power of cure equation (Chapter 4)
s	Coefficient depending on strength class of cement (Chapter 6)
t	Time [min – hour – day]
t_a	Thickness of adhesive layer [mm]
t_{cure}	Curing time [min]
t_{eq}	Equivalent time to achieve a property level under lab conditions
t_{ex}	Exposure time [hr]
t_m	Time required to attain value of $P_\infty/2$ [hr]
t_{pc}	Post-curing time [hr]
t_{rec}	Recovery time [hr]
x	Crosslink density

Greek lower case

Concept	Signification
α	Curing degree in [%]
α_c	Critical curing degree
α_L	Curing degree of samples cured under lab conditions [%]
α_p	Curing degree at peak temperature [%]
$\beta_{cc}(t)$	Function describing development of compressive strength with time
$\beta_E(t)$	Function describing development of modulus of elasticity with time
$\beta_P(t)$	Function describing development of adhesive mechanical property with time
γ_m	Partial safety factor
ε	Lattice energy [kJ/mol]
λ	Structure-dependant factor (= $\Delta C_{p\infty} / \Delta C_{p0}$)
μ	Coefficient of friction
v	Poisson's ratio
σ_a	Bending stresses in adhesive bond layer between concrete deck and steel girders [MPa]
σ_n	Compressive stresses in adhesive bond layer in concrete segmental bridging [MPa]

Concept	Signification
$\sigma_{t,d}$	Design tensile stress
τ_a	Shear stresses in adhesive bond layer between concrete deck and steel girders [MPa]
τ_d	Design shear stress

Projektabschluss

Schweizerische Eidgenossenschaft
Confédération suisse
Confederazione Svizzera
Confederaziun svizra

Eidgenössisches Departement für
Umwelt, Verkehr, Energie und Kommunikation UVEK
Bundesamt für Strassen ASTRA

FORSCHUNG IM STRASSENWESEN DES UVEK **Strassen, Brücken, Tunnel**

Formular Nr. 3: Projektabschluss

erstellt / geändert am: 04.07.2012

Grunddaten

Projekt-Nr.:	AGB2005/008
Projekttitel:	Thermophysikalisches und thermomechanisches Verhalten von kalthärtenden strukturellen Klebstoffen im Brückenbau
Enddatum:	31.12.2011

Texte

Zusammenfassung der Projektresultate:

Tragende Klebeverbindungen sind mittlerweile etablierte Verbindungstechniken in der Automobil- und Flugzeugindustrie, wo sie meistens im Werk und unter kontrollierten Bedingungen eingesetzt werden. Im Bereich des Bauwesens, wo Bauwerke in der Regel im Freien errichtet werden, unterliegen Klebeverbindungen den klimatischen Bedingungen vor Ort, Temperaturen und Feuchtigkeitsgrade variieren. Insbesondere im Winter während langen Perioden niedriger Temperaturen muss es dabei möglich bleiben, geklebte Verbindungen komplexer Bauteile herzustellen. Deshalb, aber auch wegen der Größe der zu verbinden Bauteile, kommen meist kalthärtende Klebstoffe zum Einsatz – im Gegensatz zu in den andern Industriezweigen verwendeten warmaushärtenden Klebstoffen.

Obwohl tragende Klebeverbindungen im Brückenbau sehr viele Vorteile aufweisen können, werden diese bisher nur selten verwendet. Dies ist unter anderem auf fehlende Kenntnisse über das Langzeitverhalten unter den variierenden klimatischen Bedingungen zurückzuführen. Trotz vieler Erkenntnisse auf dem Gebiet der Charakterisierung von strukturellen Klebstoffen besteht weiterhin Forschungsbedarf hinsichtlich der thermophysikalischen und thermomechanischen Eigenschaften, insbesondere in der frühen Härtungsphase sowie unter tiefen Temperaturen. Das Ziel der vorliegenden Arbeit ist es deshalb, basierend auf experimentellen und analytischen Untersuchungen, das thermophysikalische und thermomechanische Verhalten kalthärtender Klebstoffe, von der Mischung der verschiedenen Komponenten bis hin zum Langzeitverhalten, zu verstehen und zu beschreiben.

Die Untersuchungen der Anfangsphase des Härtungsverhaltens unter tiefen Temperaturen (im Winter) haben gezeigt, dass der Härtungsprozess bereits bei Temperaturen geringfügig über 0°C einsetzt. Allerdings verläuft der Prozess sehr langsam, sodass mehrere Tage nötig sind um signifikante Härtungsgrade zu erzielen. Die Glasübergangstemperatur, Tg, entwickelt sich infolge des frühen Einsetzens der Vitrifikation noch langsamer. Eine neue und praxisorientierte Methode wurde entwickelt um den Zusammenhang zwischen Glasübergangstemperatur und Härtungsgrad für verschiedene Klebstoffe zu beschreiben. Des Weiteren konnte gezeigt werden, dass die für warmhärtende Klebstoffe entwickelten Härtungsmodelle auch für kalthärtende Klebstoffe unter tiefen Temperaturen anwendbar sind. Im Gegensatz zu den thermophysikalischen Eigenschaften entwickeln sich die thermomechanischen Eigenschaften erst nach dem Einsetzen der Vitrifikation. Geringere Härtungstemperaturen führen auch zu einer signifikanten Verlangsamung der Entwicklung. Ein empirisches Modell zur Vorhersage von Festigkeit und Steifigkeit wurde entwickelt - dies in Abhängigkeit von einfachen oder komplexen Temperaturprofilen, insbesondere von tiefen Temperaturen und unter Einbezug der temperaturabhängigen Vitrifikation.

Im Sommer kann die Temperatur an exponierten Stellen, z.B. unter dem Asphalt, Tg übersteigen, was zu einer signifikanten Reduktion der mechanischen Eigenschaften führen kann. Die Untersuchungen haben gezeigt, dass wenn die Klebeverbindung sich wieder abgekühlt (unterhalb Tg), die mechanischen Eigenschaften sich wieder vollständig erholen. Dank einer erfolgten Nachhärtung werden diese sogar leicht erhöht. Ein Modell zur Vorhersage der mechanischen Eigenschaften bei und nach dem Überschreiten von Tg wurde entwickelt.

Die Untersuchungen haben weiter gezeigt, dass die mechanischen Eigenschaften langfristig, über Jahre und Jahrzehnte, infolge Nachaushärtung signifikant zunehmen. Ein Modell zur langzeitigen Entwicklung von Festigkeit und Steifigkeit von kalthärtenden strukturellen Klebstoffen wurde entwickelt. Das Modell basiert auf einem bestehenden Modell zur entsprechenden Vorhersage für Beton.

Abschließend zeigen verschiedene Fallbeispiele wie die Ergebnisse dieser Arbeit praktisch angewendet werden können, insbesondere zur Vorhersage der mechanischen Eigenschaften in der Anfangsphase der Aushärtung unter tiefen Temperaturen. Diese Ergebnisse können beispielsweise zur Planung von Bauphasen oder Wartezeiten bis zur Inbetriebnahme von Brücken verwendet werden.

Schweizerische Eidgenossenschaft
Confédération suisse
Confederazione Svizzera
Confederaziun svizra

Eidgenössisches Departement für
Umwelt, Verkehr, Energie und Kommunikation UVEK
Bundesamt für Strassen ASTRA

Zielerreichung:

Die ersten experimentellen Untersuchungen haben ergeben, dass nicht nur das mechanische Verhalten der Klebstoffe untersucht werden kann. Da es sich im Baubereich um kaltaushärtende Klebstoffe handelt, sind die mechanischen Eigenschaften stark zeitabhängig, da die Aushärtung - in Funktion der Aushärtungstemperatur - über längere Zeiträume erfolgt (im Gegensatz zu warmaushärtenden Klebstoffen im Industriebereich, die praktisch immer voll ausgehärtet sind). Nebst den mechanischen mussten deshalb auch die zeit- und temperaturabhängigen thermophysikalischen Eigenschaften - Aushärtungsgrad und Glasübergangstemperatur - in die Untersuchung einbezogen werden. Die mechanischen Eigenschaften hängen direkt von den thermophysikalischen Eigenschaften ab. Für kaltaushärtende Klebstoffe wurden mit diesen Fragestellungen Neuland betreten.

Aufgrund dieser Zeit- und Temperaturabhängigkeit beider Eigenschaftsgruppen ergaben sich hinsichtlich Brückenbau neue Fragestellungen, die in der ursprünglichen Zielsetzung nicht enthalten waren, wie z.B. die Entwicklung der Eigenschaften bei Aushärtung unter niedrigen Temperaturen, das temporäre Überschreiten der Glasübergangstemperatur und dessen Effekt nach Abkühlung oder die langfristige Entwicklung der Eigenschaften. Um diese neuen Fragestellungen angehen zu können musste das ursprüngliche Forschungsprogramm reduziert werden, insbesondere das Thema Dauerhaftigkeit wurde gestrichen (nach Absprache mit der BK C). Entsprechend wurde auch der Titel der Arbeit geändert. Ebenso nicht behandelt werden konnten duktile Klebstoffe - die Arbeit konzentriert sich auf spröde Epoxidklebstoffe, wie sie heute grossmehrheitlich eingesetzt werden.

Kompliziert wurde die Arbeit durch einen krankheitsbedingten Wechsel des Doktoranden und Schwierigkeiten bei den experimentellen Arbeiten. Letztere sind auf die hohe Temperaturempfindlichkeit bei geringen Aushärtungsgraden sowie die Kopplung von mechanischen und thermophysikalischen Eigenschaften zurückzuführen. Um konsistente Resultate zu erhalten musste zuerst eine SOP entwickelt werden. Diese Schwierigkeiten haben zu einer wesentlichen Projektverlängerung geführt.

Folgerungen und Empfehlungen:

Da der wesentliche Aspekt der Dauerhaftigkeit nicht bearbeitet werden konnte, wird empfohlen, diesen in einem Folgeprojekt anzugehen. Dabei stehen Fragen nach der physikalischen und chemischen Alterung von kaltaushärtenden Klebstoffen im Vordergrund. Physikalische Alterung beinhaltet eine Relaxation des Polymers, während unter chemischer Alterung die langfristige Nachaushärtung, die thermische und wetterbedingte Alterung verstanden wird. Die langfristige Nachaushärtung und deren positive Effekte auf die mechanischen Eigenschaften wurde im Rahmen dieses Projektes behandelt. Die thermische und wetterbedingte Alterung führt zu einem Abbau der Molekülvernetzung und entsprechend den mechanischen Eigenschaften. Auch hier wird für kaltaushärtende - und eben zumeist nicht voll ausgehärtete - Klebstoffe Neuland betreten. Es ist sehr wahrscheinlich, dass diese Prozesse bei unvollständiger Aushärtung beschleunigt werden.

Ein weiterer Aspekt betrifft die Materialermüdung. Insbesondere bei geklebten Bewehrungen in der Fahrbahnplatte kann die Ermüdungsbeständigkeit relevant sein. Die heutigen Kenntnisse über das Ermüdungsverhalten von Klebstoffen sind diesbezüglich ungenügend. Insbesondere die Beschreibung des viskoelastischen Einflusses bedarf noch weiterer Forschung.

Publikationen:

Moussa, Omar (2011). Thermophysical and thermomechanical behavior of cold-curing adhesives used in bridge construction. EPFL Thesis No. 5244.

Moussa O, Vassilopoulos AP, Keller T. Experimental DSC-based method to determine glass transition temperature during curing of structural adhesives. Construction & Building Materials 28 (2012) 263-268.

Moussa O, Vassilopoulos AP, Keller T. Effects of low-temperature curing on physical behavior of cold-curing epoxy adhesives in bridge construction. International Journal of Adhesives and Adhesion 32/1 (2012) 15-22.

Moussa O, Vassilopoulos AP, de Castro J, Keller T. Early-age tensile properties of structural epoxy adhesives subjected to low-temperature curing. International Journal of Adhesives and Adhesion 35/1 (2012) 9-16.

Moussa O, Vassilopoulos AP, de Castro J, Keller T. Time-temperature dependence of thermomechanical recovery of cold curing structural adhesives. International Journal of Adhesives and Adhesion 35/2 (2012) 94-101.

Moussa O, Vassilopoulos AP, Keller T. Long-term development of thermophysical and mechanical properties of cold-curing structural adhesives due to post-curing. Journal of Applied Polymer Science, in press.

Der Projektleiter/die Projektleiterin:

Name: Keller Vorname: Thomas

Amt, Firma, Institut: EPFL-ENAC-IIC-CCLab

Unterschrift des Projektleiters/der Projektleiterin:

Thomas Keller

Schweizerische Eidgenossenschaft
Confédération suisse
Confederazione Svizzera
Confederaziun svizra

Eidgenössisches Departement für
Umwelt, Verkehr, Energie und Kommunikation UVEK
Bundesamt für Strassen ASTRA

FORSCHUNG IM STRASSENWESEN DES UVEK **Strassen, Brücken, Tunnel**

Formular Nr. 3: Projektabschluss

Beurteilung der Begleitkommission:

Beurteilung:

Kalthärtende strukturelle Klebstoffe halten im Bausektor zunehmend Einzug auch im Brückenbau, wo sie auch für tragende Verbindungen wie beispielsweise geklebte Bewehrungsanschlüsse oder oberflächlich geklebte Stahl- oder Kohlefaserlamellenverstärkungen verwendet werden. Obschon geklebte Verbindungen zahlreiche Vorteile aufweisen, ist die Ausdehnung der Einsatzbereiche nur relativ beschränkt. Dies ist zum Einen auf unvollständige Kenntnisse des thermophysikalisch und thermomechanischen Verhaltens und zum Anderen auf die klimatischen Einflüsse auf die Erhärtungsphase zurückzuführen.

Im Rahmen des vorliegenden Forschungsprojekts wurden Modelle erarbeitet, welche Aussagen zur Vorhersage der mechanischen Eigenschaften in Abhängigkeit der klimatischen Bedingungen entwickelt, die für die Praxis von grossen Nutzen sind. Diese Modelle ermöglichen es, Antworten auf vielen Fragen zu geben, welche im Rahmen von Planung und Ausführung geklebter Verbindungen im Brückenbau auftreten.

Umsetzung:

Die erarbeiteten Modelle zur Beschreibung der Entwicklung der mechanischen Eigenschaften des Klebers ermöglichen eine präzisere Vorhersage des Tragverhaltens geklebter Verbindungen mit kaltaushärtenden Klebstoffen.

Es ist davon auszugehen, dass der Anwendungsbereich kalthärtender Klebstoffe durch die Erkenntnisse ausgedehnt werden kann und die Anwendungssicherheit in der Baupraxis erhöht wird.

weitergehender Forschungsbedarf:

Obschon im Rahmen der Forschungsarbeit einige zentrale Fragen beantwortet werden konnten, bleiben Fragen zur Dauerhaftigkeit, des Rheologischen Verhaltens und der Ermüdungsfestigkeit der Klebstoffe weiterhin offen.
Um die Kenntnisse auch in Hinblick auf diese Fragen zu vertiefen, wurde ein Folgeprojekt verfügt, dass sich diesen Fragen widmet. Dieses Projekt AGB 2012-012 träge den Titel "Dauerhaftigkeit und Ermüdungsfestigkeit von kalthärtenden strukturellen Klebstoffen im Brückenbau"

Einfluss auf Normenwerk:

Die Erkenntnisse können im Rahmen der Revision der entsprechenden Normen ins Normenwerk einfliessen.

Der Präsident/die Präsidentin der Begleitkommission:

Name: Fürst Vorname: Armand

Amt, Firma, Institut: Fürst Laffranchi Bauingenieure GmbH

Unterschrift des Präsidenten/der Präsidentin der Begleitkommission:

Verzeichnis der Berichte der Forschung im Strassenwesen

Forschungsberichte seit 2009

Bericht-Nr.	Projekt Nr.	Titel	Datum
1356	SVI 2007/014	Kooperation an Bahnhöfen und Haltestellen *Coopération dans les gares et arrêts* *Coopération at railway stations and stops*	2011
1362	SVI 2004/012	Aktivitätenorientierte Analyse des Neuverkehrs Activity oriented analysis of induced travel demand Analyse orientée aux acitivtés du trafic induit	2012
1361	SVI 2004/043	Innovative Ansätze der Parkraukmbewirtschaftung Approches innovantes de la gestion du stationnement Innovative approaches to parking management	2012
1357	SVI 2007/007	Unaufmerksamkeit und Ablenkung: Was macht der Mensch am Steuer? Driver Inattention and Distraction as Cause of Accident: How do Drivers Behave in Cars? L'inattention et la distraction: comment se comportent les gens au volant?	2012
1360	VSS 2010/203	Akustische Führung im Strassentunnel Acoustical guidance in road tunnels Guidage acoustique dans les tunnels routiers	2012
1365	SVI 2004/014	Neue Erkenntnisse zum Mobilitätsverhalten dank Data Mining? De nouvelles découvertes sur le comportement de mobilité par Data Mining? New findings on the mobility behavior through Data Mining?	2011
1359	SVI 2004/003	Wissens- und technologientransfer im Verkehrsbereich Know-how and technology transfer in the transport sector Transfert de savoir et de technologies dans le domaine des transports	2012
1363	VSS 2007/905	Verkehrsprognosen mit Online -Daten Pronostics de trafic avec des données en temps réel Traffic forecast with real-time data	2011
1367	VSS 2005/801	Grundlagen betreffend Projektierung, Bau und Nachhaltigkeit von Anschlussgleisen Principes de bases concernant la conception, la construction et la durabilité de voies de raccordement Basic Principles on the Design, Construction and Sustainability of Sidings	2011
1370	VSS 2008/404	Dauerhaftigkeit von Betongranulat aus Betongranulat	2011
1373	VSS 2008/204	Vereinheitlichung der Tunnelbeleuchtung	2012
1369	VSS 2003/204	Rétention et traitement des eaux de chaussée	2012
648	AGB 2005/023 + AGB 2006/003	Validierung der AAR-Prüfungen für Neubau und Instandsetzung	2011
1371	ASTRA 2008/017	Potenzial von Fahrgemeinschaften *Potentiel du covoiturage* *Potential of Car Pooling*	2011

Bericht-Nr.	Projekt Nr.	Titel	Datum
1374	FGU 2004/003	Entwicklung eines zerstörungsfreien Prüfverfahrens für Schwiessnähte von KDB *Dévelopment d'une méthode d'éssais non-déstructif pour des soudures de membranes polymères d'étanchéité* *Development of a nondestructive test method for welded seams of polymeric sealing membranes*	2012
1375	VSS 2008/304	Dynamische Signalisierungen auf Hauptverkehrsstrassen *Signalisations dynamiques sur des routes principales* *Dynamic signalling at primary distributors*	2012
1376	ASTRA 2011/008_004	Erfahrungen im Schweizer Betonbrückenbau *Expériences dans la construction de ponts en Suisse* *Experiences in Swiss Bridge Construction*	2012
1379	VSS 2010/206_OBF	Harmonisierung der Abläufe und Benutzeroberflächen bei Tunnel-Prozessleitsystemen *Harmonisation of procedures and user interface in Tunnel-Process Control Systems* *Harmonisation des processus et des interfaces utilisateurs dans les systèmes de supervision de tunnels*	2012
1380	ASTRA 2007/009	Wirkungsweise und Potential von kombinierter Mobilität *Mode of action and potential of combined mobility* *Mode d'action et le potentiel de la mobilité combinée*	2012
1381	SVI 2004/055	Nutzen von Reisezeiteinsparungen im Personenverkehr *Bénéfices liés à une réduction des temps de parcours du trafic voyageur* *Benefits of travel time savings in passenger traffic*	2012
1383	FGU 2008/005	Einfluss der Grundwasserströmung auf das Quellverhalten des Gipskeupers im Chienbergtunnel *Influence de l'écoulement souterrain sur le gonflement du Keuper gypseux dans le Tunnel du Chienberg* *Influence of groundwater flow on the swelling of the Gipskeuper formation in the Chienberg tunnel*	2012
1386	VSS 2006/204	Schallreflexionen an Kunstbauten im Strassenbereich *Réflexions du trafic routier aux ouvrages d'art* *Noise reflections on structures in the street*	2012
1387	VSS 2010/205_OBF	Ablage der Prozessdaten bei Tunnel-Prozessleitsystemen *Data storage in tunnel process control systems* *Enregistrement ds données de systèmes de supervision de tunnels*	2012
649	AGB 2008/012	Anforderungen an den Karbonatisierungswiderstand von Betonen *Exigences par rapport à la résistance à la carbonatationdes bétons* *Requirements for the carbonation resistance of concrete mixes*	2012
650	AGB 2005/010	Korrosionsbeständigkeit von nichtrostenden Betonstählen *Résistance à la corrosion des aciers d'armature inoxydables* *Use of stainless steels in concrete structures*	2012